SCHOOL OF

NUCLEAR ENGINEERING

COO-2826-11
PNE-79-136

FAST BREEDER BLANKET FACILITY
Quarterly Progress Report for the Period October 31, 1978 — December 31, 1978

Edited by
F. M. Clikeman

Prepared for
The U.S. Department of Energy
Under Contract No. EY-76-S-02-2826

December, 1978
Purdue University, West Lafayette, Indiana 47907

DISCLAIMER

NOTICE

This report was prepared as an account of work sponsored by the United States Government. Neither the United States nor the United States Department of Energy, nor any of their employees, makes any warranty, express or implied, or assumes any legal liability or responsibility for the accuracy, completeness, or usefulness of any information, apparatus, product of process disclosed or represents that its use would not infringe privately owned rights.

NOTICE

This report was prepared as an account of work sponsored by the United States Government. Neither the United States nor the United States Department of Energy, nor any of their employees, nor any of their contractors, subcontractors, or their employees, makes any warranty, express or implied, or assumes any legal liability or responsibility for the accuracy, completeness or usefulness of any information, apparatus, product or process disclosed, or represents that its use would not infringe privately owned rights.

ABSTRACT

This quarterly progress report summarizes the work performed using Purdue University's Fast Breeder Blanket Facility for the Department of Energy during the months October - December 1978. The summary includes a final report on the safety evaluation of the hypothetical flooding accident which has had a major influence on the design of the facility. Progress on the development and testing of the experimental technique is also summarized. Preliminary results of the $^{115}In(n,\gamma)^{116m}In$ and $^{115}In(n,n')^{115m}In$ reactions are presented in Sec. C. IV.

LIST OF CONTENTS

LIST OF FIGURES

Task B

LIST OF TABLES

TASK B
(R.C. Borg)

Safety evaluation of the hypothetical flooding accident has had a major influence on the design of the Fast Breeder Blanket Facility (FBBF). The results presented in this report are concerned with the safety studies performed during the period January 1976 to September 1978.

In Sec. I, the need for such investigations is discussed. Those individuals contributing to the safety effort are noted. The models for evaluating k_{eff} and group constants are described in Sec. II. Safety of partially flooded and the normally operated facility are reported in Sec. III. Safety of extreme advanced loadings were necessary to identify design related modification. The results of this study are given in Sec. IV. The bulk of the safety study which considers cladding and pitch variation are presented in Sec. V for 360° loadings and extended in Sec. VI for 180° loadings. Finally, in Sec. VII the safety of various dry flooded conditions are summarized.

I. INTRODUCTION

The FBBF is a fast neutron subcritical facility. Thus, for normal operation, there is an insignificant number of low energy and thermal neutrons due to the absence of moderating materials. Safety of the FBBF is primarily concerned with the hypothetical flooding accident, which would inject water, as a moderator, into the system causing moderation of neutrons which would then decrease the degree of subcriticality. Since the FBBF is located below ground level, flooding could possibily occur if there were a fire and large amounts of water were necessary to extinguish it. The FBBF is designed so that it could not accidently become critical or come close to a critical state for any flooded condition.

The object of this topical report is to make available, in the form of a single manuscript, the safety calculations and investigations preformed during the period January, 1976 to September, 1978.

In Sec. II the models for evaluating k_{eff} and calculating group constants are presented. The two-dimensional computer code 2DB[1] was used in evaluating k_{eff}. The group constants were evaluated with the aid of the HAMMER[2] code cross section generating capability. In Sec. III, the values of k_{eff} for partially flooded blankets, which could occur during the loading phase, and for normal operation are reported. Safety calculations for extreme advance loadings, which were necessary for scoping studies, are presented in Sec. IV. The bulk of the final safety calculations which consider cladding and pitch variations are presented in Sec. V for 360° loadings and extended in

Sec. VI for 180° loadings. Finally, in Sec. VII the safety of the FBBF under various dry-flooded conditions are summarized.

Several former and current students of the School of Nuclear Engineering contributed significantly to the safety studies of the FBBF for the reported period, (J.E. Arpa, K.R. Koch, D.M. Waite, D.J. Malloy, T.F. Lin, M.P. Sohn, J.H. Paczolt, and M. Golbabai). Professor O.H. Gailar assisted in most of the early safety investigations. Also, Professor K.O. Ott contributed to the effort with helpful discussion and suggestions.

II. DESCRIPTION AND DISCUSSION OF CALCULATIONAL MODELS

A. Introduction

The safety evaluation of the FBBF has been an ongoing investigation since the early development stages of the FBBF. During this time period many improvements and modifications have been incorporated into the models for evaluating k_{eff} of the hypothetical flooding accident and group constant generation. In Sec. B. the calculational models used for evaluating k_{eff} are presented. The group constants were generated from unit cell type calculations. The geometrical and material specifications of the unit cells are given in Secs. C and D.

B. Models for Evaluating k_{eff}

B.1. Models without B_4C Transition Regions

The geometrical model without B_4C transition regions for evaluating k_{eff} of a hypothetical flooding accident is given in Fig. II.1. The dimensions illustrated in Fig. II.1 were obtained from the original blue prints of the FBBF. Material indentification is given in Table II.1. The two converter regions, region 1 and 2, contain 4.8% enriched uranium oxide fuel pins which are clad with stainless steel. The spaces between the fuel pins in the outer converter region are almost completely filled with sealed sodium-containing stainless steel tubes. The excess space in both converters is filled with B_4C which was vibrated into each of the containers prior to being sealed. Because of this type of construction, flooding of either region is remote. But to be conservative, it was assumed that only 60% of the excess available space is occupied by B_4C; the other 40% is assumed to be H_2O. The actual percentages of B_4C which were available after construction, are 61.24 percent and 53.58 percent for the inner and outer converters, respectively.

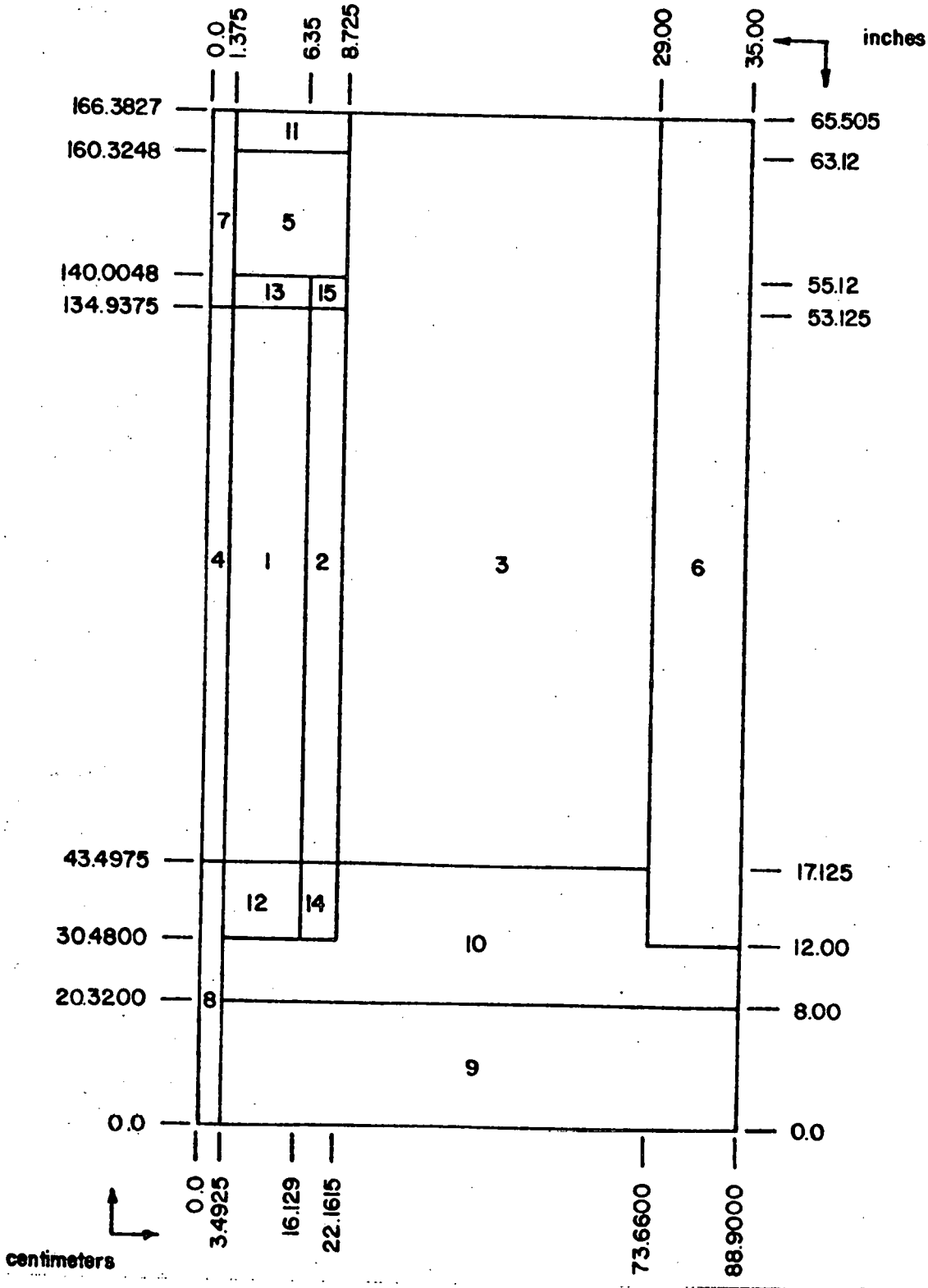

Figure II.1. FBBF two-dimensional hypothetical flooding mock-up without B_4C transition regions.

TABLE II.1

FBBF two-dimensional region descriptions
without B_4C transition regions

Region 1 -- Inner Converter
- 4.8% enriched uranium oxide fuel pins
- 316 stainless steel cladding
- 0.468 inch hexagonal pitch
- (assumed) 60% of void filled with natural B_4C
- (assumed) 40% of void filled with water

Region 2 -- Outer Converter
- 4.8% enriched uranium oxide fuel pins
- 316 stainless steel cladding
- 0.702 inch hexagonal pitch
- 2 sodium filled pins per fuel pin
- (assumed) 60% of void filled with natural B_4C
- (assumed) 40% of void filled with water

Region 3 -- Blanket
- Natural uranium oxide fuel pins
- Aluminum primary cladding
- Al or SS316 secondary cladding - open ends
- Variable hexagonal pitch
- Voids entirely filled with water

Region 4 -- Source
- Californium neglected
- Solid 316 stainless steel source holder
- 316 stainless steel source guide tube
- Void entirely filled with water or SS plug

Region 5 -- Axial Blanket
- Natural uranium metal fuel pins
- Aluminum cladding
- 1.175 inch hexagonal pitch
- Void entirely filled with water

Region 6 -- Reflector
- Carbon steel cans filled with
  - 60% carbon steel punchings
  - 40% NaCl crystals
- Including the can walls the volume fractions are
  - 66% carbon steel
  - 34% NaCl

Region 7 -- Source Drive Rod
- Essentially the same as Region 4 since the drive rod is the same diameter as the source holder.

Region 8 -- Water Below Source
- Since the source is assumed to be up, water entirely fills the source guide tube.

Region 9 -- Concrete
- Normal concrete used

Region 10 -- Steel Base and Spacers
- Carbon Steel

Region 11 -- Lead
- Solid lead

Region 12 & 13 -- ICR Pin Ends
- Same as Region 1 except no fuel in pin

Region 14 & 15 -- OCR Pin Ends
- Same as Region 2 except no fuel in pin

The blanket region, region 3, contains natural uranium oxide fuel with aluminum clad. The inner rows are stainless steel double clad and the outer rows are aluminum double clad for the initial load. All of the available voided space is assumed to be filled with water in the case of a hypothetical flooding accident.

Region 4, in Figure II.1, represents the source area. It consists essentially of the source, source holder, source guide tube and the inner converter can wall. In all safety calculations, the source is assumed to be in place unless specifically stated to the contrary, or if the source is not in place, a stainless steel rod of identical diameter is assumed to be in the source tube. This constraint enables the displacement of water from the source region and may allow more flexibility for advanced loading schemes. The region directly above the source, region 7, consists essentially of the same type of materials as the source region. The region below the source was conservatively assumed to be filled with water. This follows from the previous discussion since the source may be in place, leaving the region below voided.

Region 5, the axial blanket, was assumed to be essentially identical to the radial blanket region or filled with lead. Regions 6, 9, 10 and 11 are the reflector, concrete base, stainless steel base plates and upper lead cap. Regions 12, 13, 14 and 15 are the pin ends for the converter regions.

B.2. Models with B_4C Transition Regions

Early in the series of safety calculations it was realized that the boundary regions of the inner and outer converters could have a significant quantity of B_4C, which could considerably effect the results of safety calculations. For this reason the original model was extended to explicitly consider B_4C transition regions. This model is illustrated in Fig. II.2, with the region descriptions given in Table II.2. Evaluation of the dimensions and region materials in the inner and outer converters are described in the following with the aid of Fig. II.3.

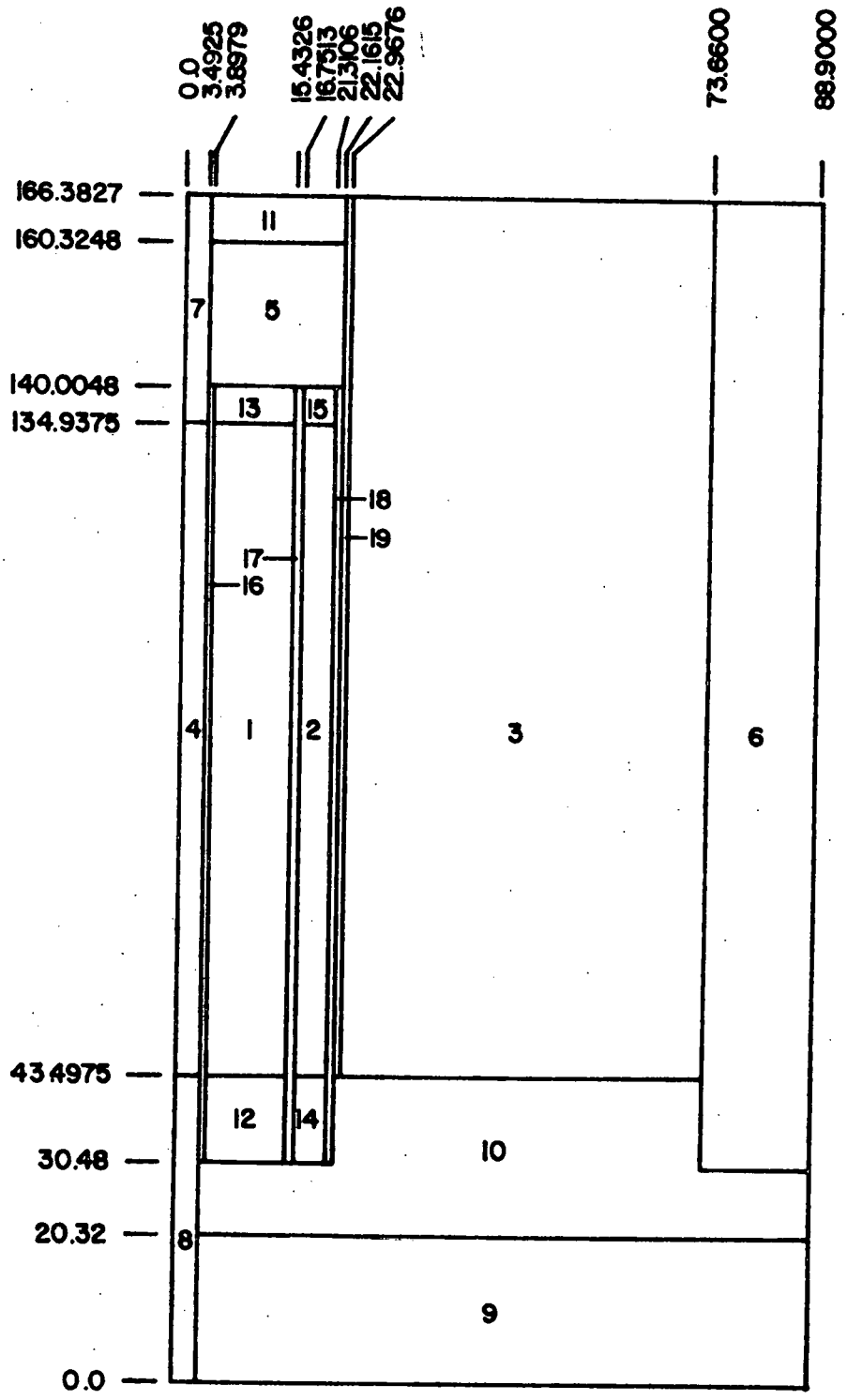

Figure II.2: FBBF two-dimensional hypothetical flooding mock-up with B_4C transition regions.

TABLE II.2.

FBBF two-dimensional region descriptions
with B_4C transition regions

Region 1 -- Inner Converter
- 4.8% enriched uranium oxide fuel pins
- 316 stainless steel cladding
- 0.468 inch hexagonal pitch
- (assumed) 60% of void filled with natural B_4C
- (assumed) 40% of void filled with water

Region 2 -- Outer Converter
- 4.8% enriched uranium oxide fuel pins
- 316 stainless steel cladding
- 0.702 inch hexagonal pitch
- 2 sodium filled pins per fuel pin
- (assumed) 60% of void filled with natural B_4C
- (assumed) 40% of void filled with water

Region 3 -- Blanket
- Natural uranium oxide fuel pins
- Aluminum primary cladding
- Al or SS316 secondary cladding - open ends
- Variable hexagonal pitch
- Voids entirely filled with water

Region 4 -- Source
- Californium neglected
- Solid 316 stainless steel source holder
- 316 stainless steel source guide tube
- Void entirely filled with water or SS plug

Region 5 -- Axial Blanket
- Natural uranium metal fuel pins
- Aluminum cladding
- 1.175 inch hexagonal pitch
- Void entirely filled with water

Region 6 -- Reflector
- Carbon steel cans filled with
  - 60% carbon steel punchings
  - 40% NaCl crystals
- Including the can walls the volume fractions are
  - 66% carbon steel
  - 34% NaCl

Region 7 -- Reflector
Essentially the same as Region 4 since the drive rod is the same diameter as the source holder.

Region 8 -- Water Below Source
Since the source is up, water entirely fills the source guide tube.

Region 9 -- Concrete
Normal concrete used

Region 10 -- Steel base and Spacers
Carbon steel

Region 11 -- Lead
Solid lead

Region 12 & 13 -- ICR Pin Ends
Same as Region 1 except no fuel in pin

Region 14 & 15 -- OCR Pin Ends
Same as Region 2 except no fuel in pin

Region 16 -- Source/ICR Transition
Areas in which fuel rods will not be located form an irregular annular ring in the ICR. This region is filled with:
- 60% natural B_4C
- 40% water

Region 17 -- ICR/OCR Transition
Similar to Region 16 but this region contains parts of both the ICR and OCR including their can walls

Region 18 -- OCR/Blanket Transition A
Similar to Region 16 but in OCR

Region 19 -- OCR/Blanket Transition B
Region in the blanket which contains only H_2O

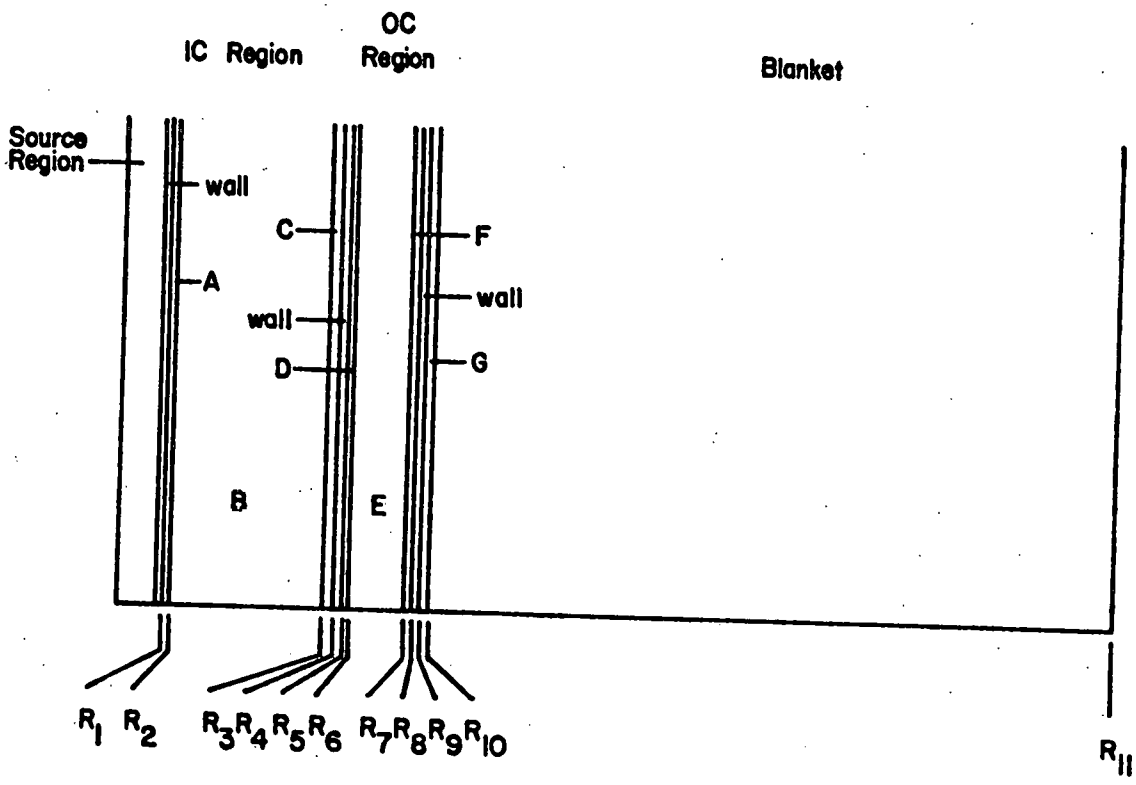

Figure II.3: FBBF mockup with transition regions explicitly described; regions A and C are the inner converter inner and outer transition regions; regions D and F are the outer converter inner and outer transition regions; region G is the blanket inner transition region; and regions B and E are the portions of inner and outer converters which contain both B_4C and fuel.

B.2.1 Inner Converter (IC)

The inner converter, which was originally considered as a single region, is divided into three regions (comp. Fig. II.3).

Region A: Inner converter inner boundary region.

Region A contains water or B_4C mixed with water depending on the investigation. The area of the region, which does not contain any fuel pins, is identical to the voided area between R_1 and R_2. The value of R_2 in Fig. II.3, is calculated with the aid of Fig. II.4 by noting that:

$$\frac{\pi}{6}\,(R_2^2 - R_1^2) = \frac{L^2\sqrt{3}}{4} - \frac{11}{6}\cdot\pi\frac{s^2}{4} - \frac{\pi}{6}R_1^2$$

with

$$R_1 = 3.4925 \text{ cm}$$

$$L = 4s$$

$$s \equiv \text{pitch} = 1.20396 \text{ cm}$$

thus,

$$R_2 = 3.8979 \text{ cm} \quad .$$

Region B: Homogenized inner converter region based on the unit cell description.

The value of R_3 is calculated by knowing that the volume (area) of region B must be equal to the volume (area) of the total number of unit cells in in the region. The basic equation is given by

$$\frac{\pi}{6}\,(R_3^2 - R_2^2) = n_1 A_1 \quad ,$$

with

R_2 = 3.8979 cm

n_1 = number of unit cells in a sector of 60° = 93,

A_1 = area of unit cell = 1.2553 cm, (comp. Sec. II.C)

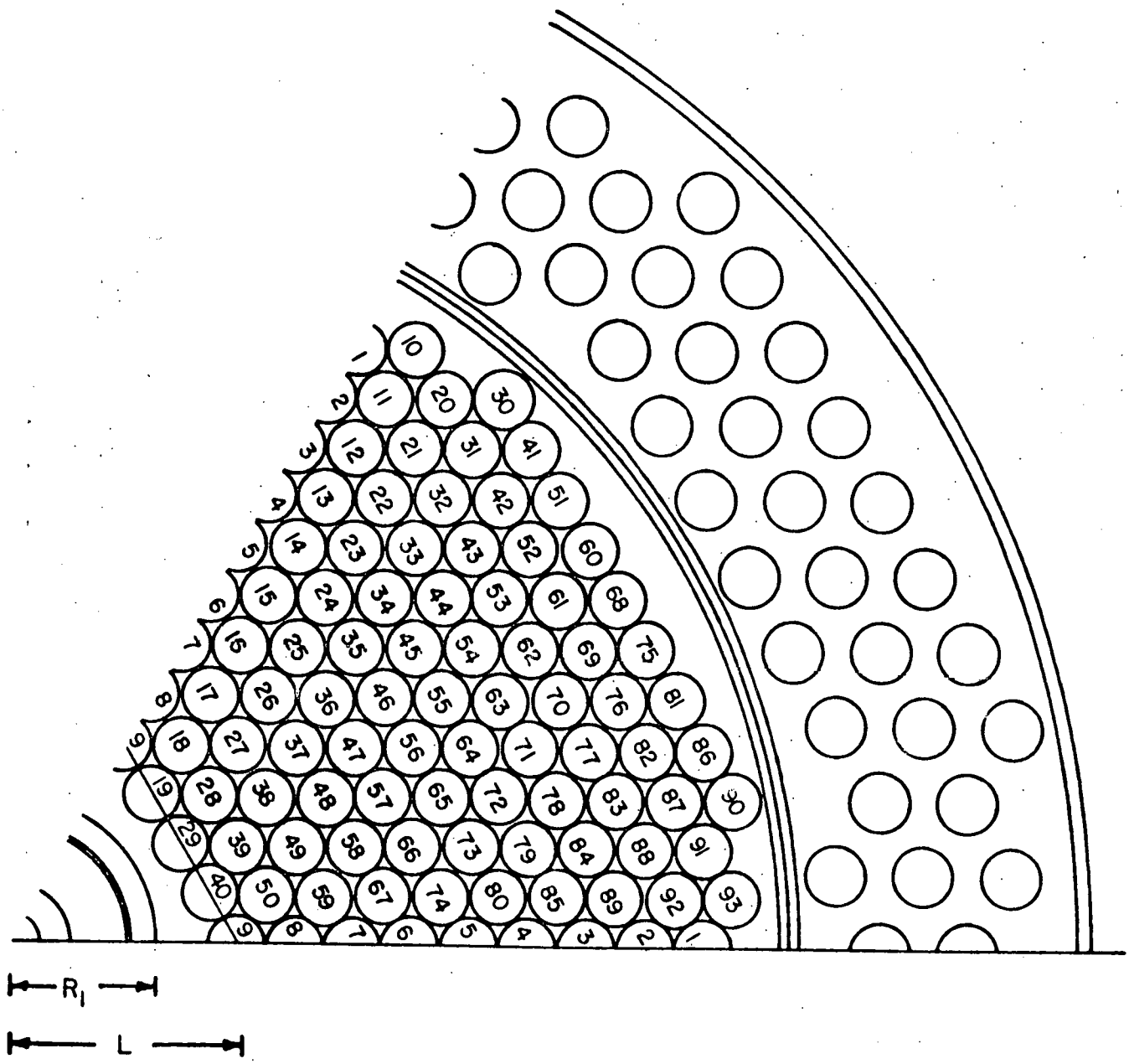

Figure II.4: One-sixth section of the converters.

thus,

$$R_3 = 15.4326 \text{ cm} \quad .$$

Region C: Inner converter outer boundary region.

Region C contains water or B_4C mixed with water depending on the investigation. The external dimension, R_4 (comp. Fig. II.3), is identical to 15.7996 cm which corresponds to the radius of the outer can wall.

B.2.2 Outer Converter (OC)

The outer converter is divided into three regions in the same way as the inner converter (comp. Fig. II.3). Calculation of the radial dimensions is slightly different than that applied for the inner converter. The area of the interface region between the converters does not contain any fuel pins. It is almost equal to one-third the total voided area of the outer converter region. Therefore, the radial dimensions for regions D and F (comp. Fig. II.3) were evaluated so that region F has twice the area of region D. Region E has a volume (area) equal to that of the cell description for the total number of fuel pins in the OC (in the same way as region B in the IC). Therefore, the values of R_6 and R_7 were calculated with the following expressions:

$$\frac{\pi}{6}(R_6^2 - R_5^2) = \frac{1}{2}\frac{\pi}{6}(R_8^2 - R_7^2)$$

$$\frac{\pi}{6}(R_7^2 - R_6^2) = A_2 n_2$$

where

$R_8 = 21.9718$ cm

$R_5 = 16.31874$ cm

A_2 = area of the unit cell of OC = 2.7534 cm^2,

n_2 = number of unit cells in a 60° sector = 33,

thus

$$R_6 = 16.7513 \text{ cm}$$

$$R_7 = 21.3106 \text{ cm} \quad .$$

B.2.3 Blanket Region

The outer radius of the inner blanket boundary where there is no fuel can be calculated with the aid of Fig. II.5, Fig. II.3 and the following equation:

$$\frac{\pi}{6} R_{10}^2 - \frac{\pi}{6} R_9^2 = L^2 \frac{\sqrt{3}}{4} - \frac{55}{3} A_3$$

with

R_9 = 22.1615 cm (from the construction of the facility),

$L = R_9 + 3s$ (from Fig. II.5),

$s \equiv$ Pitch = 1.7094 cm

$A_3 \equiv$ area of unit cell of the blanket region = 2.5306 cm^2

The factor $\frac{55}{3}$ accounts for the number of fuel pins inside the triangle with a side of length L. This gives:

$$R_{10} = 22.9626 \text{ cm} \quad .$$

B.2.4 Transition Regions

The specific B_4C and wall regions indicated in Fig. II.3 were homogenized to form the transition regions illustrated in Fig. II.2. The inner converter inner wall and region A were combined to form region 16 in Fig. II.2. Regions C, D and the inner-outer converter walls were homogenized to obtain region 17 in Fig. II.2 and region 18 was homogenized from region F and the outer converter outer wall. Region 19 is identical to region G.

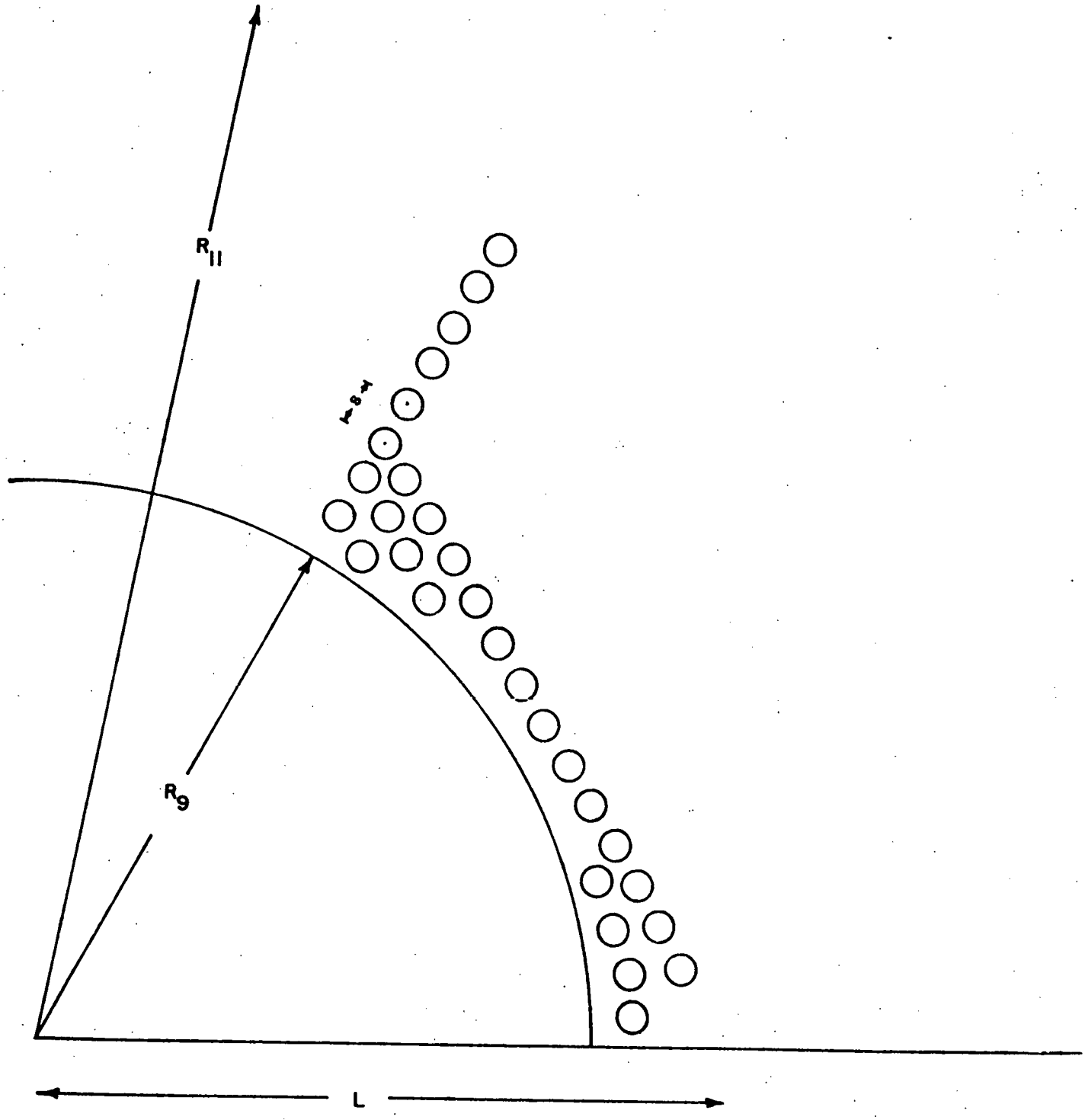

Figure II.5: One-sixth of the FBBF blanket region.

B.3 Advanced Loading Models

Future blanket loadings of the FBBF will contain some enriched material. To investigate the safety of these advanced loadings the most reactive configuration was considered. It consisted of replacing some of the inner rows of nautral uranium with the remaining 4.8% enriched fuel and the middle rows with 1.3% enriched material. The outer rows of natural uranium rods were retained. The model is illustrated in Fig. II.6. Dimensions of the converter regions are the same as those given in Fig. II.3. The basic difference between the models illustrated in Fig. II.3 and Fig. II.6 is the splitting of the blanket region. Since the length of the 4.8% and 1.3% enriched rods is different than the natural uranium rods, the base plate had to be slightly adjusted as indicated in Fig. II.6. The outer radius of each enriched region is not specifically indicated since various dimensions were considered (comp. Sec. VI and VII). Region identifications are given in Table II.3. The material descriptions of each region are essentially the same as those indicated in Table II.2.

C. Models for the Calculation of Group Constants

The cross sections for the inner converter, outer converter, blanket and source region were calculated with the aid of the HAMMER[2] code based on a unit cell description. The general description of the procedure is given, followed by a subsection for each region which gives the needed unit cell information. Figure II.7 illustrates a general unit cell characteristic of regions in the FBBF.

The generalized unit cell must be transformed into a cylindrical unit cell for input to HAMMER. The fuel pin and cladding are already cylindrical. But the outer most region which is hexagonal must be converted to a cylinder with the same enclosed area retained (comp. Fig. II.7):

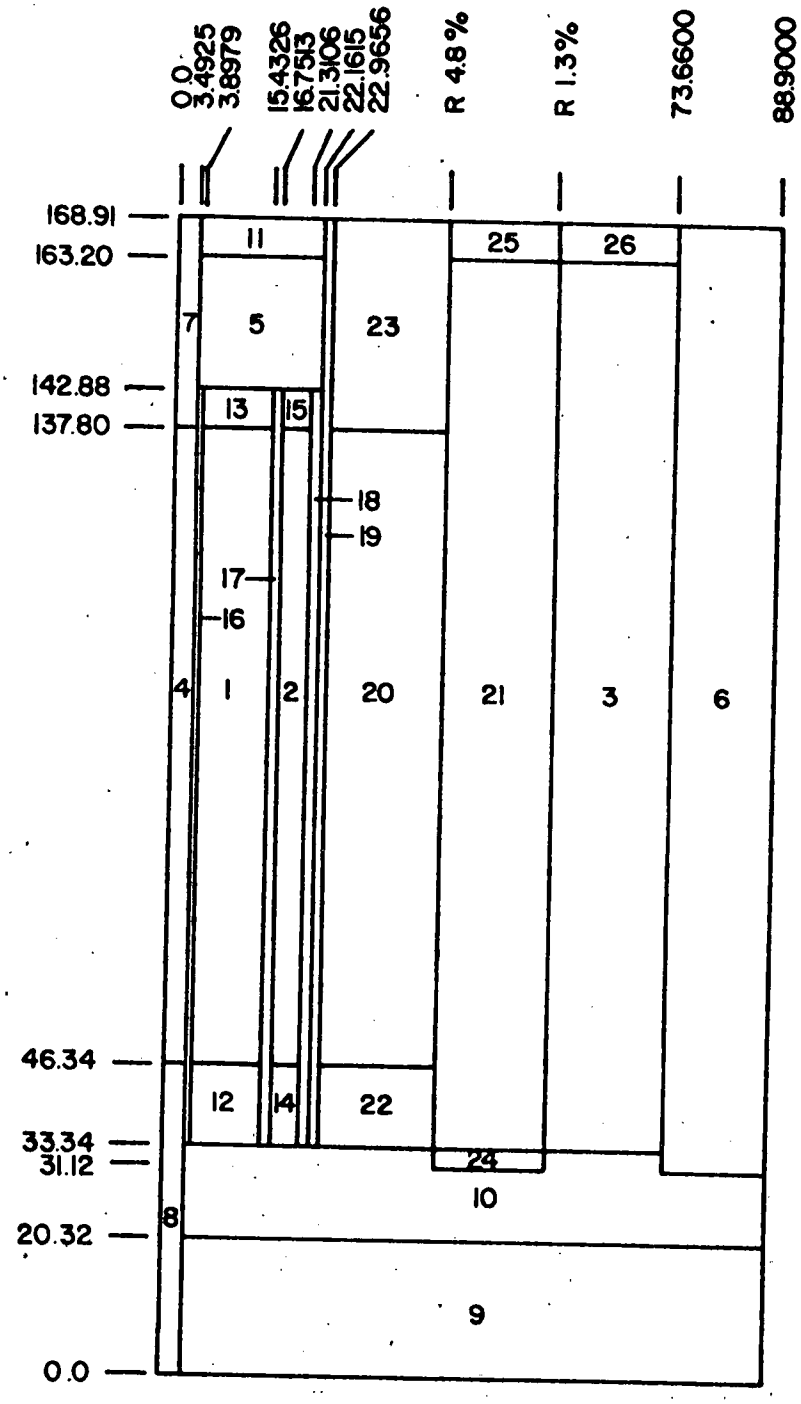

Figure II.6: FBBF mock-up for advance loading safety study.

TABLE II.3

Two-dimensional FBBF advanced loading descriptions

1. Inner Converter
2. Outer Converter
3. Nat. UO_2 Blanket Region
4. Source
5. Axial Blanket
6. Reflector
7. Source Drive Rod
8. Water Below Source
9. Concrete
10. Steel Base and Spacers
11. Lead Cap
12. ICR Lower Pin Ends
13. ICR Upper Pin Ends
14. OCR Lower Pin Ends
15. OCR Upper Pin Ends
16. Source/ICR Transition
17. ICR/OCR Transition
18. OCR/Blanket Transition A
19. OCR/Blanket Transition B
20. 4.8% enriched Blanket Region
21. 1.3% Enriched Blanket Region
22. Non-Active 4.8% Region
23. Non-Active 4.8% Region
24. Non-Active 1.3% Region
25. Non-Active 1.3% Region
26. Non-Active Nat. UO_2 Region

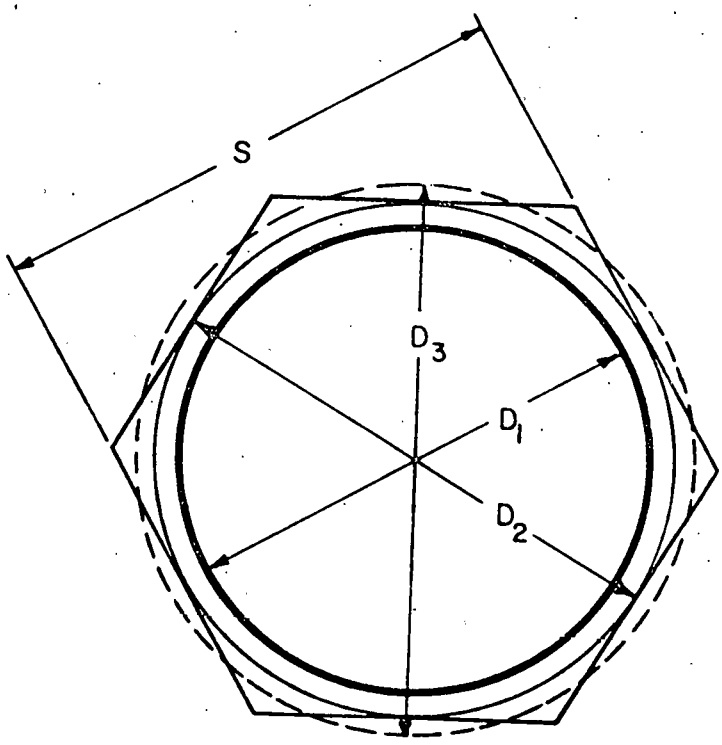

Figure II.7: Generalized hexagonal unit cell.

$$\text{Area of hex} = 3/2\ s^2 \tan 30°$$

$$\text{Area of equiv. cyl.} = \frac{\pi D_3^2}{4}$$

$$\frac{\pi D_3^2}{4} = \frac{3}{2} s^2 \tan 30°$$

$$D_3 = s\sqrt{\frac{6\tan 30°}{\pi}}$$

A 0.008" thick ring of Unit Heavy Scatterer is called for by HAMMER. The diameter of the unit cell with a heavy scatter ring (D_4) is given by:

$$D_4 = D_3 + 2 \times 0.008" \quad .$$

The volume fraction of each region is based on the original unit cell, i.e., unit heavy scatterer is neglected. As illustrated, inclusion of irregular shaped regions of a unit cell is simply performed by converting these regions into cylindrical rings of equivalent area. The ordering of the rings is choosen to best represent the geometry of the original cell.

The axial buckling is needed by the HAMMER code. A standard extrapolation length of 37.6 cm is used, since for the flooded case the spectrum is not extremely thermalized. The buckling is calculated by:

$$B^2 = \left(\frac{\pi}{H'}\right)^2 \quad .$$

where H' is the extrapolated height of the active region.

C.1 Inner Converter

The unit cell for the inner converter is illustrated in Fig. II.8. The following indicates the cell characteristics and region description:

Equivalent Diameter:

$$\frac{\pi D_4^2}{4} = \text{Area of Hex} = \frac{3}{2} s^2 \tan 30$$

$$D_4 = s\sqrt{\frac{6\tan 30}{\pi}} = 0.498" = 1.2649 \text{ cm}$$

$s \equiv$ pitch = 0.474" = 1.2040 cm

Scatter Ring:

$$D_5 = D_4 + 2 \times 0.008"$$

Area:

Total area = Area of Hex = 0.1946 in^2 = 1.2553 cm^2

Buckling

Only the axial buckling is used.

Active height of IC = 36" = 91.44 cm

Extrapolation length = 37.6 cm

$$B^2_{axial} = \left(\frac{\pi}{H'}\right)^2 = 5.9272\text{E-}04 \text{ cm}^{-2} = 5.9272 \text{ m}^{-2}$$

Cell Description

Region	Material	Unit Cell Dimensions in.	cm.	Volume fraction
1	4.8% UO_2	0.420	1.0668	0.7120
2	Air Gap (approx. O_2)	0.426	1.0820	0.0205
3	SS316 (approx. SS304)	0.466	1.1836	0.1440
4	Moderator	0.498	1.2649	0.1235
	40% H_2O			0.0494
	60% B_4C			0.0741
5	Scatter Ring	0.514	1.3056	

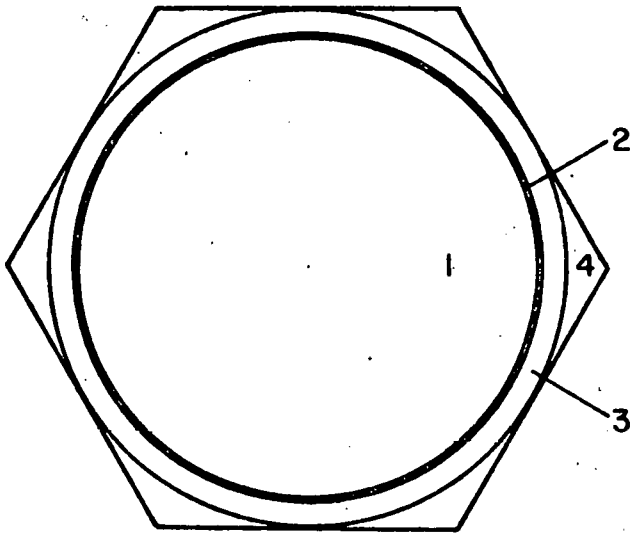

Figure II.8: Inner converter unit cell. Regions 1 to 4 are the fuel region, air gap, SS clad and water mixed with B_4C, respectively.

C.2. Outer Converter

The unit cell for the outer converter and the diagram of a sodium pin are illustrated in Fig. II.9 and Fig. II.10 respectively. In the following the information for evaluating the dimensions for the unit cell are indicated.

Equivalent Diameter:

$\frac{\pi D_4^2}{4}$ = Area total - Area sodium - Area sodium pins

$D_4 = \sqrt{\frac{4}{\pi}(A_t - A_{Na} - A_{pins})} = 0.4945" = 1.2560$ cm

Scatter Ring

0.008" thick Unit Heavy Scatter (Matl. 306)

$D_7 = D_6 + 2 \times 0.008"$

Volume Fractions

Total Area = $A_t = 0.4274$ in^2 = 2.7574 cm^2

Buckling

Only Axial Buckling used.

Active height of ICR = 36" = 91.44 cm

Extrapolation length = 37.6 cm

$$B^2_{axial} = \left(\frac{\pi}{H'}\right)^2 = 5.9272\text{E-}04 \text{ cm}^{-2} = 5.9272 \text{ m}^{-2}$$

Unit Cell Description:

Region	Material	Unit Cell Dimensions in.	cm.	Volume Fraction
1	4.8% UO_2	0.420	1.0668	0.3241
2	Air Gap (approx. O_2)	0.426	1.08204	0.009328
3	SS316 (approx. SS304)	0.466	1.18364	0.06557
4	Moderator	0.4945	1.2560	0.05027
	40% H_2O			0.01828
	60% B_4C			0.02743
5	SS304	0.5374	1.3650	0.08146
6	Na (approx. Al)	0.73769	1.8737	0.4692
7	Scatter Ring	0.75369	1.9144	

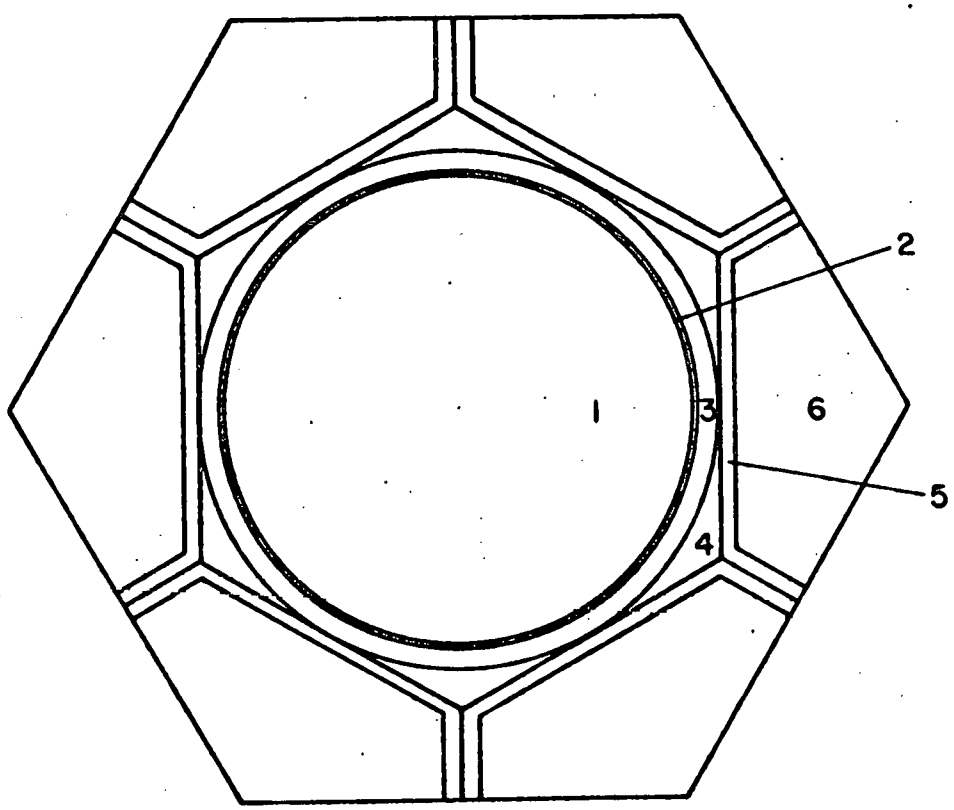

Figure II.9: Outer converter unit cell. Regions 1 to 6 are the fuel region, air gap, SS clad, water mixed with B_4C, SS pin and sodium, respectively.

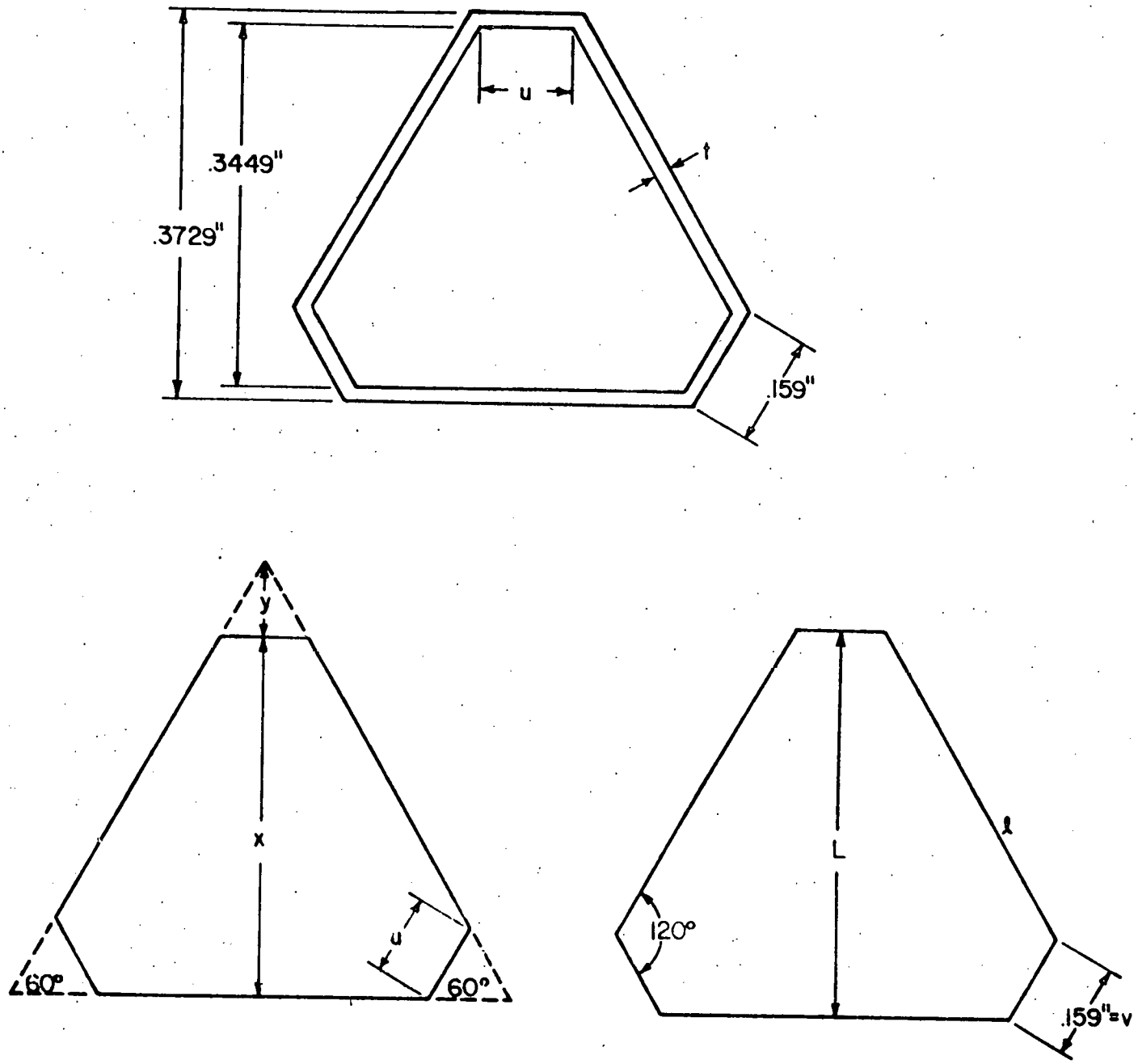

Figure II.10: One of the sodium pins in the outer converter.

OUTER CONVERTER cont.

Area of Pins: (see Figure II.9 for variable description- unit cell contains two sodium pins)

Unit cell contains 2 whole sodium pins
sodium pin is 0.014" thick

$\ell \cos 30° + v \cos 30° = L$

$\ell = L/\cos 30° - v$

$\ell = 0.3729/\cos 30° - 0.159 = 0.27159"$

Perimeter = $P_e = 3(\ell+v) = 1.29176"$

Area of 1 pin clad = $A_p = 0.01808\ in^2$

Area of 2 pins clad = $2A_p = 0.03617\ in^2 = 0.23335\ cm^2$

$u = v - 2t/\tan 60°$

$y = u \cos 30$

Area of 1 pin

$$= \frac{(x+y)^2}{\tan 60°} - 3\,\frac{uy}{2}$$

$$= \frac{(x+u\cos 30°)^2}{\tan 60°} - 3/2\ U^2 \cos 30°$$

$x = 0.3449"$ $v = 0.159"$ $t = 0.014"$

$u = v - 2t/\tan 60 = 0.14283"$

A_{Na} = 2 x Area of 1 pin = $0.20054\ in^2 = 1.2939\ cm^2$

Area total = Area Cell = $\frac{3}{2}\ s^2 \tan 30$, s = pitch = 0.702"

$A_t = 0.4274\ in^2 = 2.7574\ cm^2$

C.3. Single Clad Blanket Unit Cell

The unit cell for the single clad blanket is illustrated in Fig. II.11. In the following, the unit cell characteristics are given:

Equivalent Diameter:

$$\frac{\pi D_4^2}{4} = \text{Area total} = \frac{3}{2} s^2 \tan 30°$$

$$D_4 = s\sqrt{\frac{6\tan 30°}{\pi}} = 0.6300" = 1.6003 \text{ cm}, \quad s = 0.6"$$

Scatter Ring:

0.008" thick unit heavy scatter (Matl. 306)

$$D_5 = D_6 + 2 \times 0.008"$$

Volume Fractions:

$$\text{Area total} = \frac{3}{2} s^2 \tan 30° = 0.3118 \text{ in}^2 = 2.0116 \text{ cm}^2$$

Buckling:

Only Axial Buckling used.
Active Height of Blanket = 48" = 121.92 cm
Standard extrapolation = 37.6 cm

$$B^2_{axial} = \left(\frac{\pi}{H'}\right)^2 = 3.8786\text{E-}4 \text{ cm}^{-2} = 3.8786 \text{ m}^{-2}$$

Unit Cell Descriptions

Region	Material	Unit Cell Dimensions in.	Unit Cell Dimensions cm.	Volume Fraction
1	0.711% UO_2	0.546	1.38684	0.7511
2	Air gap	0.550	1.39700	0.01105
3	Al cladding	0.600	1.52400	0.1449
4	100% H_2O	0.630	1.52908	0.09297
5	Scatter Ring	0.646	1.64084	

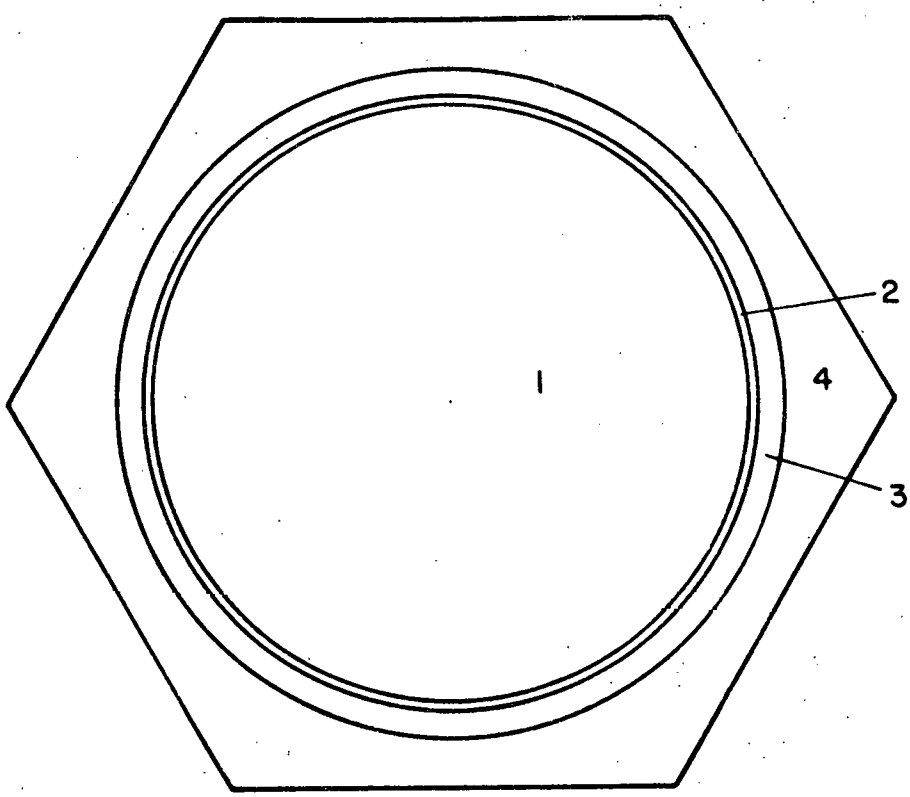

Figure II.11: Single Clad Blanket Unit Cell. Regions 1 to 4 are the fuel, air gap, Al clad and water, respectively.

C.4. Double Clad Blanket Unit Cell

The unit cell for the double clad blanket is illustrated in Fig. II.12. The following indicates the eell characteristics.

Equivalent Diameter:

$$\frac{\pi D_6^2}{4} = \text{Area Total} = \frac{3}{2} s^2 \tan 30°$$

$$D_6 = s\sqrt{\frac{6\tan 30°}{\pi}} = 0.7067" = 1.7950 \text{ cm}, \quad s = \text{pitch} = 0.673"$$

Scatter Ring:

0.008" thick Unit Heavy Scatter (Matl. 306)

$$D_7 = D_6 + 2 \times 0.008"$$

Volume Fractions:

$$\text{Area Total} = \frac{3}{2} s^2 \tan 30° = 0.3922 \text{ in}^2 = 2.5303 \text{ cm}^2$$

Buckling:

Only Axial Buckling used.
Active Height of Blanket = 48" = 121.92 cm

$$B^2_{axial} = \left(\frac{\pi}{H'}\right)^2 = 3.8786\text{E-}04 \text{ cm}^{-2} = 3.8786 \text{ m}^{-2}$$

Unit Cell Description:

Region	Material	Unit Cell Dimensions in.	Unit Cell Dimensions cm.	Volume Function
1	0.711% UO_2	0.546	1.38684	0.5969
2	Air Gap	0.550	1.39700	0.008778
3	Al Cladding	0.600	1.52400	0.1151
4	100% H_2O	0.602	1.52908	0.004814
5	SS316 (approx. SS304)	0.668	1.79502	0.1678
6	100% H_2O	0.7067	1.79502	0.1065
7	Scatter Ring	0.7227	1.83566	

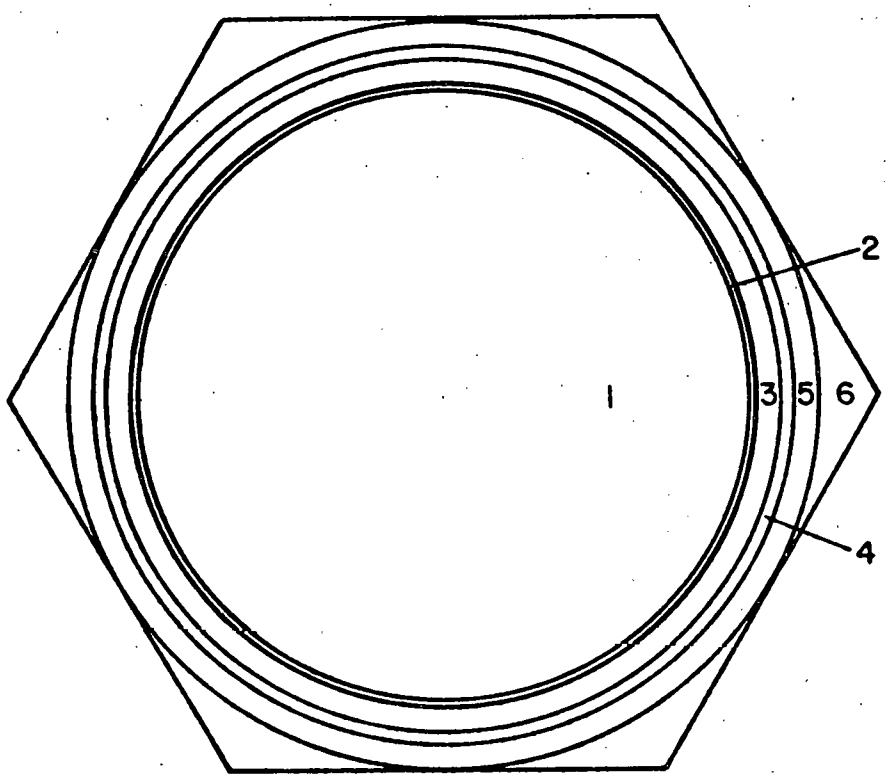

Figure II.12: Double clad blanket unit cell. Regions 1 to 6 are the fuel, air gap, Al clad, water, SS or Al secondary clad and water, respectively.

C.5. Enriched Blanket Unit Cell

The Enriched Blanket Unit Cell was used for advanced blanket loadings and is illustrated in Fig. II.13. The following indicates the cell characteristics.

Equivalent Diameter:

$$D_4 = s\sqrt{\frac{4}{\pi} \times \frac{3}{2} \tan 30^\circ \; (1 - VF_{ss\text{-}rod})}$$

$$D_5 = s\sqrt{\frac{6 \tan 30^\circ}{\pi}}$$

s = pitch

The pitch can be varied.

Scatter Ring:

0.008" thick Unit Heavy Scatter (Matl. 306)

$D_6 = D_5 + 2 \times 0.08"$

Volume Fractions:

Area Total = $\frac{3}{2} s^2 \tan 30^\circ$

Buckling:

Only Axial Buckling used.
Active Height of Blanket = 51.13 in = 129.86 cm
Standard Extrapolation = 37.6 cm

$$B^2_{axial} = \left(\frac{\pi}{H'}\right)^2 = 3.5195\text{E-}4 \text{ cm}^{-2} = 3.5195 \text{ m}^{-2}$$

Unit Cell Description:

Region	Material	Unit Cell Dimensions 4.8% UO_2 in.	4.8% UO_2 cm.	1.3% UO_2 in.	1.3% UO_2 cm.
1	Fuel	0.420	1.0668	0.383	0.9728
2	Air Gap	0.426	1.0820	0.391	0.9931
3	Al Clad	0.466	1.1836	0.453	1.1506
4	100% H_2O	D_4			
5	SS-Rods	D_5			
6	Scatter Ring	D_6			

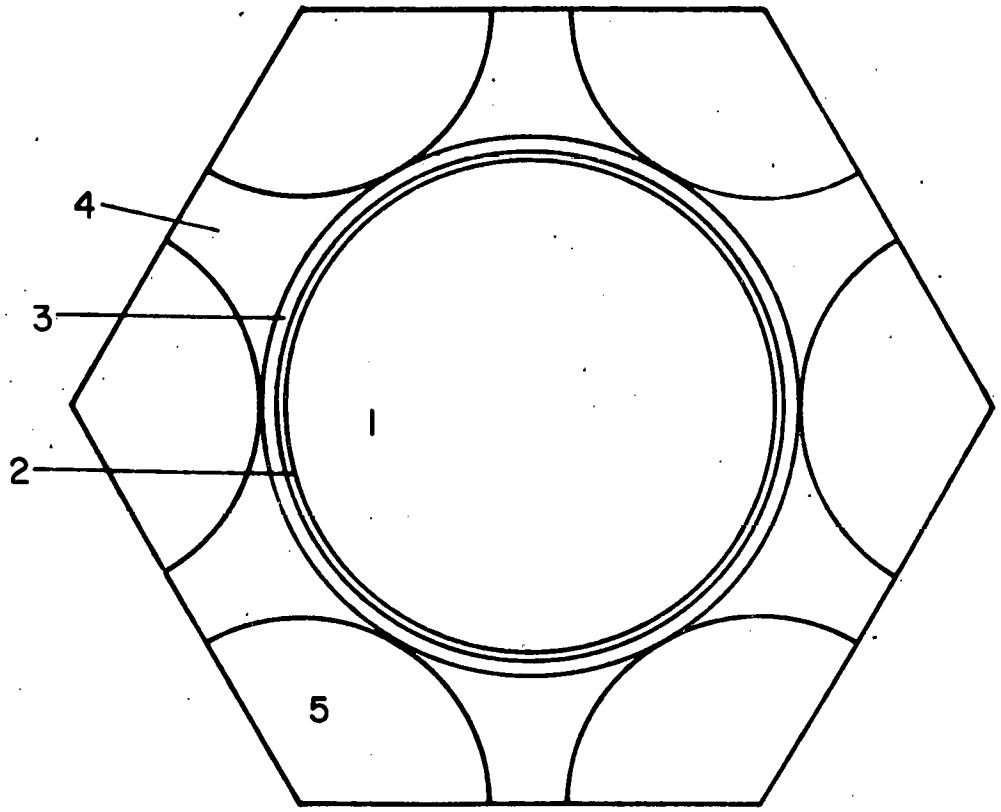

Figure II.13: Enriched Blanket Unit Cell. Regions 1 to 5 are the fuel, air gap, Al clad, water and SS rod, respectively.

C.6. Source Unit Cell

The unit cell for the source is illustrated in Fig. II.14. The following indicates the cell characteristics.

Equivalent Diameter:

Area of region 8 = $\frac{\text{Area total}}{2}$ (approx)

$$\frac{\pi D_8^2}{4} = \frac{\pi D_7^2}{4} \times 2$$

$$D_8 = \sqrt{2}\, D_7$$

Scatter Ring:

$$D_9 = D_8 + 2 \times 0.008"$$

Volume Fractions:

Based on both total area and unit cell area

Buckling:

Active length = 36" = 91.44 cm

Standard Extrapolation length = 37.6 cm

$$B^2_{axial} = \left(\frac{\pi}{H'}\right)^2 = 5.9272\text{E-}04\ cm^{-2} = 5.9272\ m^{-2}$$

Homogenized ICR:

HAMMER Material Number	Number densities from IC HAMMER run x V.F. from IC	Smeared Number Density
92235.	0.0011159 x 0.7120	= 0.0007945
92238.	0.0218861 x 0.7120	= 0.0155829
8000.	0.0460040 x 0.7120 + 0.000125 x 0.0210 + 0.0133889 x 0.1235	= 0.0347091
304.	0.0854702 x 0.1440	= 0.0123077
2001001.	0.0267778 x 0.01235	= 0.0033071
5000.	0.0659200 x 0.1235	= 0.0081411
6012.	0.0164800 x 0.1235	= 0.0020353

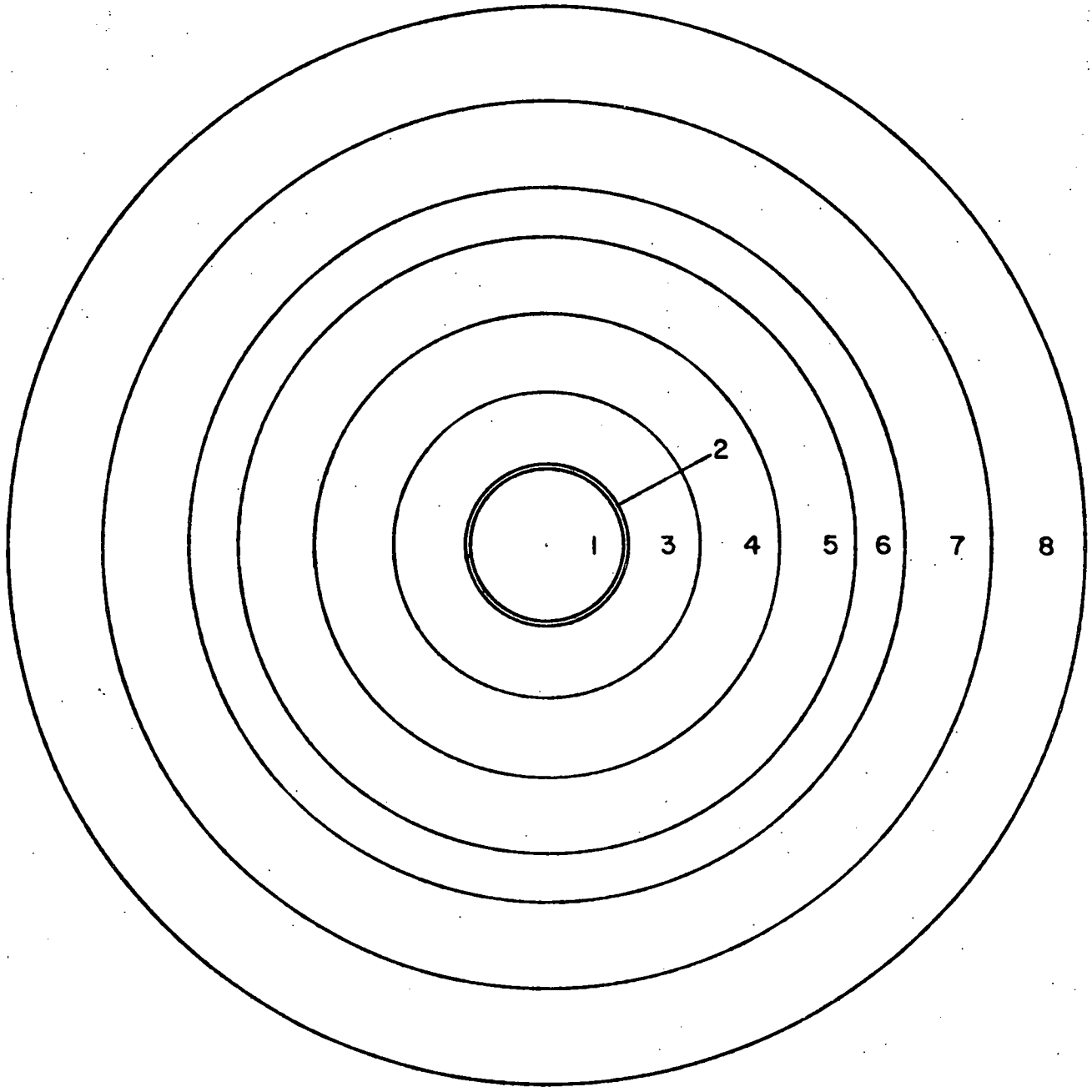

Figure II.14: Source unit cell. Regions 1 to 7 are the source, air gap, source holder, water, source guide, water and inner can wall respectively.

SOURCE cont.

Unit Cell Description:

Region	Material	Unit Cell Dimensions in.	Unit Cell Dimensions cm.	Volume Fraction	V.F. of Whole Area
1	Source-approx SS 304	0.500	1.2700	0.03306	0.01653
2	Air Gap	0.510	1.29540	0.001336	0.0006678
3	Source holder = SS 304	1.000	2.54000	0.09784	0.04892
4	100% H_2O	1.500	3.81000	0.1653	0.08264
5	Source guide tube = SS 304	2.000	5.08000	0.2314	0.1157
6	100% H_2O	2.25	5.7150	0.1405	0.07025
7	Inner can wall = SS 304	2.75	6.9850	0.3306	0.1653
8	Homogenized ICR	3.8891	9.87831	---	0.5000
9	Scatter Ring	3.9051	9.91895		

C.7. Axial Blanket Unit Cell

The unit cell for the axial blanket is illustrated in Fig. II.13. The following indicates the cell characteristics.

Hex. Pitch = 1.175 in

Region				
1	Natural U metal	1.125	2.8575	0.8314
2	Aluminum	1.175	2.9845	0.7554
3	100% H_2O	1.234	3.1344	0.09336
4	Scatter Ring	1.250	3.1750	---

Axial Buckling = 224.76 m^{-2}

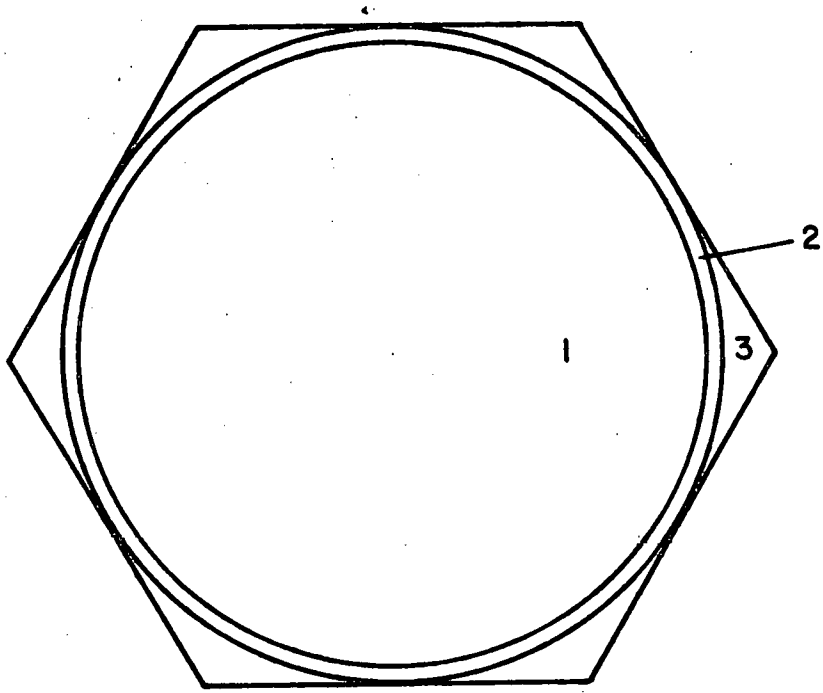

Figure II.15: Axial blanket unit cell. Regions 1 to 3 are the natural uranium metal, Al clad and water, respectively.

C.8. Calculation of Cross Sections for Transition Regions

The set of cross sections for the four converter boundary regions were calculated using the HAMMER code. In order to determine group constants which would give the best characteristics of the system and also the best estimation of the actual cross sections, several strategies were considered for the wet case. The models are described with the aid of Fig. II.14:

Model A: The unit cell of the inner (outer) converter as the central region is surrounded by a ring describing the boundary region and another ring consisting of the stainless steel wall. Determination of the dimensions of this modified unit cell was dictated by the conservation of the proportionality of the region volumes.

Model B and Model E: The unit cell of the inner (outer) converter as the central region is surrounded by a ring describing the boundary region mixed with the stainless steel wall (configuration B in Fig. II.14) or surrounded by water (configuration E).

Model C: The unit cell input for HAMMER was based on Fig. II.3 with inner and outer converter mid-planes as boundaries.

Model D: Use of the unit cell of the inner (outer) converter as the central region surrounded by several rings described by:

1. Ring of water in the inner (outer) converter
2. Ring of stainless steel (wall)
3. Ring of water in the outer (inner) converter
4. Ring of the unit cell of the outer (inner) converter:

The results of the cross section calculations were compared and those of configuration D were assumed to be the best values because they represent the actual physical characteristics in more detail and also give the most conservative values for the group constants, i.e., lowest value of absorption in the thermal energy group. Therefore, the group constants for the additional regions with maximum boron in both converters were calculated using only configuration D.

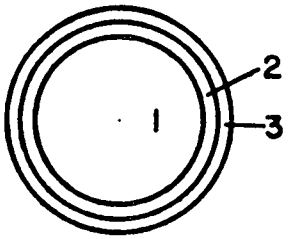

Model A

1-unit cell
2-H_2O
3-SS

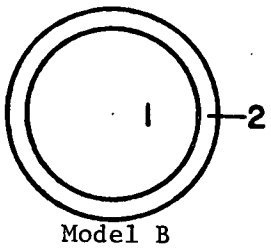

Model B

1-unit cell
2-H_2O + SS mixed

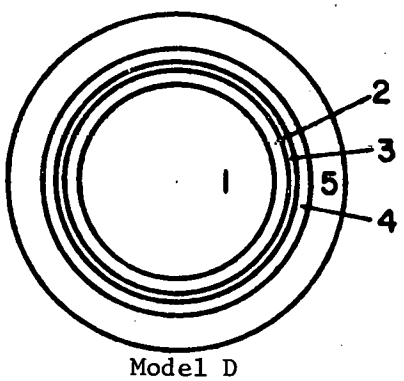

Model D

1-OC unit cell
2-H_2O
3-SS
4-H_2O
5-IC unit cell

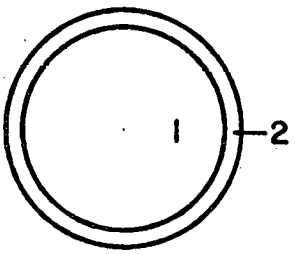

Model E

1-unit cell (IC)
2-water

Figure II.16: Unit cells for group constant calculation of the converter boundary regions.

C.9. Treatment of Non-Unit Cell Regions

The cross-sections of the IC, OC, Blanket, and Axial Blanket were obtained from unit cell descriptions using the HAMMER code. Calculation of group constants for other regions is not directly applicable to the HAMMER code cell type procedure. The cross-sections of the reflector, steel base, concrete, and lead cap regions were obtained by a flux weighting procedure based on the blanket flux as weighting function. The group constants for the converter pin ends were obtained by flux-volume weighting the respective converter unit cells with the fuel eliminated. The cross sections of the source unit cell were obtained by flux-volume weighting with the homogenized IC left out (comp. Sec. C.4). It is assumed that the source drive rod region has the same cross-sections as the source region since the geometry and materials are almost identical. The cross-sections of the water below the source were obtained by flux-volume weighting in the same way as for the source with water cross-sections used in regions where the water replaces the source.

D. Material Number Densities

The HAMMER high energy library does not contain sodium. Aluminum was chosen to replace sodium because of there similar scattering properties. The number density of the Al was chosen to conserve the slowing down of the Na, i.e.,

$$(\xi\Sigma_s)_{Al} = (\xi\Sigma_s)_{Na} \quad .$$

Values of ξ and σ_s were obtained from the group constant set of Ref. 3, and the average values of $\xi\Sigma_s$ was conserved over the energy range from 6.5 MeV to 0.465 ev. It was found that the Al number density required for this conservation was 4.331 times that of the Na. The neutron capture in both Na and Al is negligible and has therefore minimual impact on the substitution. Similary, the library does not have Pb. Zr was selected to replace Pb on the same basis that Al was chosen to replace Na. In case of flooding the spectrum of the FBBF will be rather thermalized, therefore the slowing down powers of both elements should be matched over a large portion of the spectrum. The adjustment of the Zr density to yield the same slowing down power as the Pb has been performed over the energy range 0.2 keV to thermal. It was found that the Zr number density required to conserve the slowing down power was 0.80 that of Pb.

The following indicates number densities of the materials used in the safety calculations. Reference 4 supplied many of the numbers for the evaluation of air and steel.

$\underline{UO_2}$ 4.8% enriched

ρ = 10.96 g/cc

ρ = (94% theoretical density) = 10.3024 g/cc

MW = 270.03

N(U-235) = 1.10301×10^{-3} (1/barn-cm)

N(U-238) = 2.18764×10^{-2} (1/barn-cm)

N(O-16) = 4.59589×10^{-2} (1/barn-cm)

Air $\rho(20°c) \approx 0.0012$ g/ml ≈ 0.0012 g/cc

	Volume Fractions	$\rho x 10^{-3}$ g/cc	MW
O_2	20.945%	1.429	31.998
N_2	78.084%	1.2506	28.0135
CO_2	0.033%	1.977	44.01
Ar	0.934%	1.784	39.948

Trace Elements

	ppm by vol.
Ne	18.18
He	5.25
Kr	1.14
Xe	0.087
H_2	0.5
CH_4	2
N_2O	0.5

	N(/barn-cm)	σ_a(b)	ξ	σ_s(b)	$\Sigma_a(cm^{-1})$	$\Sigma_s(cm^{-1})$	$\xi\Sigma_s(cm^{-1})$
O	1.129×10^{-5}	20×10^{-5}	0.120	4.2	2.258×10^{-9}	4.742×10^{-5}	5.690×10^{-6}
N	4.199×10^{-5}	1.88	0.136	10	7.894×10^{-5}	4.199×10^{-4}	5.711×10^{-5}
C	8.929×10^{-9}	0.004	0.158	4.8	3.572×10^{-11}	4.286×10^{-8}	6.772×10^{-9}
Ar	2.512×10^{-7}	0.66	0.0492	1.5	1.658×10^{-7}	3.768×10^{-7}	1.854×10^{-8}
					7.911×10^{-5}	4.677×10^{-4}	6.283×10^{-5}

Equivalent O-16 for $\xi\Sigma_s = 6.283 \times 10^{-5}$

$N(O\text{-}16) = 1.247 \times 10^{-4}$/barn cm

SS-316 and SS-304

Chemical Composition percent

Type	C Max	Mn Max	P Max	S Max	Si Max	Cr	Ni	Mo	Fe
304	0.08	2.00	0.045	0.030	1.00	18/20	8/12	--	rest
316	0.08	2.00	0.045	0.030	1.00	16/18	10/14	2/3	rest

	σ_a	σ_s	ξ	$\xi\sigma_s$
Cr	3.1	3	0.0385	0.116
Ni	4.6	17.5	0.0335	0.586
Mo	2.70	7	0.0640	0.448
Fe	2.62	11	0.0848	0.933

ρ(SS-316) = 7.75 g/cm^3
MW(SS-316) = 56.53
N(SS-316) = 8.259 x10^{-4} /barn-cm

ρ(SS-304) = 7.75 g/cm^3
MW(SS-304) = 55.39
N(SS-304) = 8.430 x10^{-4} /barn-cm

H_2O

ρ = 1.0 g/cc at 20°c, 40% of moderator by volume.
equiv. ρ = 0.4 g/cc (cc of mod), MW = 18.01534

B_4C

60% of moderator by volume
ρ = 2.52 g/cc MW = 55.26
Equiv. ρ = (0.6)(2.52) = 1.512 g/cc (cc of mod)
N(B) = 0.06592 /barn-cm
N(C) = 0.01648

Na

ρ = 0.97 g/cc MW - 22.9898
approximated by Al
N(N_a) = 0.02541 /barn-cm
Equiv. N(Al) = 0.1101

Concrete - normal

Element	Elemental density (g/cm^3)	MW
H	0.02	1.00797
C	0.118	12.01115
O	1.116	15.9994
Na*	0.011	22.9898
Fe	0.026	55.847
Al	0.085	26.9815
Mg*	0.057	24.312
Ca*	0.58	40.08
Si*	0.34	28.086
K*	0.004	
S*	0.007	
	ρ_{total} = 2.368 g/cm^3	

*not available for HAMMER

Concrete - normal cont.

1) Ignore trace elements K and S
2) Substitute equivalent amount of Al for Na
   from earlier $N^{Al} = 4.331\ N^{Na}$
3) Substitute equivalent amount of C for Mg, Ca, and Si

Isotope	ξ	σ_s	σ_a	N(1/barn-cm)	$\xi\Sigma_s$	Σ_a
H	1.0	17	0.33	0.01195	0.20316	0.0039437
C	0.158	4.8	0.004	0.0059171	4.4875×10^{-3}	2.3669×10^{-5}
O	0.120	4.2	0.00020	0.042012	2.1174×10^{-2}	8.4024×10^{-6}
Na	0.0845	4	0.525	2.8818×10^{-4}	9.7406×10^{-5}	1.5130×10^{-4}
Fe	0.0353	11	2.62	2.8041×10^{-4}	8.4354×10^{-4}	7.3466×10^{-4}
Al	0.0723	1.4	0.241	1.8974×10^{-3}	1.9206×10^{-4}	4.5728×10^{-4}
Mg	0.0811	3.6	0.069	1.4121×10^{-3}	4.1228×10^{-4}	9.7435×10^{-5}
Ca	0.0492	3.0	0.44	8.7159×10^{-3}	1.2865×10^{-3}	3.8350×10^{-3}
Si	0.0698	1.7	0.16	7.2912×10^{-3}	8.6518×10^{-4}	1.1666×10^{-3}

Reflector Material

SS 304 spheres 60%, with containers 66%
NaCl crystals 40%, with containers 34%

ρ(SS-304) = 7.92 g/cm^3 Equiv. ρ(SS-304) = 5.2272 g/cm^3
N(SS-304) = 0.0854702 /barn-cm
MW(NaCl) = 58.44
ρ(NaCl) = 2.165 g/cm^3 Equiv. ρ(NaCl) = 0.7361 g/cm^3
N(Na) = 0.0075865/barn-cm N(Cl) = 0.0075865/barn-cm
replace Na by equiv. Al N(Al) = 4.331 N(Na)

Axial Blanket

Solid Pb
MW = 207.19
ρ = 11.3437 g/cm^3
N(Pb) = 0.0329761/barn-cm

III. SAFETY OF PARTIAL LOADINGS

Safety of any loading sequence is primarily concerned with the hypothetical flooding accident. Also of importance is the safety of the converters during initial assembly since there is a span of time that they will not be within the facility. Values of k_{eff} for normal operation are also desirable.

Procedure for evaluating k_{eff} of the hypothetical flooding accident involve determination of the group constants from cell calculations for each of the distinct regions, and mockup of the facility. HAMMER and 2DB were used to evaluate the group constants and mockup the facility, respectively. Description of the unit cells and the two-dimensional mockup are given in Section II.

In Table III.1 the value of k_{eff} is shown for the individual converters and both of them together. These values represent an upper bound since no boron was assumed to be in either converter. It was also assumed that 35 cm of water surrounded the converters. The values of k_{eff} indicate subcriticality well below the limits specified by the first license value of 0.75.

Table III.2 illustrates values for k_{eff} of a partially loaded facility. It was assumed that 35 cm of water was on the top and sides and that the converters contained the maximum boron. The tabulated values for k_{eff} are proportional to the blanket thickness and well below the limit specified by the license. The results of Table III.2 are substantially lower than those of Table III.1 because of the boron.

It is of interest to know the values of k_{eff} for the normal facility. These calculations were based on the one-dimensional description given in Ref. 5. LAZARUS[6] was used to calculate k_{eff} for all cases. Table III.3 illustrates values of k_{eff} for the converters with the maximum boron content. Since LAZARUS is a diffusion theory computer code, aluminum was assumed to be placed in the

TABLE III.1

Values of k_{eff} for Flooded Converters Without Boron

	k_{eff}
Inner Converter	0.6821
Outer Converter	0.4310
Both Converters	0.6989

TABLE III.2

Values of k_{eff} for Flooded Partial Blanket Loadings

	k_{eff}
Full Blanket	0.4535
Half Blanket	0.4469
No Blanket	0.3727

TABLE III.3

Values of k_{eff} for Converter Regions

	k_{eff}
Inner Converter	0.1737
Outer Converter	0.0224
Both Converters	0.2303

TABLE III.4

Values of k_{eff} for Partial Blanket Loadings

	k_{eff}
Full Blanket	0.3194
Half Blanket	0.2876
No Blanket	0.2285

central region which is physically occupied by air. Thus, the reported values of k_{eff} should be conservative. In Table III.4, values for k_{eff} of partial blanket loadings are given. Again as was seen for the flooded case, as the blanket thickness increases, k_{eff} becomes larger and below the 0.45 normal licensed operating value of k_{eff}.

IV. SAFETY EVALUATION OF EXTREME ADVANCED LOADING CONFIGURATIONS

A. Introduction

For advanced FBBF blanket loadings, some of the natural-uranium rods in the radial blanket are replaced by 4.8% and 1.3% enriched fuel. A large variety of different configurations can be obtained by combining the available 6060 rods of natural UO_2, 2845 rods of 1.3% enriched UO_2 and 1510 rods of 4.8% enriched UO_2.[1] The purpose of this investigation was to:

1. study the upper range of configurations for advanced blanket loadings;
2. perform the hypothetical flooding accident criticality calculation for all selected configurations, and analyze the impact of different boron concentrations in the converters; and
3. derive safety-related design improvements.

The HAMMER and 2DB computer codes have been used in this study for the cell calculations and the criticality evaluations, respectively.

It is emphasized that the configurations presented in this section are extreme and that experimental loadings will not be experimentally investigated. The study was primarily carried out in order to investigate possible design improvements related to the safety of the FBBF.

B. Criticality Evaluation

B.1. Selection of a Suitable Range of Configurations for the Radial Blanket

The precise configurations of advanced FBBF loadings have not been defined. In accordance with this, a very conservative choice for the range of configurations

---

[1] There are 2300 rods of 4.8% enriched fuel; 790 of them are used in the converter regions (592 in the Inner Converter and 198 in the Outer Converter). The remaining 1510 rods are available for advanced blanket loadings.

to be evaluated in this study has been made. The most extreme configuration has been assumed in which all of the available uranium-enriched fuel is loaded into the radial blanket replacing some of the natural uranium fuel. For this purpose, the blanket is subdivided into three regions, as shown in Fig. IV.1, which contain the 4.8%, the 1.3% and the natural uranium fuel respectively. The number density of UO_2 in each region is constrained to be identical and the total blanket thickness is specified to be 51 cm. Therefore, since the rod diameter is different for each of the three enrichments, the pitch in each region is not the same and the region thickness will vary. By changing the pitch of the rods in the regions, a wide range of different configurations have been studied. Starting from the driest possible configuration (comp. Sec. B.2), the pitch of each region has been progressively increased at the expense of the number of rods in the natural uranium region. As the pitch of the rods in each region increases, the reactivity of the hypothetical flooded facility also increases until a trade-off between moderation and absorption is reached. Beyond this point (reactivity maximum), any further increase of the water content yields a reduction in k_{eff}.

B.2. Search for the Most Critical Configuration

The search for the most critical configuration has been performed by evaluating a series of different radial-blanket-region thicknesses within the following boundaries:

1) Lower Boundary. The driest configuration corresponds to the minimum possible pitch of the 1.3% enriched-fuel region because they have the smallest diameter (comp. Table IV.1).
2) Upper Boundary. The wettest configuration is defined when the natural uranium region has been eliminated. A further increase of the pitch beyond this point would require a reduction of the number of loaded enriched-fuel rods.

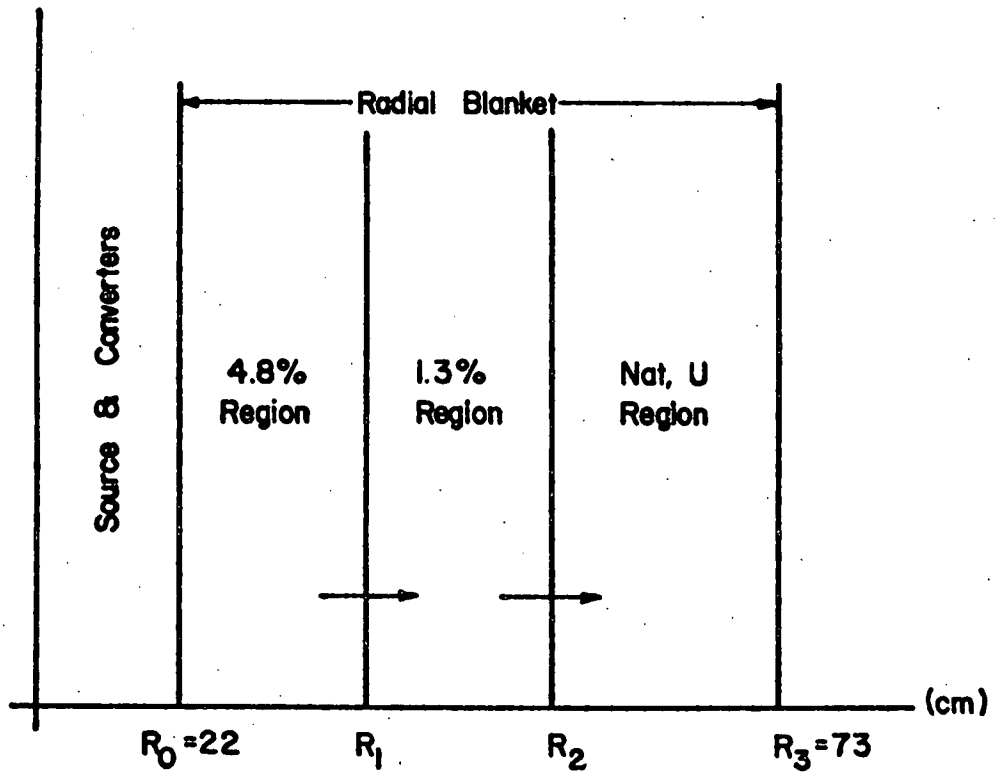

Figure IV.1: Radial blanket regions for advanced loading design.

Condition 1: Fuel Description

The dimensions of the three different types of fuel pins have been taken from Fig. IV.2 and Table IV.1.

Condition 2: Region Pitch

The pitch for each of the three regions has been calculated for each configuration by first choosing a pitch for the 1.3% enriched-fuel region and then constraining the smeared uranium number density to be the same in all three regions. The initial case is for a pitch with a minimum water content in the radial blanket. This corresponds to a situation in which the 1.3% enriched fuel rods are touching each other.

The set of equations used to determine the pitches are given below.

$$p_2 = \text{chosen value} \quad ,$$

$$N_1 = N_2 \rightarrow 0.02299 \left(\frac{0.5334}{0.5250}\right)^2 \frac{1}{p_1^2} = 0.022981 \left(\frac{0.4864}{0.5250}\right)^2 \frac{1}{p_2^2} \, ,$$

$$N_3 = N_2 \rightarrow 0.02298 \left(\frac{0.6934}{0.5250}\right)^2 \frac{1}{p_3^2} = N_2 \quad .$$

These relations can be simplified into the following:

$$N_2 = 0.019726 \frac{1}{p_2^2} \quad ,$$

$$p_1 = 0.15405 \frac{1}{\sqrt{N_2}} \quad ,$$

$$p_3 = 0.2002 \frac{1}{\sqrt{N_2}} \quad ,$$

where:

The index i = 1, 4.8% enriched fuel region

= 2, 1.3% enriched fuel region

= 3, natural uranium region

p = Pitch of the triangular lattice (in cm)

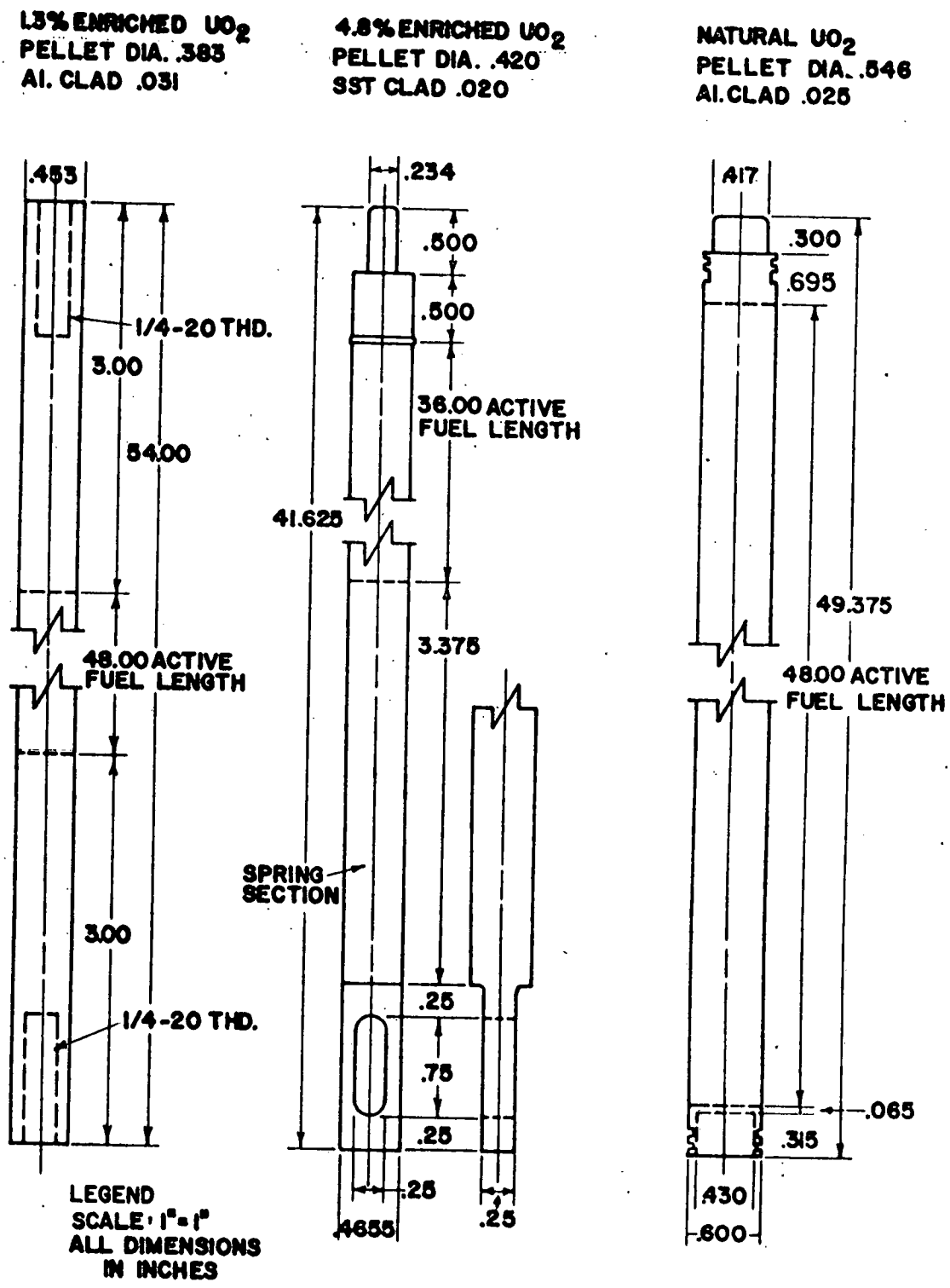

Figure IV.2: FBBF fuel pins.

TABLE IV.1

Fuel Pin Dimensions

	Natural Uranium	1.3%	4.8%
Pellet Diameter	0.546"?	0.383"	0.4200"
Clad	Al	Al	348 St.St.
Clad OD	0.600"	0.453"	0.466"
Active length	48"	48"	36"
Overall length	49 3/8"	54"	41 5/8"
Bottom hardware	0.681"	3"	1"
Top hardware	0.990"	3"	4 5/8"
Approx. Wt.	4 3/4 lbs.	3 lbs.	2 1/3 lbs.
Est. Clad ID	0.550"	0.391"	0.426"
Clad Thickness	0.025"	0.031"	0.020"
Clad Area	0.04516 in^2	0.04110 in^2	0.02802 in^2
Gap Area	0.00344 in^2	0.00486 in^2	0.00399 in^2
Fuel Area	0.23414 in^2	0.11520 in^2	0.13854 in^2
Total	0.2827 in^2	0.16117 in^2	0.17055
Clad VF	0.160	0.255	0.164
Gap VF	0.012	0.030	0.023
Fuel VF	0.828	0.715	0.812

N = Uranium density (in atoms U/barn cm)

The cell uranium density for each region is calculated according to:

$$N_i = N_i^{Fuel} \left(\frac{\text{Volume Fuel}}{\text{Volume Cell}} \right)_i$$

Condition 3: Region Boundary

A radial blanket thickness of 51 cm. and the number of enriched-fuel rods loaded into it, has been maintained in all configurations studied. Therefore, any increase in the pitches of each region, has been done at the expense of the radii R_1 and R_2 (comp. Fig. IV.1) and the consequent reduction in the number of natural uranium rods. The wettest configuration studied corresponds to the case in which the natural uranium region has vanished. The radii R_1 and R_2 are calculated with the following expression:

$$A_i = n_i A_{cell}^i = n_i \pi r_{cell}^{i\,2} = n_i \pi (0.525 p_i)^2 \quad ,$$

where

i = 1 4.8% region

= 2 1.3% region

n_i = Number of rods available for the region

n_1 = 1510 rods

n_2 = 2845 rods

A_{cell}^i = Area of the equivalent circularized cell

r_{cell}^i = Radius of the equivalent circularized cell

p_i = Pitch of the triangular lattice

The above equation does not account for irregular boundaries nor the intermingling of different fuel rods between the regions. The neglect of these boundary effects yields an underestimated value for R_1 and R_2 which will cause

the regions to be slightly undermoderated. Nevertheless this error has been neglected in this preliminary study because the nature of the configuration selected is conservative enough to compensate for such underestimates.

Constraint 1: Minimum Thickness of the Natural Uranium Region

As the radius R_2 increases, the thickness of the natural uranium region tends to be eliminated (comp. Fig. IV.1). A minimum thickness of a circularized natural uranium fuel cell has been imposed for this region.

$$R_3 - R_2 \geq 2r_{3,cell} = 1.05\ p_3 \quad ,$$

where:

R_3 = 73 cm outer radius of the natural uranium region

R_2 = inner radius of the natural uranium region

$r_{3,cell}$ = Radius of the equivalent cell for the natural uranium region

p_3 = Pitch of the triangular lattice in the natural uranium region

Constraint 2: Minimum Number of Natural Uranium Rods

The minimum number of natural uranium rods has been imposed to correspond to the number of rods of a single ring of touching natural uranium equivalent-circular cells

$$n_3 \geq \frac{2\pi R'_2}{2r_{3,cell}} = \frac{2\pi(R_2 + r_{3,cell}}{2r_{3,cell}} = \pi\left(1 + 1.9048\ \frac{R_2}{P_3}\right) \quad ,$$

where

$$R'_2 = R_2 + r_{3,cell}$$

B.3. Results of the Criticality Evaluation

The results of the criticality evaluation for the FBBF-advanced loading configurations considered in this section using different boron concentrations in the converters are presented in Table IV.2. The most reactive configuration is the

TABLE IV.2

Flooded criticality evaluation for the most extreme hypothetical advanced blanket loadings*

RADIAL BLANKET							k_{eff}			
Case	4.8% Region		1.3% Region		Natural Uranium Region		No boron in converters	Both converters with the maximum boron content of the OC(1)	Maximum boron in both converters(2)	Uranium density atu/b.cm. in the zone
	Pitch (cm)	k_∞ (cell)	Pitch (cm)	k_∞ (cell)	Pitch (cm)	k_∞ (cell)				
1	1.2621	1.0461	1.1506	0.6702	1.6403	0.7520	0.8020	0.7407	0.7236	1.4896 E-2
2	1.5958	1.3458	1.4549	1.0964	2.0741	0.9153	1.1202	1.0915	1.0882	9.3191 E-3
3	1.7962	1.4021	1.6376	1.1234	2.3345	0.8951	1.1969	1.1712	1.1685	7.3557 E-3
4	1.9297	1.4164	1.7593	1.1142	2.5080	0.8663	-	1.2004	1.1981	6.3732 E-3
5	1.9965	1.4187	1.8202	1.1053	2.5948	0.8500	-	1.2102	1.2080	5.9539 E-3
6	2.0402	1.4188	1.8601	1.0983	2.6517	0.8387	-	1.2151	1.2131	5.7012 E-3
7	2.1299	1.4151	1.9419	1.0814	-(3)	-	-	1.2211	1.2192	5.2310 E-3
8	2.1512	1.4124	1.9613	1.0769	-	-	-	1.2182	1.2163	5.1260 E-3

(1) Both converters with the maximum boron content of the outer converter (2.74% vol. f. B_4C)

(2) Inner converter with its maximum boron content (6.05% vol. f. B_4C_1) and outer converter with its maximum boron content (2.74% vol. f. B_4C_1).

(3) Means that there is no natural uranium region.

*These loadings will not be experimentally evaluated.

one that corresponds to case 7, which coincides with the upper boundary of the search. To check that this is the absolute maximum, case 8[1] was evaluated. In the opposite direction, the closest permitted point[2] to case 7 is case 6. Between cases 6 and 7 there is an interval of uncertainty in which the absolute maximum might be placed. Nevertheless, since this interval is not physically permitted, the most reactive configuration is considered to be the one corresponding to case 7.

It is seen from Table IV.2, that loading the converters with boron has very little impact on the criticality of the facility, because the 4.8% and the 1.3% enriched region tend to drive the facility. (Comp. k_∞ in Table IV.2). The results of the criticality evaluation performed in this study yield k_{eff} values which are rather high, (comp. Table IV.2). It must be noted that the large values of k_{eff} could have been expected from the nature of the fuel loading selected. Again, it is important to stress that these configurations will not be considered as experimental loadings but they are needed to obtain information about safety related design requirements for more realistic advanced loadings.

C. Design Improvements

The loading configurations investigated in this study can be improved in terms of safety if an additional thermal neutron absorber which also displaces water is provided in the blanket zones. This could be done by:

1. The use of double-cladded fuel.

   A choice of the material selected for the extra clad and also whether it is more convenient to double-clad only the 4.8% enriched fuel or all the blanket fuel must be made prior to the

[1] Case 8 is a +1% perturbation of the pitches corresponding to case 7. This had to be done at the expense of a 3% reduction in the number of rods of the 1.3% region.

[2] Between cases 6 and 7 the constraints of the natural uranium region described in Sec. B are violated.

explicit consideration of advanced loadings. Economic factors must be taken into account when making a final decision. Here, all possibilities have been examined for the materials: Al, SS and Boron-SS. The results are presented in Table IV.3. It is seen from Table IV.3 that both the 4.8% and 1.3% enriched regions must be double clad in order to obtain a substantially subcritical facility.

2. Combining double-cladded rods with some other neutron absorbing material.

   For cost reasons case 4 (comp. Table IV.3) might become appealing provided that a small amount of additional absorption could be obtained. With this respect the possibility of using thin absorbent annuli at the boundaries of the enrichment zones could be investigated.

3. Replacing some of the fuel-rods (especially the 4.8% enrichment rods) by absorbent rods which in the case of flooding would act in the same way as the control rods in LWRs.

4. Inserting rods of Boron-SS, SS or Al between the fuel rods in each enrichment region, causing water to be displaced and undermoderating the region. B-SS and SS have an added advantage of absorbing neutrons.

In making the decision on the type of extra-absorption to be added to the advanced loading design, one must be very careful in evaluating the heterogeneity effects introduced, which later on might contaminate the results of the experiments performed on the FBBF.

TABLE IV.3

Impact of using double claddings of the fuel in the radial blanket regions.

Case	Design Characteristics	4.8% Region		1.3% Region		Nat. U Region Pitch (cm)	FBBF k_{eff}	FBBF k_{eff} corresponds to the same Nu of the radial blanket but without the double clad.
		k_{∞} (cell)	Pitch (cm)	k_{∞} (cell)	Pitch (cm)			
1	Double Al clad for all fuel. Case with minimum water content. (Fuel rods of the 1.3% region touching each other).	1.3724	1.8714	1.0806	1.7062	2.4323	1.1235	1.1898
2	Same as CASE 1 but with SS304 double clad.	1.1748	1.8714	0.7354	1.7062	2.4323	0.9509	1.1898
3	Same as CASE 1 but with the maximum water content possible. (The natural uranium region has vanished).	1.4020	2.1299	1.0741	1.9419	-	1.1878	1.2211
4	Same as CASE 3 but with SS304 double clad.	1.1959	2.1299	0.7397	1.9419	-	1.0077	1.2211
5	Same as Case 3. The double clad for the 4.8% region is 1% boron steel and the 1.3% region is not double cladded.	0.5076	2.1299	1.0814	1.9419	-	0.8654	1.2211
6	Same as 5 but with Al double clad for the 1.3% region.	0.5076	2.1299	1.0741	1.9419	-	0.8270	1.2211
7	Same as 5 but with SS double clad for the 1.3% region.	0.5076	2.1299	0.7397	1.9419	-	0.6043	1.2211

D. Conclusion

The object of the study presented in this section was to initiate evaluation of advance loading configurations and define possible limitations of the types of experiments which could be safely preformed with the FBBF. Future studies, which were based on configurations suggested above, i.e., insertion of rods of stainless steel or aluminum between the fuel pins, are presented in a subsequent section (comp. Sec. V).

Again, it is emphasized that the results presented in this section were necessary for scoping safety studies of advanced loadings and that they are not proposed configurations.

V. INVESTIGATION OF 360° LOADINGS

A. Introduction

Safety of any loading sequence is primarily associated with the hypothetical flooding accident. The safety investigations for the initial loading and advance loading sequences can be described in two parts: changes in k_{eff} due to pitch variations, etc. and the safety of a designated loading configuration. The investigations present in this section have been devised in such a way that both types of safety investigations are simultaneously evaluated.

The procedure for evaluating k_{eff} of hypothetical flooding accident involves determination of the group constants for each distinct region and mock-up of the facility. HAMMER and 2DB were used to evaluate the group constants and mock-up the facility, respectively.

The safety analysis of four configurations are presented. They are blanket loadings with:

1. single clad natural UO_2 pins,
2. double clad natural UO_2 pins,
3. initial blanket configurations
4. advanced blanket loadings based on a combination of:
   a. stainless steel secondary rods with 4.8% enriched pins,
   b. stainless steel secondary rods with 1.3% enriched pins,
   c. natural uranium UO_2 pins.

B. Single Clad Natural Uranium Blanket

The single clad blanket consists of natural UO_2 fuel with aluminum clad. The unit cell description used as input to HAMMER is given in Sec. II.C.3. The geometrical model of the FBBF used for the two-dimensional k_{eff} calculations is shown in Fig. II.3 with a material description given in Table II.3.

The hexagonal pitch of the fuel pins was varied from 1.524 cm where the cladding of adjacent pins just touch, to a large pitch of 6.35 cm. Results of this investigation are illustrated in Fig. V.1 and in Table V.1.

The k_{eff} of the facility follows the same trends as the blanket k_{∞} as the pitch is increased. The blanket region strongly influences the value of k_{eff} up to about a 4.5 cm pitch. For a pitch greater than 4.5 cm, the contribution of the blanket to k_{eff} is negligible and the facility effective multiplication is determined by the converter regions. The k_{eff} of the flooded FBBF with a single clad blanket reaches a maximum of 0.813 for a pitch of about 2.1 cm.

C. Double Clad Natural Uranium Blanket

The double clad blanket consists of the same aluminum clad natural UO_2 pins as the single clad blanket. A secondary clad of either stainless steel or aluminum tubing is placed around the fuel pins. The secondary cladding tubes have an ID of 1.5291 cm and an OD of 1.6967 cm. The unit cell description used as input to HAMMER is given in Sec. II.C.4. The 2DB geometrical model is identical to that of the single clad blanket case, (comp. Sec. II.B).

The hexagonal pitch of the double clad fuel pins was varied from the minimum of 1.6967 cm where the secondary cladding of adjacent pins just touch to a pitch of 6.35 cm. The results of this investigation are shown in Figs. V.2 and V.3 and Tables V.2 and V.3 for aluminum and stainless steel, respectively.

As in the case of the single clad blanket, the k_{eff} of the FBBF follows the k_{∞} of the blanket. The blanket region influences k_{eff} up to about a 5 cm pitch with Al as secondary cladding and up to about a 4 cm pitch with stainless steel as secondary cladding. For a pitch greater than these values, the converters cause the value of k_{eff} to level off while the blanket k_{∞} continues to decrease.

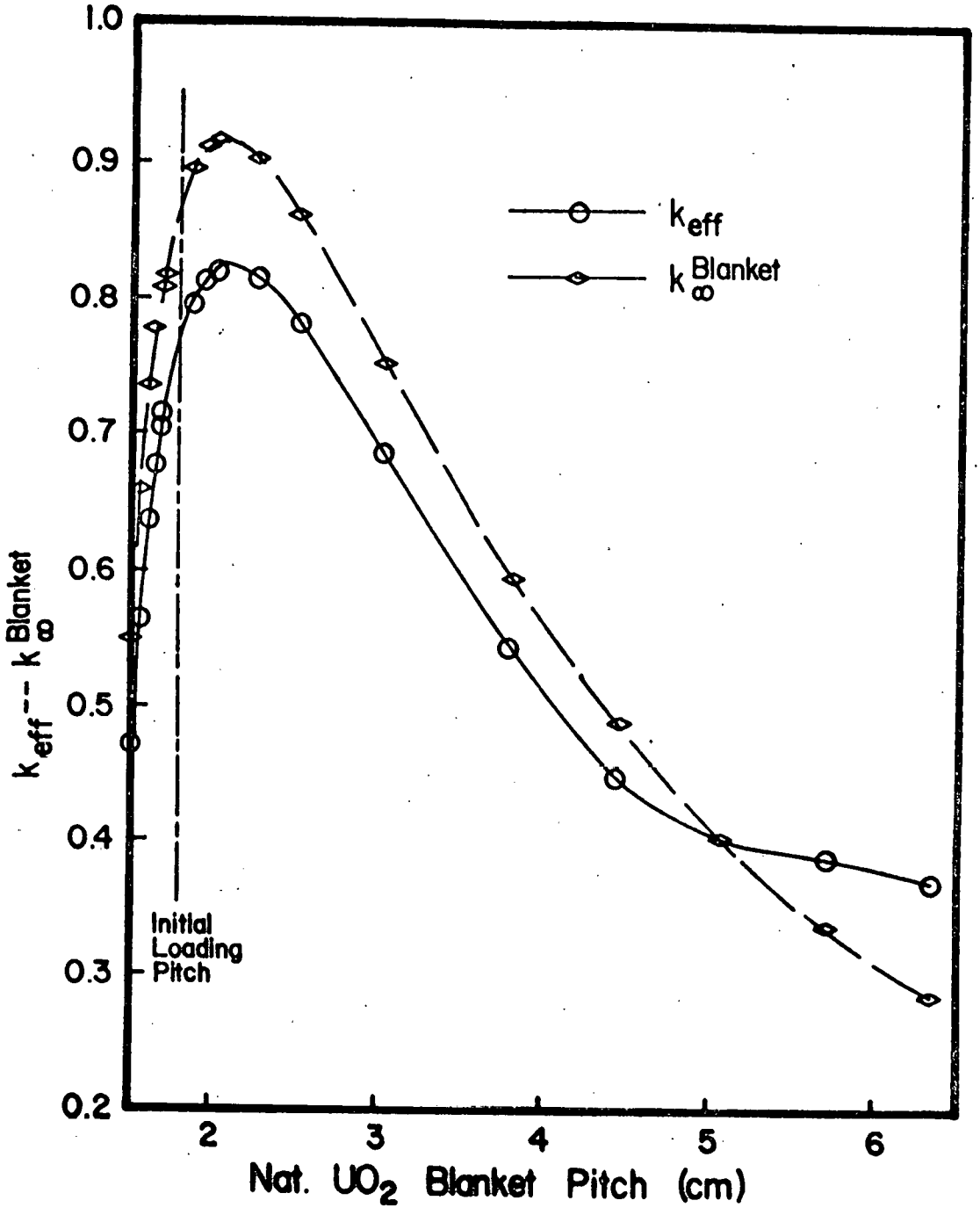

Figure V.1: FBBF safety study single clad blanket.

TABLE V.1

Single Clad Blanket Results

Pitch (in)	Pitch (cm)	Number Density atoms/barn-cm	Blanket k_∞	k_{eff}
0.600	1.524	0.0172581	0.55005	0.46919
0.620	1.575	0.0161626	0.65884	0.56458
0.640	1.626	0.0151682	0.73496	0.63576
0.655	1.664	0.0144814	0.77737	0.67684
0.668	1.697	0.0139233	0.80669	0.70584
0.673	1.709	0.0137172	0.81647	0.71565
0.740	1.880	0.0113457	0.89382	0.79654
0.770	1.956	0.0104788	0.90799	0.81329
0.800	2.032	0.0097977	0.91439	0.82148
0.900	2.286	0.0076703	0.90127	0.81566
1.000	2.540	0.0062129	0.86045	0.78145
1.200	3.048	0.0043145	0.75314	0.68594
1.500	3.810	0.0027613	0.59478	0.54255
1.750	4.445	0.0020287	0.48680	0.44674
2.000	5.080	0.0015532	0.40109	0.40184
2.250	5.715	0.0012272	0.33646	0.38803
2.500	6.350	0.0009941	0.28357	0.36926

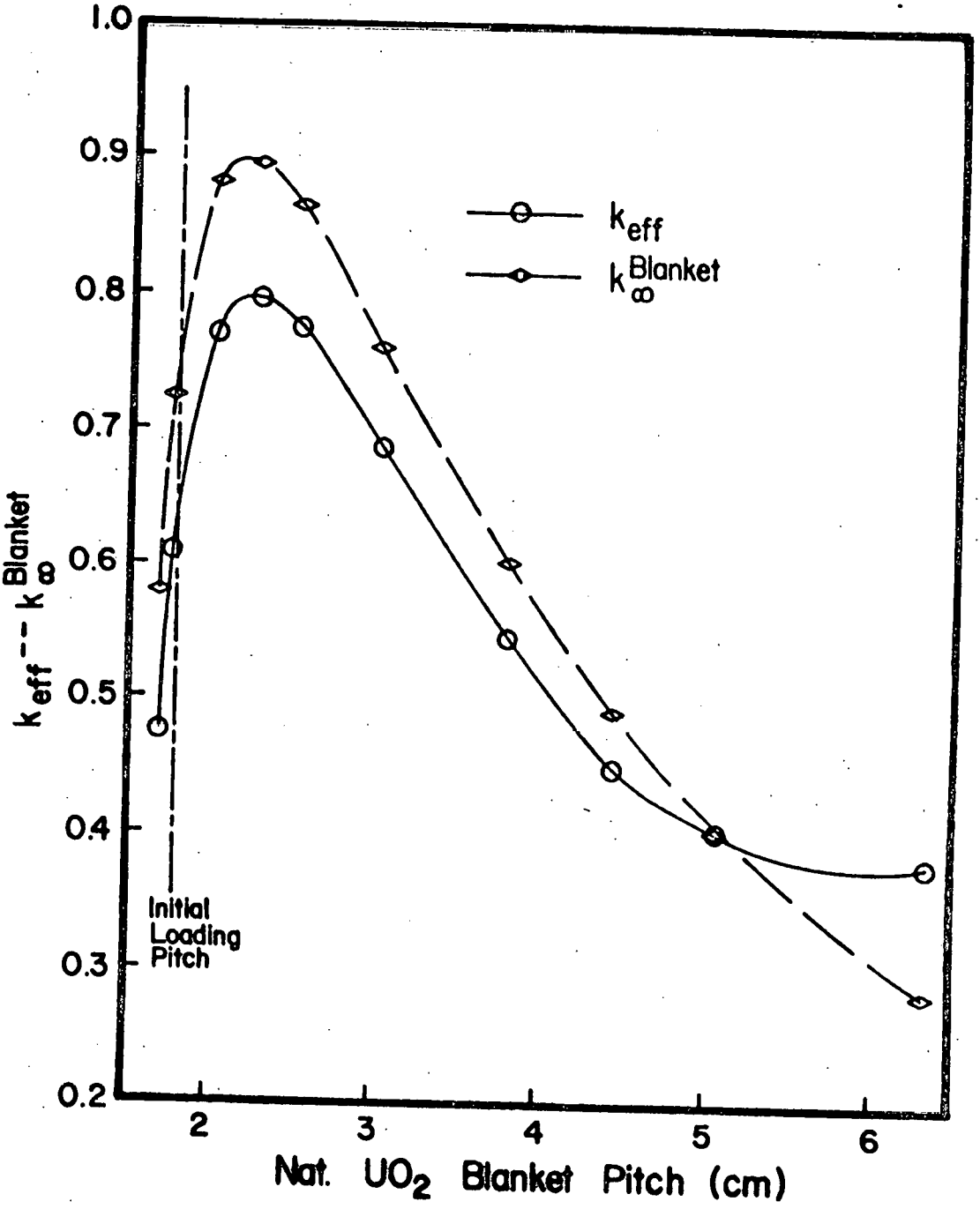

Figure V.2: FBBF safety study Al double clad blanket.

TABLE V.2

Aluminum Double Clad Blanket Results

Pitch (in)	Pitch (cm)	Number Density atoms/barn-cm	Blanket k_{∞}	k_{eff}
0.668	1.697	0.0139233	0.57767	0.47736
0.700	1.778	0.0126799	0.72395	0.60962
0.800	2.032	0.0097077	0.87970	0.77206
0.900	2.286	0.0076703	0.89282	0.79640
1.000	2.540	0.0062129	0.86271	0.77558
1.200	3.048	0.0043145	0.75953	0.68756
1.500	3.810	0.0027613	0.60160	0.54672
1.750	4.445	0.0020287	0.49242	0.45007
2.000	5.080	0.0015532	0.40763	0.40308
2.500	6.350	0.0009941	0.28595	0.38038

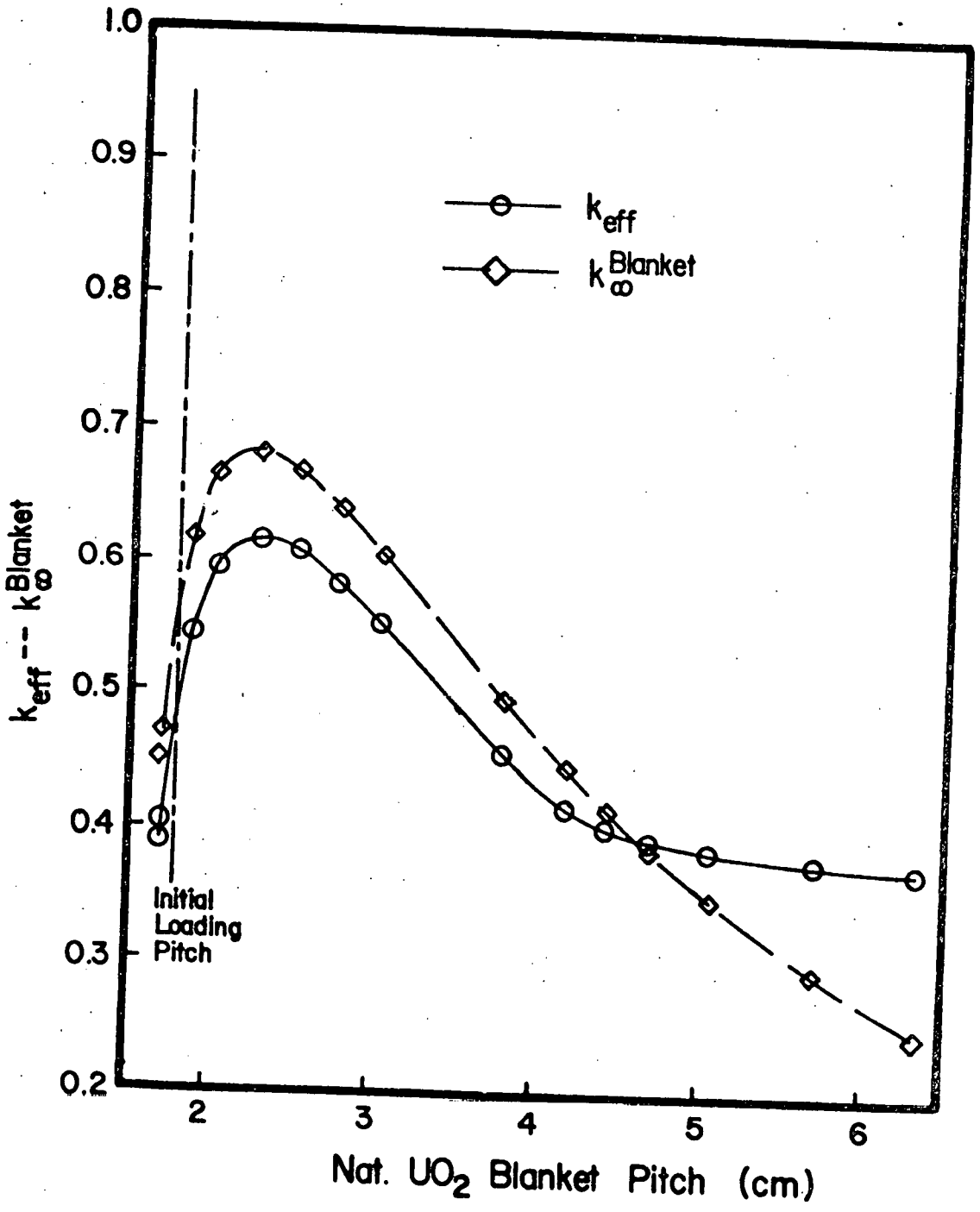

Figure V.3: FBBF safety study SS double clad blanket.

TABLE V.3

Stainless Steel Double Clad Blanket Results

Pitch (in)	Pitch (cm)	Number Density atoms/barn-cm	$k_{\infty}^{Blanket}$	k_{eff}
0.668	1.697	0.0139233	0.45104	0.38952
0.673	1.709	0.0137172	0.47048	0.40499
0.740	1.880	0.0113457	0.61903	0.54410
0.800	2.032	0.0097077	0.66602	0.59406
0.900	2.286	0.0076703	0.68305	0.61679
1.000	2.540	0.0062129	0.66882	0.60750
1.100	2.794	0.0051346	0.64031	0.58338
1.200	3.048	0.0043145	0.60568	0.55234
1.500	3.810	0.0027613	0.49745	0.45609
1.650	4.191	0.0022821	0.44746	0.41714
1.750	4.445	0.0020287	0.41666	0.40297
1.850	4.699	0.0018153	0.38803	0.39509
2.000	5.080	0.0015532	0.35129	0.38606
2.250	5.715	0.0012272	0.29647	0.37953
2.500	6.350	0.0009941	0.25237	0.37462

The k_{eff} of the flooded FBBF with a double clad blanket reaches a maximum of about 0.80 for a pitch of 2.3 cm for aluminum secondary cladding and a maximum of about 0.62 for a pitch of 2.3 cm when stainless steel is the secondary clad. Both types of secondary cladding cause the maxima to be lower and also shift it to a larger pitch when compared to the single clad blanket.

D. Initial Blanket Loading

The initial blanket loading has approximately two thirds of the inner-most natural uranium pins surrounded by stainless steel secondary clad and the outer one-third surrounded by aluminum secondary clad. Two types of safety investigations were preformed for the initial loadings.

The first type of investigation was an evaluation of k_{eff} for the initial blanket pitch with different portions of the blanket loaded. The results of these investigations are given in Table V.4. They indicate that the initial FBBF blanket loading and partial loadings are substantially below the 0.75 k_{eff} limit set by the license. The value of k_{eff} increases as the number of natural uranium pins loaded increases. A full loading has the maximum value of 0.432.

The second type of investigation considered variations of the pitch. The calculations were formulated identical to those presented in the previous subsections for the unclad, aluminum secondary clad and stainless steel secondary clad loadings. The calculational procedure is also identical. In Fig. V.4 and Table V.5, the value of k_{∞} for both the stainless steel and aluminum secondary clad portions and the value of k_{eff} of the FBBF are plotted for different values of the pitch. Since the blanket thickness is constrained to 51 cm, as the pitch is increased from the minumum where adjacent secondary clad tubes touch, the number of aluminum secondary clad pins is reduced. After a pitch of approximately 2.2 cm the number of pins have been reduced significantly enough to eliminate all aluminum secondary clad tubes. The values of k_{eff} from

TABLE V.4

Values of k_{eff} for Flooded Initial Blanket Loadings

	k_{eff}
Full Blanket	0.423
Half Blanket	0.382
No Blanket	0.341

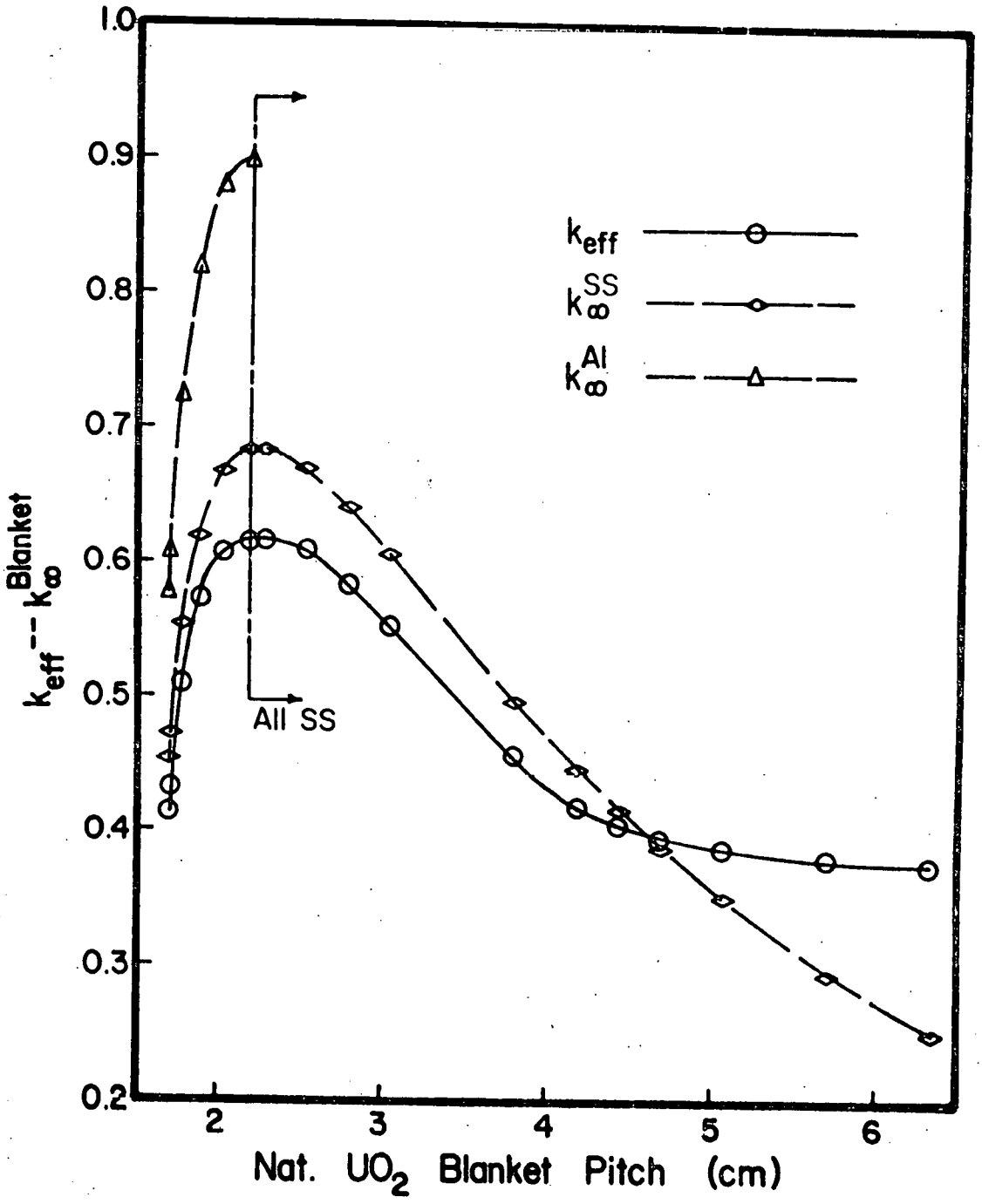

Figure V.4: FBBF safety study initial blanket loading.

TABLE V.5

Initial Blanket Loading Results

Pitch		Number Density	R Interface	k_∞ SS Blanket	k_∞ Al Blanket	k_{eff}
(in)	(cm)	atoms/barn-cm	(cm)			
0.668	1.697	0.0139233	57.1237	0.45104	0.57767	0.41261
0.673	1.709	0.0137172	57.4878	0.46048	0.60706	0.43150
0.700	1.778	0.0126799	59.4610	0.55073	0.72395	0.51021
0.740	1.880	0.0113457	62.4031	0.61903	0.81885	0.57262
0.800	2.032	0.0097077	66.8529	0.66602	0.87970	0.60626
0.862	2.189	0.0083615	71.4893	0.68237	0.89625	0.61525
0.900	2.286	0.0076703	--	0.68305	--	0.61679
1.000	2.540	0.0062129	--	0.66882	--	0.60750
1.100	2.794	0.0051346	--	0.64031	--	0.58338
1.200	3.048	0.0043145	--	0.60568	--	0.55234
1.500	3.810	0.0027613	--	0.69745	--	0.45609
1.650	4.191	0.0022821	--	0.44746	--	0.41714
1.750	4.445	0.0020287	--	0.41666	--	0.40297
1.850	4.699	0.0018153	--	0.38803	--	0.39509
2.000	5.080	0.0015532	--	0.35129	--	0.38606
2.250	5.715	0.0012272	--	0.29647	--	0.37953
2.500	6.350	0.0009941	--	0.25237	--	0.37462

the 2.2 cm pitch to the maximum pitch are identical to those presented in Fig. V.3, which considered stainless steel as secondary clad. Initially the smallest value of k_{eff} corresponds to the smallest pitch. A maximum value of approximately 0.617 is obtained for a pitch of about 2.2 cm. As was also illustrated in the previous subsection, the value of k_{eff} follows the trend of the value of k_{∞} for the stainless steel secondary clad until there is a trade off between moderation and the amount of fuel. This occurs for a pitch of about 4.6 cm. Since the aluminum secondary clad pins are on the outer parameter of the blanket, they do not significantly influence the value of k_{eff}.

E. Advanced Loaded Blanket

For advanced FBBF blanket loadings, some of the natural-uranium rods in the radial blanket are replaced by 4.8% and 1.3% enriched fuel with secondary rods of stainless steel placed between the enriched pins. A large variety of different configurations can be obtained by combining the available 6060 rods of natural UO_2, 2845 rods of 1.3% enriched UO_2 and 1510 rods of 4.8% enriched UO_2. The purpose of this investigation was to select a range of configurations for advanced loadings and perform the hypothetical flooding accident criticality calculation for all selected configurations.

The same conditions and constraints applied in the previous section are again valid for the studies presented in this subsection. The difference between the two investigations is the implementation of absorbing and water displacement rods considered in this study. Therefore, the unit cells are modified slightly as seen in Sec. II.C.5.

The results of the criticality evaluation for the FBBF-advanced-loading configurations are presented in Fig. V.5 and Table V.6. The 4.8% enriched region has the largest value of k_{∞}. As the pitch of the region increases, k_{∞}

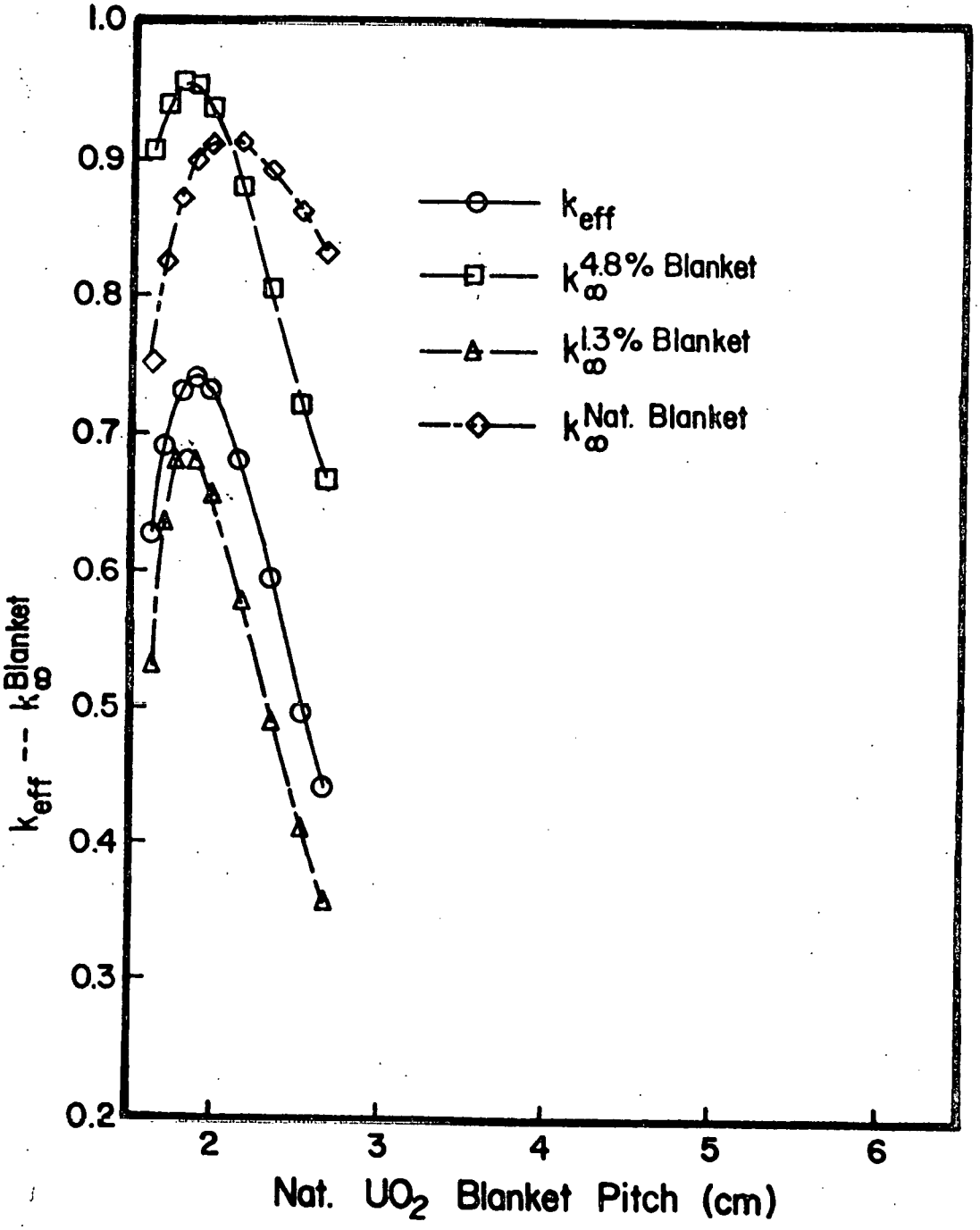

Figure V.5: FBBF safety study advanced blanket.

TABLE V.6

Advanced Loading Blanket Results

Natural Uranium Blanket Region		1.3% Blanket Region			4.8% Blanket Region				
Pitch (cm)	k_∞	Outer Radius (cm)	Pitch (cm)	k_∞	Outer Radius (cm)	Pitch (cm)	k_∞	Number Density atoms/barn-cm	k_{eff}
1.6403	0.75252	46.763	1.1506	0.53066	33.889	1.2620	0.90516	0.0148980	0.62748
1.7199	0.82399	48.539	1.2065	0.63654	34.849	1.3233	0.93993	0.0135500	0.69189
1.8105	0.87180	50.578	1.2700	0.68231	35.961	1.3930	0.95660	0.0122289	0.72983
1.9010	0.89874	52.636	1.3335	0.68169	37.094	1.4626	0.95418	0.0110919	0.74103
1.9915	0.91180	54.712	1.3970	0.65572	38.247	1.5323	0.93828	0.0101065	0.73347
2.1725	0.91184	58.907	1.5240	0.57738	40.603	1.6716	0.87955	0.0084923	0.68191
2.3536	0.89246	63.153	1.6510	0.49031	43.017	1.8108	0.80443	0.0072360	0.59487
2.5346	0.86145	67.438	1.7780	0.41347	45.481	1.9501	0.72261	0.0062392	0.49494
2.6831	0.83239	70.976	1.8821	0.35720	47.534	2.0644	0.66699	0.0055679	0.44031

reaches a maximum of about 0.957 and then continues to decrease due to the increase in stainless steel absorption and reduction of moderation from the water. The value of k_∞ for the natural uranium region has a maximum of about 0.912. It decreases with increased pitch but at a slower rate than the 4.8% enriched region. Since the natural uranium region does not contain any secondary stainless steel rods, moderation is greater and there is no loss of neutrons in a secondary absorber as in the case of the 4.8% enriched region. The values of k_∞ for the 1.3% enriched region are the lowest. Again, this is due to the displacement of water by the secondary stainless steel rods and the additional absorption. The small size of the natural UO_2 region and its location at the outer edge of the blanket cause its contribution to k_{eff} to be less than the 4.8% enriched region. The k_{eff} of the facility reaches a maximum of about 0.741 which corresponds to a natural UO_2 pin pitch of about 1.9 cm. (See Table V.6 for the corresponding pitches of the other regions and the associated UO_2 number density.)

VI. INVESTIGATION OF 180° LOADINGS

Double blanket loadings consist of two 180° sections which have different physical characteristics. For example, one half of the facility could have stainless steel as secondary cladding and the other half could have aluminum. These double loadings enable more experimental information to be generated in a shorter period of time. As indicated in the previous section there is a window for the single clad and aluminum double clad blankets where the value of k_{eff} would be slightly greater than that specified by the license for the initial loading (comp. Figs. V.4, V.5, Tables V.3, V.4). For all pitches the value of k_{eff} for the stainless steel double clad blanket is substantially below the value of 0.75. Thus, based on the reported values for k_{eff} of these three single loadings one would expect that all aluminum and unclad loading pitches with half of the facility consisting of a stainless steel secondary clad loading would have a value of k_{eff} below 0.75. The value of k_{eff} for double loadings intuitively should be between the values of the two single loadings. The intuitive consideration does not hold and is discussed in the following paragraphs.

Physically, a double loading configuration in the FBBF is a three-dimensional problem. Since there is not a three-dimensional computational capability available at Purdue University, a number of two-dimensional calculations are necessary to obtain the desired information about the safety of the double loadings. First, group constants are obtained from HAMMER by the procedure and methods reported previously. Next, two r-z calculations are preformed to determine the value of k_{eff} for each single loading based on the physical description of each half. A buckling search is performed in r-Θ geometry for each physical description with convergence specified by the value of k_{eff} calculated from the initial r-z problem. The value of k_{eff} for a double loading is obtained by mocking up the

the facility in r-Θ geometry and describing the leakage by input buckling values calculated from the previous r-Θ problems.

A number of different ways to describe the leakage of the double loading r-Θ calculations were considered. The bucklings were input as group and zone dependent values, one value for each half, and one average value. The results of this investigation indicated an insensitivity of the leakage to the buckling description indicating that most of the neutrons leak out radially. The calculated value of k_{eff} is also insensitive to the method of inputting the buckling which describes the axial leakage.

Since the basic concern of the safety analysis is to keep k_{eff} as low as possible, the stainless steel double clad half of the facility was first specified with a pitch of 1.88 cm. The value of k_{eff} for a single loading with this pitch and stainless steel as secondary clad is 0.544. Aluminum as secondary cladding was specified in the other half. A pitch of 2.286 cm, which corresponds to the point near the maximum value of k_{eff}, 0.796, of the aluminum double clad single loading, was chosen. Surprisingly, the calculated value of k_{eff} for the double loaded facility is almost the same as a single loaded facility with aluminum as secondary clad. Further investigations were preformed in order to obtain an understanding of this seemingly inconsistent finding. First, the portion of the aluminum loading was reduced from 360° to 0°. Simultaneously, the portion of the facility with stainless steel as secondary clad was increased. The results are shown in Fig. VI.1 and Table VI.1. The value of k_{eff} stays fairly constant and does not start to substantially decrease until the aluminum portion of the facility is less than 15 per cent. These results do not seem to be consistent with the physical understanding of the problem.

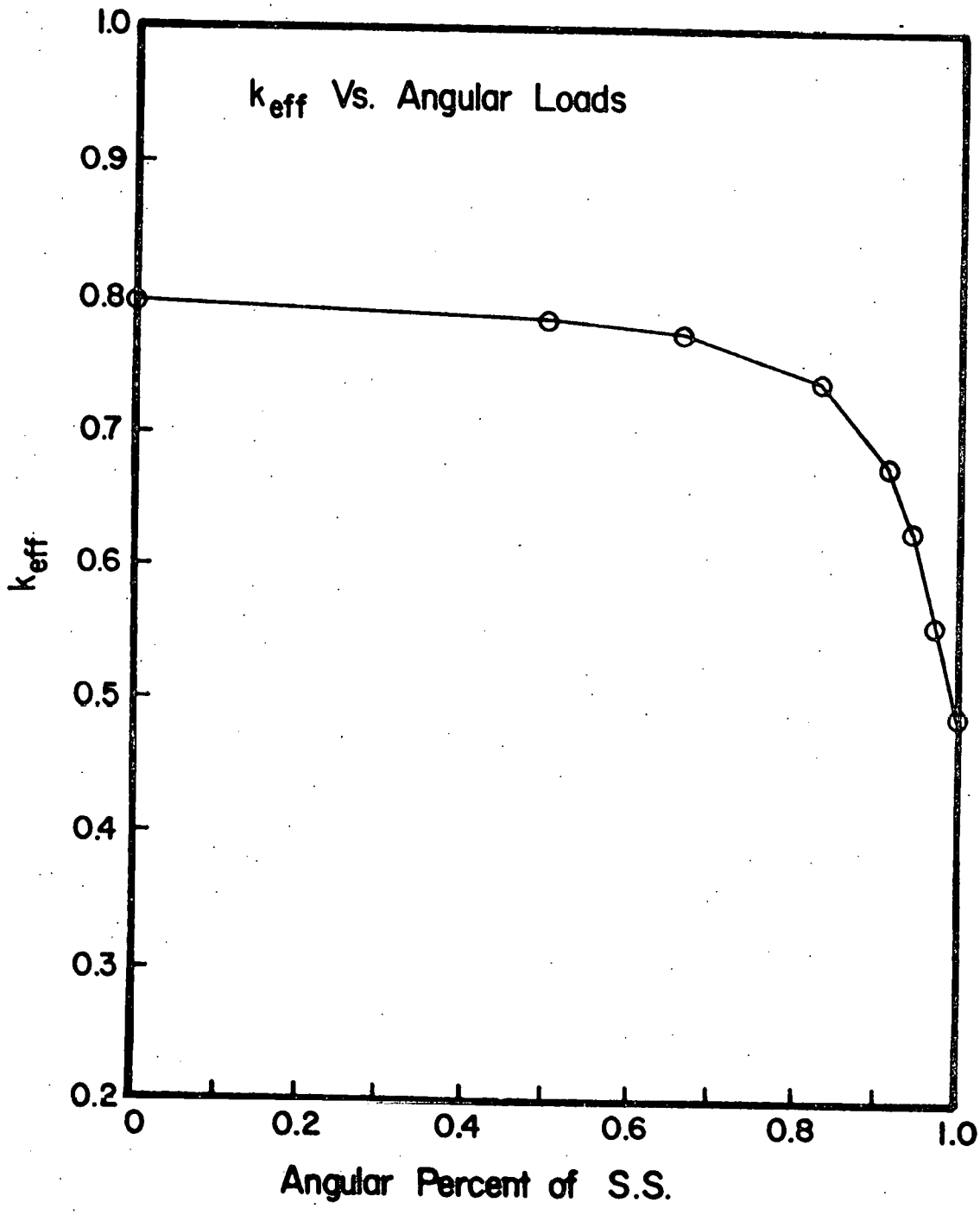

Figure VI.1: Double loading safety investigation, value of k_{eff} vs the angular per cent of stainless steel secondary cladding.

TABLE VI.1

Value of k_{eff} for Various Fractions of Aluminum and Stainless Steel as Secondary Clad.

Fraction of Stainless Steel (pitch = 1.793cm)		Fraction of Aluminum (pitch = 2.286 cm)		k_{eff}
0.0		1.0	(360°)	0.797
1/2	(180°)	1/2	(180°)	0.785
2/3	(240°)	1/3	(120°)	0.774
5/6	(300°)	1/6	(60°)	0.739
11/12	(330°)	1/12	(30°)	0.674
17/18	(340°)	1/18	(20°)	0.629
35/36	(350°)	1/36	(10°)	0.557
1.0	(360°)	0.0		0.489

In order to understand the results presented in the previous paragraph, the problem was slightly modified so that the pitch of each half of the facility was set to 1.709 cm. This constrained the water and uranium content to be the same for each half and removes interpretation difficulties. A value of k_{eff} for this double loading was again essentially the same as the value with only aluminum. The reason for this result can be better understood by investigating Fig. VI.2 which illustrates the log of the normalized flux vs radial position. The flux was normalized to the maximum value of the total flux on the aluminum side. The points cut through the middle of each half of the facility. For all groups the flux is between two and three orders of magnitude higher on the aluminum side when compared to the stainless steel side. The flux shown in Fig. VI.2 is physically not realized since it results from an eigenvalue-problem solution. One would expect a flux difference of three or four times, reflecting the difference of the absorption in each half for a physically realized flux. To check this latter point, the flux solution was determined, based on a source calculation (see Fig. VI.3). The differences of the fluxes for each half of the blanket, given in Fig. VI.3, should be representative of the differences which would be expected in the flooded facility if a source were present, rather than the λ-mode flux differences presented in Fig. VI.2. The difference in the fluxes in each half are not orders of magnitude, as depicted in Fig. VI.2, but rather three to four times greater on the aluminum side as shown in Fig. VI.3. This difference depicted in Fig. VI.3 is what one would expect from physical considerations.

The general calculational procedure to obtain the value of k_{eff} is to artifically modify the balance equation in order to obtain criticality, i.e., in one-group notation:

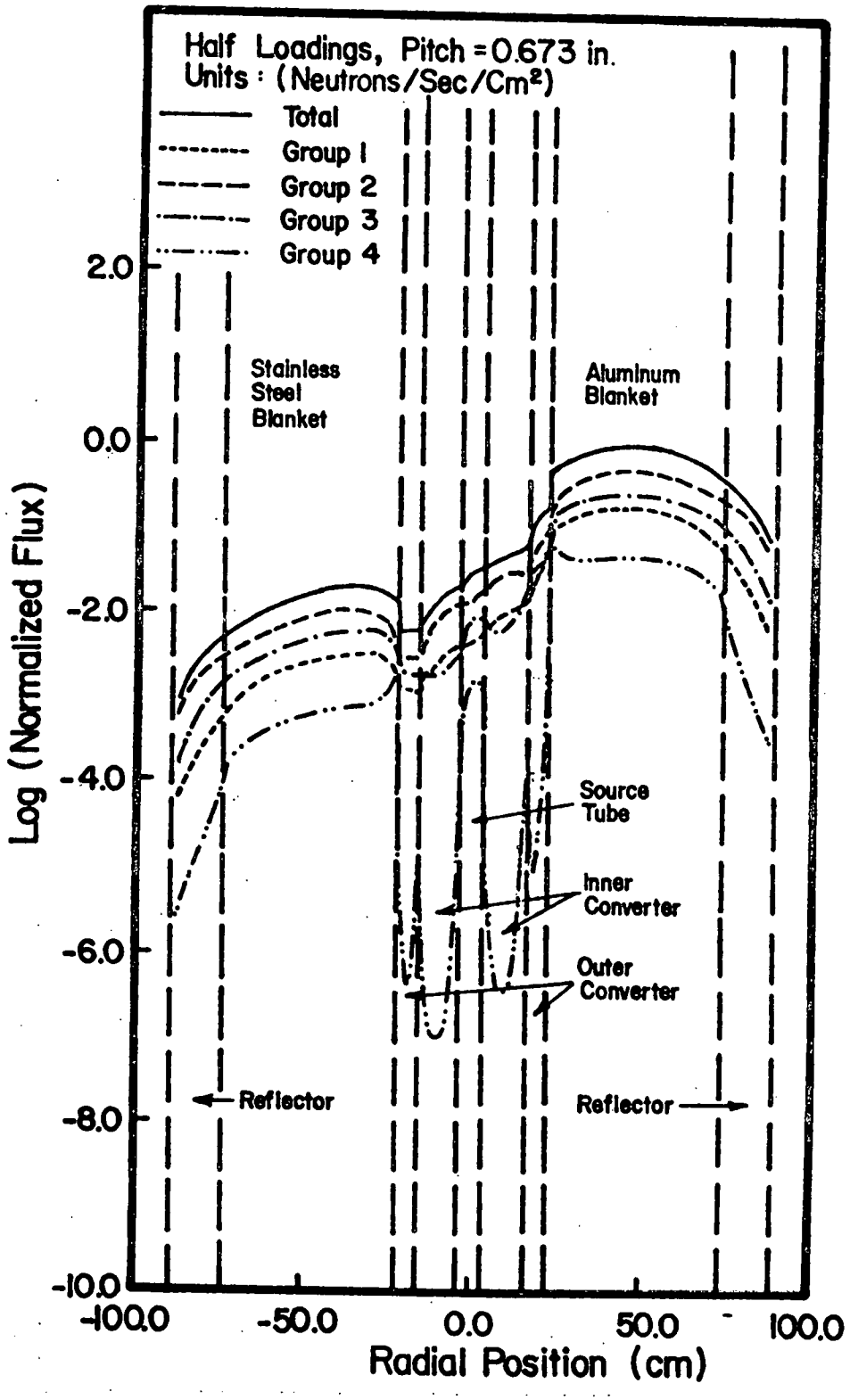

Figure VI.2: Log of the λ-mode group fluxes.

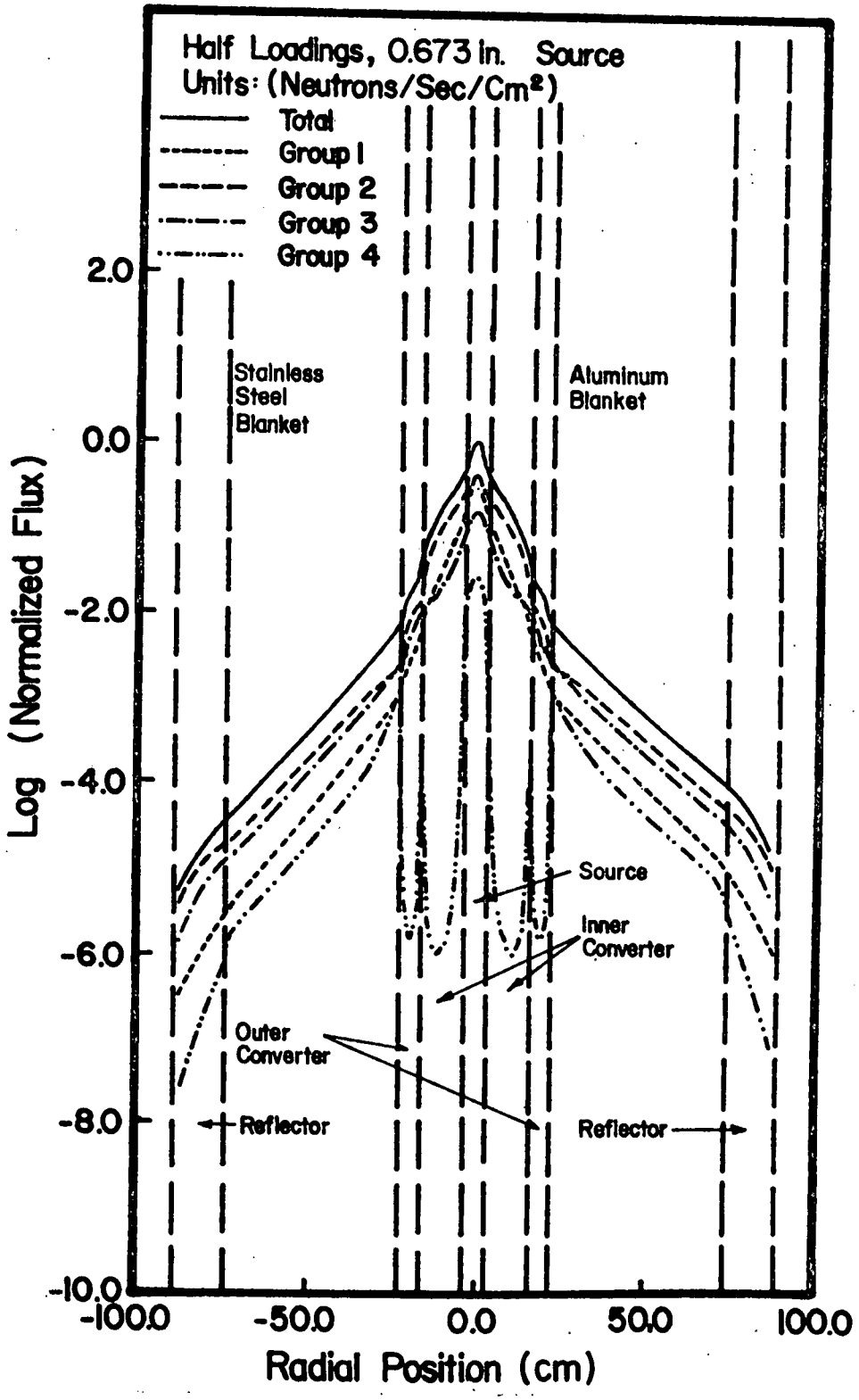

Figure VI.3: Group fluxes based on a source calculation.

$$\frac{\lambda k_\infty}{1+L^2B^2} = 1 \quad , \tag{1}$$

where λ is the eigenvalue identical to $1/k_{eff}$; the second term in the denominator describes the leakage. Thus, for each region a modified value of k_∞ can be considered as

$$k'_\infty = \lambda k_\infty \quad . \tag{2}$$

The values for k_∞, for a pitch of 2.286 cm., in the aluminum and stainless steel secondary clad halves, are 0.893 and 0.683, respectively. Multipling these values by the eigenvalue λ, which is approximately 1.25, modified infinite multiplication constants of approximately 1.12 and 0.86 are obtained. Thus, the eigenvalue artifically modifies the aluminum side to such an extent that it is treated as super productive medium but the stainless steel side is still an absorbing medium. The flux shapes illustrated in Fig. V.2 are exactly what one would expect from a medium with one side super productive and the other side an absorbing medium. Similar calculations were preformed for the initial loading pitch and the same type flux shape differences were obtained.

The investigations presented in this subsection indicate that the λ-mode flux, for the double loading subcritical problems needed to verify the safety of the FBBF, are not physically realized.

VII. SUMMARY OF FBBF SAFETY INVESTIGATIONS

A. Introduction

In the previously reported safety investigations of the hypothetical accident, all regions of the FBBF were assumed to be flooded. The effects of boron with dry rather than flooded converters were not considered in these earlier studies. Initially one-dimensional FOG code calculations were used to evaluate k_{eff} for various dry-flooded conditions for the presumed initial loading configuration without boron in the converters.[7] Later, two models for the mockup of the FBBF, one with and one without explicit treatment of B_4C transition regions, were used with the two-dimensional 2DB code. The value of k_{eff} for specified conditions such as pitch variation and the type of secondary cladding for hypothetical accident conditions were evaluated. These investigations indicated that, for a number of blanket pitches with Al as secondary clad, the value of k_{eff} could be about 0.8. In order to re-evaluate these few cases, the converters were considered dry rather than flooded.

The object of this section is to investigate and summarize the inherent safety feature of the FBBF with both the inner and outer converters dry or flooded and also to verify the initial calculations with the improved methods. Because the converters are both separately constructed and sealed by welding, it is feasible and necessary to evaluate the flooding of the FBBF with dry converters.

The composition of each region of the FBBF in this study was determined from the initial loading configuration. The radial blanket, which physically has inner rows of SS double clad natural uranium fuel pins and outer rows of Al double clad pins, was modified for the calculations by considering an all Al or SS double clad blanket. Also two blanket pitches were chosen for

investigation of the effect of pitch variation under various dry-flooded conditions. The initial blanket loading pitch, 0.673 inch and the pitch of the maximum reactive configuration, 0.900 inch, i.e., the configuration which results in maximum k_{eff}, were used (comp. Sec. V).

The pitch in the inner converter is slightly increased from the original design value of 0.468 inch to 0.474 inch. The amounts of natural B_4C vibrated into the inner and outer converters are 21.59 kg and 23.313 kg, respectively. It occupies 61.24 percent of the possible voided volume of the inner converter and 53.58 percent of the outer converter. These amounts of B_4C are very close to the previously assumed value of 60 percent. The source region was considered to be flooded with and without the source plug in order to compare results with the previous investigations.[7] Because the reflectors are also welded shut, they were treated as dry regions for most of the cases investigated.

The unit cell set up for the input to the HAMMER code for generating group constants in each region is the same as that used previously (comp. Sec. II). Two models were used to mock up the facility, one included B_4C transition regions and the other did not. They are presented in Sec. II. The corrected material number densities and explicit dimensions of the facility used here are presented in Section II.D and Ref. 9.

B. Results and Discussions

The effective multiplication factors, calculated with the model which explicitly treats the transition regions, for various conditions are presented in three tables. Table VII.1 gives values of k_{eff} for a pitch of 0.673 inch, Table VII.2 for a pitch of 0.900 inch with a SS double clad blanket and Table VII.3 for a pitch of 0.900 inch with Al as secondary cladding. The

TABLE VII.1

Values of k_{eff}
for various dry-flooded
conditions for SS double clad blanket
with a pitch of 0.673 inch

Case No.	Source	IC	OC	B_4C	Blanket	Reflector	k_{eff}
1	SS	D	D	Y	F	D	0.41027
2	SS	F	F	Y	F	D	0.40507
3	F	D	D	Y	F	D	0.41259
4	F	F	F	Y	F	D	0.40693
5	SS	D	D	N	F	D	0.46846
6	SS	F	F	N	F	D	0.72101
7	F	D	D	N	F	D	0.46953
8	F	F	F	N	F	D	0.76546

The symbols used in the table:

IC - Inner converter

OC - Outer converter

SS - Stainless Steel plug

D - Dry

F - Flooded

Y - B_4C in converters

N - No B_4C in converters

TABLE VII.2

Values of k_{eff}
for various dry-flooded
conditions for SS double clad blanket
with a pitch of 0.900 inch

Case No.	Source	IC	OC	B_4C	Blanket	Reflector	k_{eff}
1	SS	D	D	Y	F	D	0.61864
2	SS	F	F	Y	F	D	0.61668
3	F	D	D	Y	F	D	0.61858
4	F	F	F	Y	F	D	0.61669
5	SS	D	D	N	F	D	0.64959
6	SS	F	F	N	F	D	0.75855
7	F	D	D	N	F	D	0.64974
8	F	F	F	N	F	D	0.79170
9	F	F	F	N	F	F	0.69171

The symbols used here are the same as Table VII.1.

TABEL VII.3

Values of k_{eff}
for various dry-flooded
conditions for Al double clad blanket
with a pitch of 0.900 inch

Case No.	Source	IC	OC	B_4C	Blanket	Reflector	k_{eff}
1	SS	D	D	Y	F	D	0.77529
2	SS	F	F	Y	F	D	0.77168
3	F	D	D	Y	F	D	0.77518
4	F	F	F	Y	F	D	0.77167

The symbols used here are the same as Table VII.1.

k-infinite values which are helpful in understanding the results are given in Table VII.4 for the converters and blankets.

Several important features of the FBBF are found in this investigation. They are discussed in the following.

(1) Boron effect:

The presence of B_4C in the converters stabilizes the value of k_{eff} for a given blanket pitch irrespective of whether the converters are dry or flooded (compare the first four cases in Tables VII.1, VII.2 and VII.3). Every region in the FBBF has some contribution to the value of k_{eff}, but the degree of its influence depends on the magnitude of k_∞, and the size and the location of the region. All of the fuel of the FBBF is loaded in the converters and blanket, therefore, these regions have the dominate impact on the determination of the value of k_{eff}. The values of k_∞ as shown in Table VII.4, for flooded converters with boron are only slightly smaller than the k_∞ values of the dry converters with boron (comp. Cases No. 2, 4, 6 and 8 in Table VII.4). This trend is due to the compensation between the increased absorption of B_4C and fission of U-235 as the neutron spectrum becomes softer for the flooded case. Therefore, if boron is in the converters, there is not much difference in the k_{eff} results since the k_∞ value of the converters do not significantly change when comparing the dry and flooded cases.

For the boron free cases, k_{eff} greatly increases if the dry converters are assumed to be flooded for the same blanket (compare the last four cases in Tables VII.1 and VII.2). This increase is more pronounced for the initial loading pitch. The values of k_∞ are much smaller for the dry converters without boron than the flooded converters without boron (compare cases No.1, 3, 5 and 7 of Table VII.4). All of these values of k_∞ are sufficiently larger than k_∞ of the blanket with the initial loading pitch. For the blanket

TABLE VII.4

k-infinity for inner converter,
outer converter and
blanket under various conditions

Case	Region	Conditions	K_∞
1	IC	dry, no B_4C	0.7905
2	IC	dry, with B_4C	0.5589
3	IC	flooded, no B_4C	0.9403
4	IC	flooded, with B_4C	0.5218
5	OC	dry, no B_4C	0.6576
6	OC	dry, with B_4C	0.4539
7	OC	flooded, no B_4C	0.7755
8	OC	flooded, with B_4C	0.4493
9	Blanket	flooded, 0.673 inch SS double clad	0.4705
10	Blanket	flooded, 0.900 inch SS double clad	0.6831
11	Blanket	flooded, 0.900 inch Al double clad	0.8583

IC - Inner Converter
OC - Outer Converter

with a pitch of 0.900 inch, the value of k_∞ is larger than case 5 and substantially larger than case 9 (compare cases No. 1, 3, 5, 7, 9 and 10 of Table VII.4). Therefore, the converters have a larger influence on the values of k_{eff} for the case of the blanket with the initial loading pitch, while the blanket has proportionately a greater contribution for the case with a pitch of 0.900 inch. Thus, one would expect k_{eff} to increase when comparing cases with dry and flooded converters. Also, the increases should be more pronounced for the case with the blanket initial loading pitch as is indicated in Tables VII.1 and VII.2. Case 9 in Table VII.2 considered all regions of the FBBF flooded; as illustrated in the table, the value of k_{eff} is identical to that of case 8 which has a dry reflector. Thus, the impact of a dry versus wet reflectors is minimal.

(2) The effect of water in source region:

For the cases with boron in the converters, k_{eff} changes very little even if the stainless steel plug in the source region is replaced with water for both SS and Al double clad blankets (compare the first four cases in Tables VII.1, VII.2 and VII.3).

The water in the source region can soften the neutron spectrum in the adjacent regions, and thus influence these regions. The boron in the converters has a stabilizing effect as stated above. Which one of these effects is more important depends on the values of k_∞ in the converters and the blanket. Since the values of k_∞ for the converters with boron are not much larger than those of blankets (compare cases No. 2, 4, 6, 8, 9, 10 and 11 of Table VII.4), the boron stabilizing effect is dominant. Therefore, the replacement of the SS source region with water has negligible effect on the values of k_{eff} for the cases with boron in the converters.

For the boron free converters, k_{eff} has a negligible change in the dry cases, but has a slight increase in the flooded cases when the stainless steel

plug in the source region is replaced with water (compare the last four cases in Tables VII.1 and VII.2). Since no boron stabilizing effect exists, the values of k_{eff} are influenced by the presence of water in the source region which in turn depends on the k_{∞} of the converters and the blanket. The values of k_{∞} for the flooded converters without boron are much larger than those of SS double clad blankets (compare cases No. 3, 7, 9 and 10 of Table VII.4). Therefore, the water in the source region has a larger influence for the flooded cases without boron.

(3) The effect of pitch variation:

The value of k_{eff} increases as the pitch of the blanket increases from 0.673 inch to 0.900 inch. This is consistent with the previous investigations.[2] This is due mainly to the increase in k_{∞} from 0.4705 for the pitch 0.673 inch to 0.6831 for the pitch 0.900 inch SS double clad blanket (compare cases No.9 and 10 of Table VII.4).

(4) SS double clad vs Al double clad:

If the Al double clad fuel pins are used instead of SS double clad fuel pins, k_{eff} increases. This is consistent with the previous investigations. Comparing the last two cases in Table VII.4, k_{∞} increases from 0.6831 to 0.8583 for this change in the blanket.

(5) The comparison of models:

The values of k_{eff} calculated by the three models described in the introduction are given in Table VII.5 for the boron-free cases with the blanket pitch of 0.673 inch. Models 1 and 2 are used with the two-dimensional 2DB calculation with and without the transition regions treated, respectively. Model 3 is the basis of the one-dimensional FOG calculation.[1]

The values of k_{eff} obtained from Models 2 and 3 agree very well, but are a little higher than those evaluated from Model 1 for the dry case,

TABLE VII.5

Values of k_{eff}
calculated by various models
for 0.673 inch
SS double clad blanket under various conditions
without boron in converters

Case No.	Model	Source	IC	OC	Blanket	Reflector	k_{eff}
1	1	SS	D	D	F	D	0.46846
2	1	SS	F	F	F	D	0.72101
3	1	F	D	D	F	D	0.46953
4	1	F	F	F	F	D	0.76546
5	2	SS	D	D	F	D	0.49537
6	2	SS	F	F	F	D	0.64788
7	2	F	D	D	F	D	0.56906
8	2	F	F	F	F	D	0.71030
9	3	SS	D	D	F	F	0.4884
10	3	SS	F	F	F	F	0.6486
11	3	F	F	F	F	F	0.7180

The Model No.

1 - model with explicit treatment of transition regions.
2 - model without explicit treatment on transition regions.
3 - one dimensional FOG calculation.

while the converse is true for the flooded case. The increasing trend in k_{eff} from the dry case to flooded case is the same for the three models.

The improved two-dimensional model, Model 1, which is the basis of present investigation, should give more reliable results. The results of Model 3 are consistent with those from Model 2, however.

C. Conclusions

The use of improved methods and models in the safety investigation of a hypothetical flooded accident has led to several important conclusions which are summarized here.

(1) Boron in the converters has a stabilizing effect irrespective of whether they are treated as dry or flooded cases; i.e., for a hypothetical accident k_{eff} stays fairly constant when B_4C is present in the converters. If there is no B_4C in the converters, k_{eff} would greatly increase from the dry case to flooded case. However, boron in the converters can not bring the values of k_{eff} below 0.75 for Al double clad blanket for the most reactive case with a pitch of 0.900 inch (Table VII.3).

(2) The replacement of the stainless steel in the source region with water has only negligible effect on the safety of FBBF except for the case of the flooded converters without boron.

(3) The specific treatment of flooded reflectors has little impact on the value of k_{eff}.

(4) The pitch variation from the initial loading pitch to maximum reactive pitch of SS double clad blanket results in an increase in k_{eff} (comp. Sec. V.).

(5) The change from SS double clad blanket to Al double clad blanket also results in an increase in k_{eff} (comp. Sec. V.).

(6) The results from the different models and calculational procedures are in fairly good agreement and the trends for different dry-flooded conditions are the same.

TASK C
(F.M. Clikeman)

I. INTRODUCTION

The objectives of this task are: 1) the testing of experimental equipment and the development of techniques for making experimental measurements in the blanket regions in the FBBF facility; 2) performing check-out tests and preparing the operating procedures required for licensing purposes and safe operation of the FBBF facility; 3) performing measurements on the first blanket configuration of the FBBF. The progress of each of these tasks is summarized in the following subsections.

II. TESTING OF EXPERIMENTAL EQUIPMENT AND TECHNIQUES
(F.M. Clikeman)

The testing of equipment and techniques used for neutron spectroscopy, integral neutron capture rate, fission rate and gamma dosimetry measurements continued during the quarter. Measurements were also continued to determine the nature of the azimuthal asymetry observed during the last reporting period. The results of the investigation of the azimuthal asymmetry are reported in Sec. III. Preliminary results of the measurement of the $^{115}In(n,\gamma)$ and the $^{115}In(n,n')$ reaction rates are reported in Sec. IV.

A. Foil Activation Measurements
(G.A. Harms and F.M. Clikeman)

Preliminary activation of several possible activation foils were made to determine the gamma-ray spectra and optium irradiation and counting times for use in the FBBF facility. The specific reactions investigated during the period were the indium neutron capture and inelastic scattering reactions. The preliminary results for these reactions are shown in Sec. IV. In this case since two reactions are being investigated for the same set of foils and multiple gamma-rays resulted from the neutron interactions the foils were counted using the Ge(Li) spectrometer system. Work is continuing and a number of additional isotopes are expected to yield usable levels of activity for measurements in the blanket region in the FBBF facility.

B. Proton-Recoil Proportional Counter Measurements
(D.W. Vehar and F.M. Clikeman)

During the progress period several neutron energy spectra in various materials with neutron resonances have been obtained in the energy range 1 - 10 keV (Na) and in the range 20 - 200 keV (Al, Fe, and F). Measurements were made with the 8-atmosphere H_2 detector in plugs of the various materials placed in the upper axial blanket region of the FBBF facility. Structures in the measured distributions were then used to adjust the energy calibration of the detector and also verified satisfactory operation of the detector system.

Eight gain runs are used to cover the energy range from 1 keV to 3 MeV: three with the 10-atmosphere methane detector and five with the 8-atmosphere hydrogen detector. Detector voltages and approximate ranges are listed in Table II.1.

Gamma-ray discrimination is used with the hydrogen detector at all voltages and with the highest voltage used with the methane filled dectecotr. Proton recoil distributions are recorded as 8K two-parameter data and are reduced to 100 channels for analysis. No gamma discrimination is necessary for the two lowest methane-filled detector voltages, and pronton-recoil distributions are recorded as 4K single-parameter data and collapsed to 100 channels for analysis. Differential unfolding is used to obtain the neutron energy spectrum from the proton-recoil data.

Figure II.1 shows a preliminary spectrum obtained for location A-12 in the FBBF blanket (radius - 56.2 cm). No corrections have been made for electric field and wall-and-end effects in the detector. The effects of these corrections are expected to be small. In addition, some of the data for the CH_4 detector were suspect and omitted from the analysis. The dip

TABLE II.1

Bias Voltages and Energy Ranges for
Proton Recoil Detectors

Bias Voltage (volts)	Range (keV)
4800 - CH_4 - Fill Gas	623. -- 2930
5300	284. -- 1340
5800	102. -- 481.
3700 -- H_2 - Fill Gas	48.4 -- 228.
4000	16.1 -- 75.9
4300	5.37 -- 25.3
4600	1.79 -- 8.42
4900	0.596 -- 2.80

in the spectrum of 34 keV is due to resonances in aluminum and iron. Those at 90 keV and 150 keV are due to resonances in aluminum and those at 440 keV and 1100 keV are due to resonances in oxygen. Error bars shown in the curve are on standard deviation and are based on the counting statistics of the proton spectra. Future work will investigate the effects of the electric field and wall-and-end effects as well as check the reproducibility of the technique.

C. Fission Rate Measurements
(H.P. Chou, R.H. Johnson, and F.M. Clikeman)

During the past quarter, experiments with SSTR for measuring fission rates have led to the decision to use fused quartz as the recording media. Fused quartz samples have been tested both by using a small ^{252}Cf source and irradiation with fission foils in the FBBF. Results have shown that the fission track registration efficiency of fused quartz is about twice as high as that of glass. This feature reduces irradiation time significantly, and therefore speeds up data collection. Commerical fused quartz disks have been ordered for future use.

Progress has been made on the development of the automatic track counting system. The track counting program, described in the last quarterly progress report, has been debugged and used to count actual SSTR samples. In the current stat of development, the program, both counts the number of tracks and determines the track sizes. It then corrects for the overlapping of tracks according to the track size distribution. A single discrimination level is pre-set to determine tracks from background events by checking the light output signal. The output of the discriminator is fed into a microcomputer for analyzing. The track counting program has the following features:

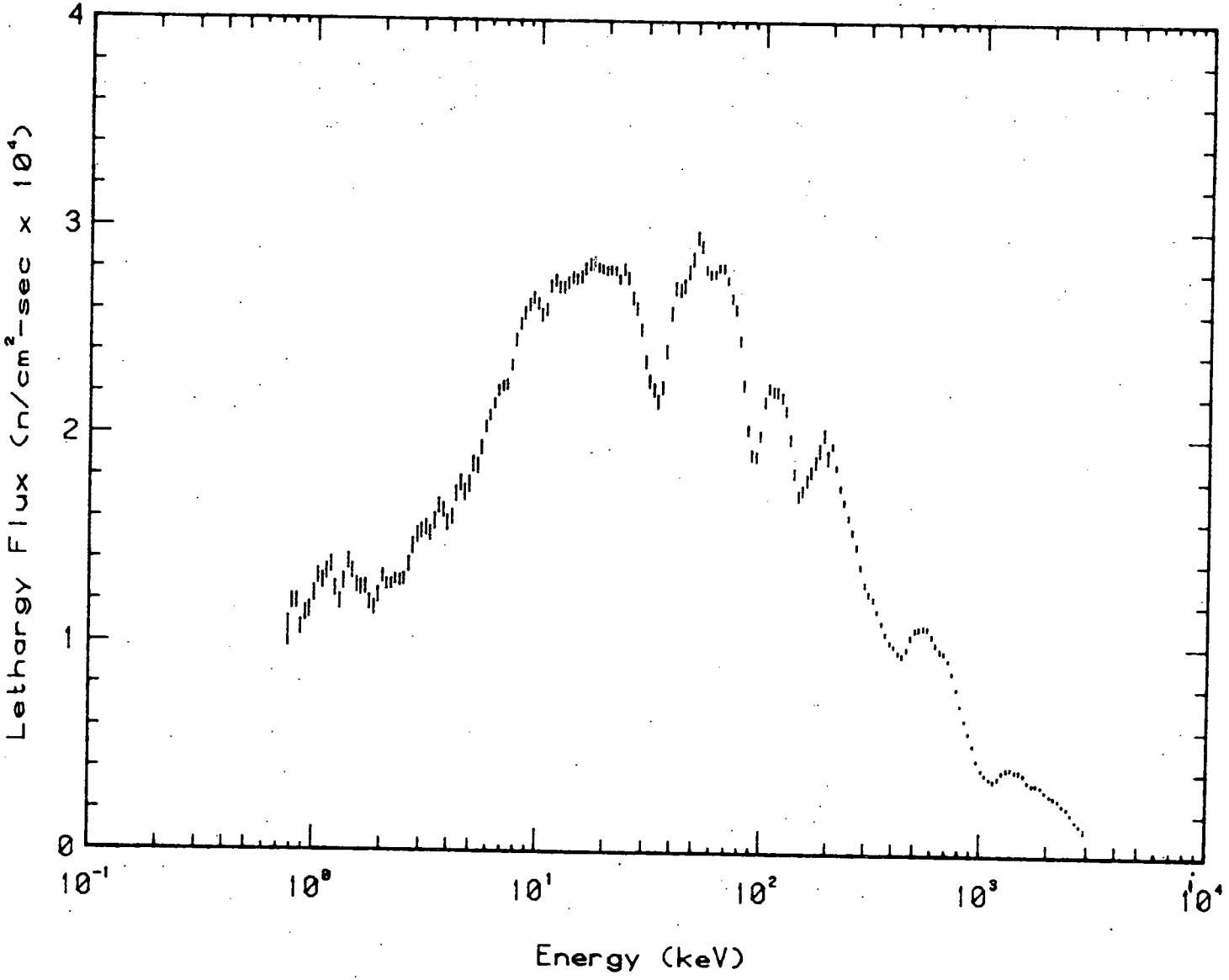

Figure II.1: Preliminary neutron-energy spectrum at location A-12.

1. The program utilizes 2-Kbytes of memory with the running time limited by the microscope scanning speed;
2. The program receives data via hardware interrupt control with an input buffer for temporary storage of four scanned lines (maximum 1000 track entries per line);
3. Each track entry is saved in the form of two bytes for track position and one byte for track size;
4. Track positions and sizes are temporarily saved in an output buffer and then dumped to a mini-disk for further use;
5. Output of the program includes the total number of tracks, track size distribution, number of tracks vs scanned lines, and the scanned pattern of a randomly selected area with the size of 50 x 50 picture elements.

For a track recorder with a diameter of 7 mm and a track number of order 10^4, the reproducibility given by the system is limited to 3% which is mainly caused by the variation of the photometer and the overshooting of the microscope stage motors. Investigation is under way to reduce these effects.

D. Gamma-ray Dosimetry Measurements
(K.R. Koch and F.M. Clikeman)

Gamma-ray heating rate measurements have now been made in the FBBF using CaF_2:Dy TLD's encased in both lead and stainless steel sleeves. These measurements have been made along radial traverses at the facility's axial midplane. Four TLD's were used in each holder as described in the previous progress report, yielding averaged measurements of $\pm$ 1% standard deviation at each radial location. Currently, measurements have been made for both

background and source up conditions using lead holders in sector D and stainless steel holders in sector A. Further measurements including axial traverses, are planned. The raw data of the lead measurements are shown in Figure II.2. These results do not include corrections for dose calibrations or f-factors. As is seen, the results are smoothly varying with no unexpected discontinuities.

The properly weighted f-factors (TLD dose/sleeve dose) for lead holders have been calculated. the properly weighted f-factor at each spatial point is given in Ref. 10 as

$$f(\vec{r}) = \frac{\int_0^\infty dT_\gamma T_\gamma \phi(\vec{r},T_\gamma) \left[\frac{\gamma_{en}(T_\gamma)}{p}\right]_{sleeve} f(T_\gamma)}{\int_0^\infty dT_\gamma T_\gamma \phi(\vec{r},T_\gamma) \left[\frac{\gamma_{en}(T_\gamma)}{p}\right]_{sleeve}}$$

The calculation requires multigroup gamma-ray spectra at each radial point and cubic spline fits of both the mass energy absorption coefficients and the 4 chip energy dependent f-factors. The mass energy absorption coefficients and the f-factor for both lead and stainless steel are given in the previous progress report. They were fit with a cubic spline. Using calculated gamma-ray spectra from ANISN-W, the weighted f-factors for lead have been calculated at each radial mesh point used by the ANISN calculation. Figure II.3 shows the radial dependence of the weighted lead f-factors. A single f-factor for each experimental position can thus be found by interpolation where necessary.

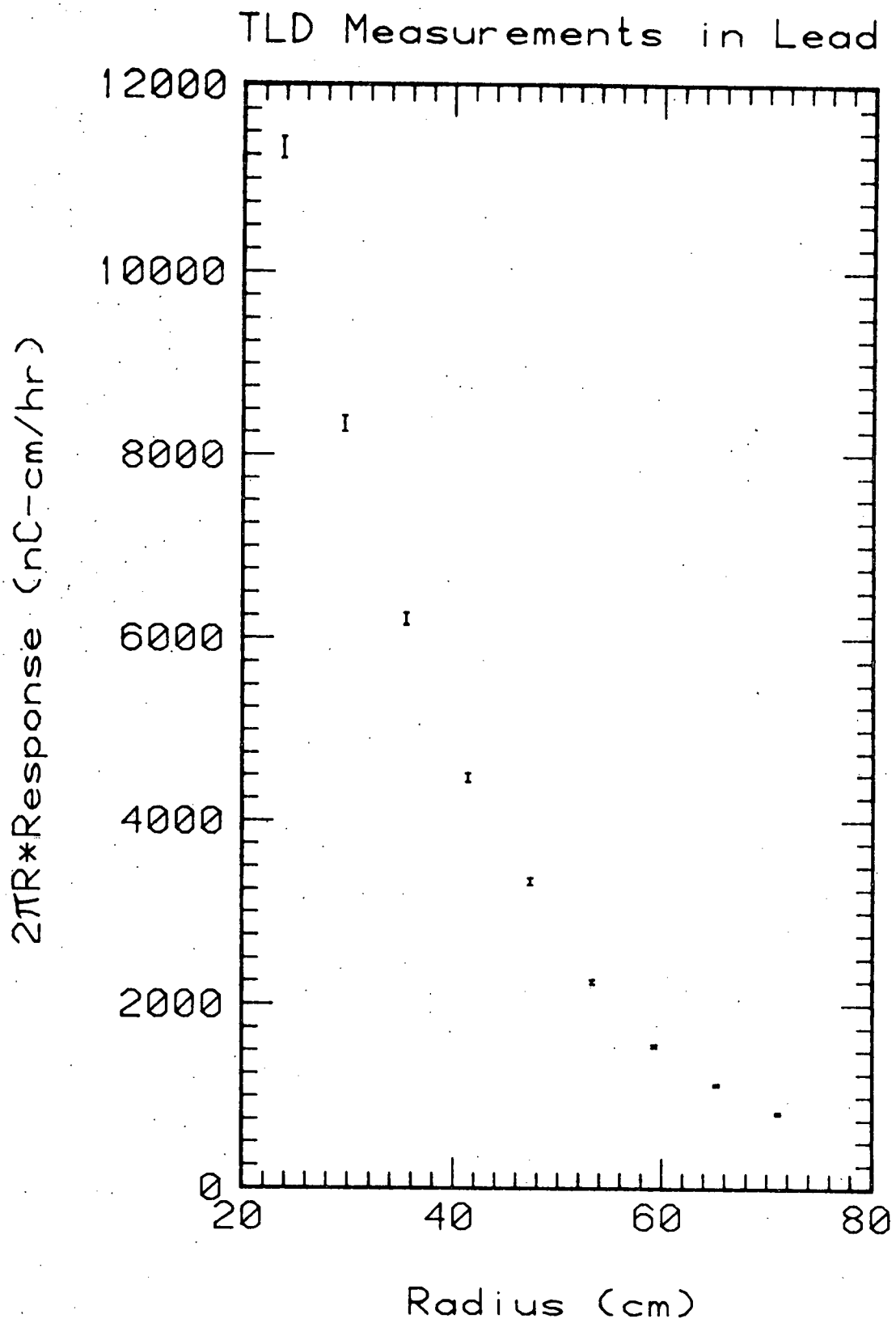

Figure II.2: Preliminary CaF(D_y) TLD measurements as a function of radial position. The TLD dosimeters were irradiated in lead sleeves. Background has not been subtracted. The error bars represent the 1% standard deviation of the average of 4 TLD dosimeters.

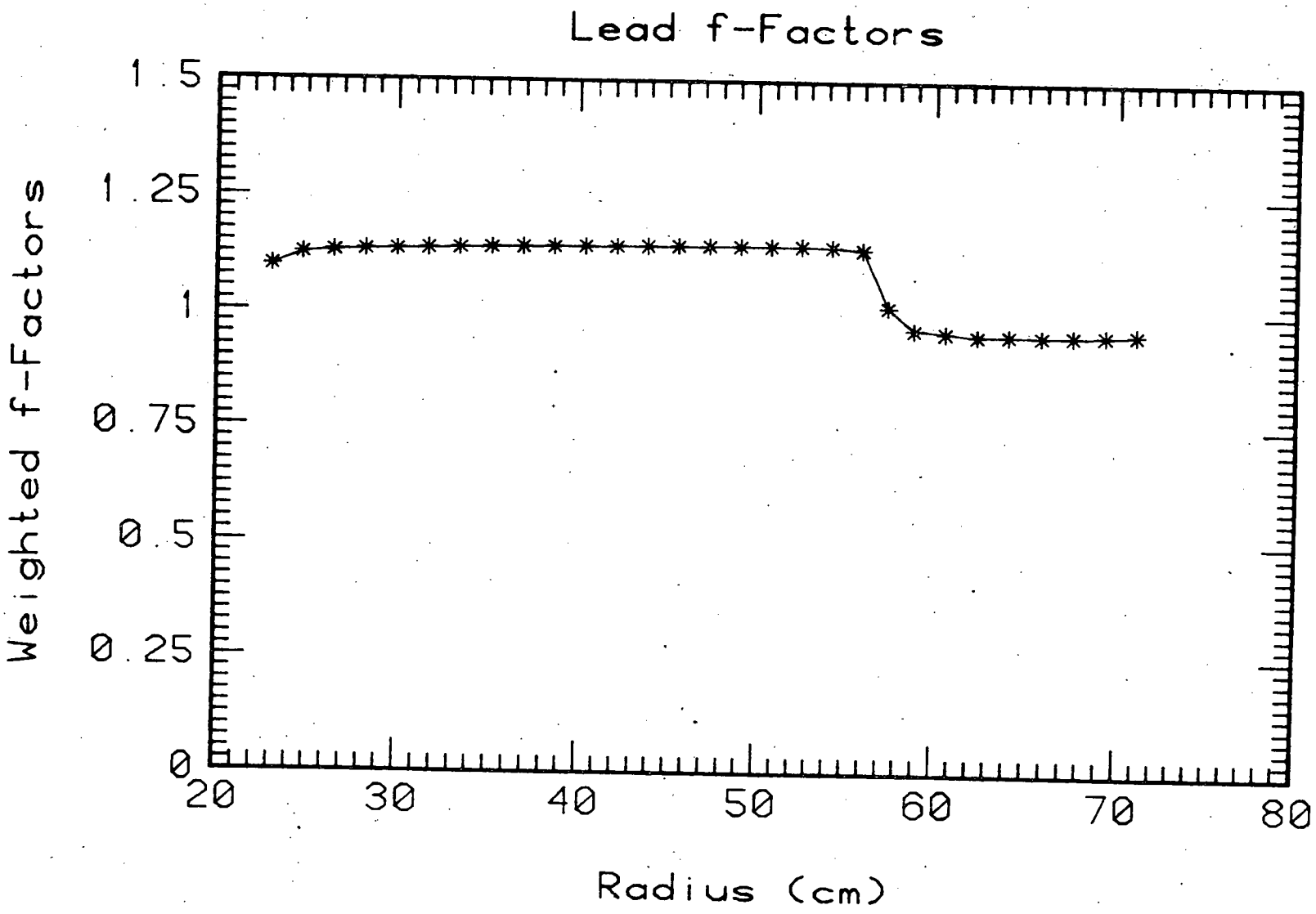

Figure II.3: Calculated f-factors for correcting CaF(Dy) dosimeter response to the lead sleeve dose.

Dose calibration of the CaF_2:Dy TLD's has yet to be performed so absolute gamma doses can not be calculated. A strong Co-60 source will be used so that high doses and dose rates, similar to those experienced in the FBBF, can be obtained.

The steps for obtaining final absolute gamma-ray heating measurements are:

1. Measurements using 4 chips per holder where all 4 chips are from the same precision set.
2. Apply precision set correction factors to each chip and averaging the 4 values for each holder.
3. Dose determination from TLD response-to-dose calibrations of each precision set as a whole.
4. Subtraction of background dose per unit time at that location (precision set correction factors applied and 4 chips averaged for background)
5. Possible corrections for neutron response of CaF_2:Dy in the fast neutron flux.
6. Apply multiplicative spatial f-factors to correct for sleeve-TLD material mismatch.

III. INSTALLATION AND TESTING OF THE FACILITY, FACILITY EQUIPMENT AND PREPERATION OF OPERATING PROCEDURES

During the progress period the observed asymmetry of the FBBF facility was investigated using the proton-recoil proportional counters. The advantage of using these detectors is that the effects or changes in neutron spectra as a fucntion of position can be readily observed. The results of the experiment are summarized in the following section.

A. Azimuthal Flux Asymmetry in the FBBF Blanket
(D.W. Vehar and F.M. Clikeman)

Previous measurements with gold foils have indicated a possible azimuthal asymmetry of the neutron flux in the FBBF blanket. That is, measured gold reaction rates at the center of sector D were about 4% higher than those at the center of sector A. In an effort to determine the source of this asymmetry, proton-recoil ionization distributions were measured over the energy range from 5 keV to 3 MeV at several locations in the FBBF blanket. A comparison was made between distributions at corresponding locations in sectors A and D, as the point-wise ratio of two distributions. If $M_{A2}(i)$; i = 1; 128 is the measured 128-energy-channel proton-recoil distribution at location A2 and $M_{D2}(i)$; i = 1, 128 is the distribution at location D2, then the ratio $R_2(i)$ is

$$R_2(i) = \frac{M_{A2}(i)}{M_{D_2}(i)} \; ; \; i = 1,128.$$

The proton-recoil distributions were recorded as 2048-channel single-parameter spectra, which were compressed in 128 channels before the ratio was taken. Reasonable statistics could thus be obtained in the upper

channels without memory overflow in the lower channels. Gamma-ray discrimination was not required for these measurements. Two gain runs were made with the 10-atmosphere methane detector and one was made with the 8-atmosphere hydrogen detector, with overlapping energy ranges. Since it was necessary to lower the neutron source to change detectors, a third detector was placed permanently at location B4 and used to verify that the neutron source strength remained constant over the course of the experiment. Distributions were obtained at positions 2, 12 and 17 in sectors A and D, corresponding to radii of 26.6, 56.2 and 71.1 cm respectively. The following figures show these results. Due to noise in the distributions at the lower channels, some of those points have been omitted from the plots.

Several conclusions can be drawn from the figures. Within statistics, the ratio is constant with energy at both positions 2 and 12, indicating that the shape of the neutron energy spectrum is the same for corresponding points in sectors A and D. Some differences were expected at the outer edges of the blanket, which seem to be reflected in the figures for position 17, although the differences are small. Second, the measured distributions at each point in sector D are all about 3 percent higher than at corresponding points in sector A, in agreement with the approximate 4 percent difference shown by the gold data. Since the discrepancy is not a function of radial position, a shift in position of the neutron source is ruled out. The effects of such a shift would tend to decrease with increasing radius. The cause of the asymmetry must therefore be in the transformer regions, possibly a non-uniform distribution of boron-carbide. The investigations will continue in efforts to determine the cause of the asymmetry.

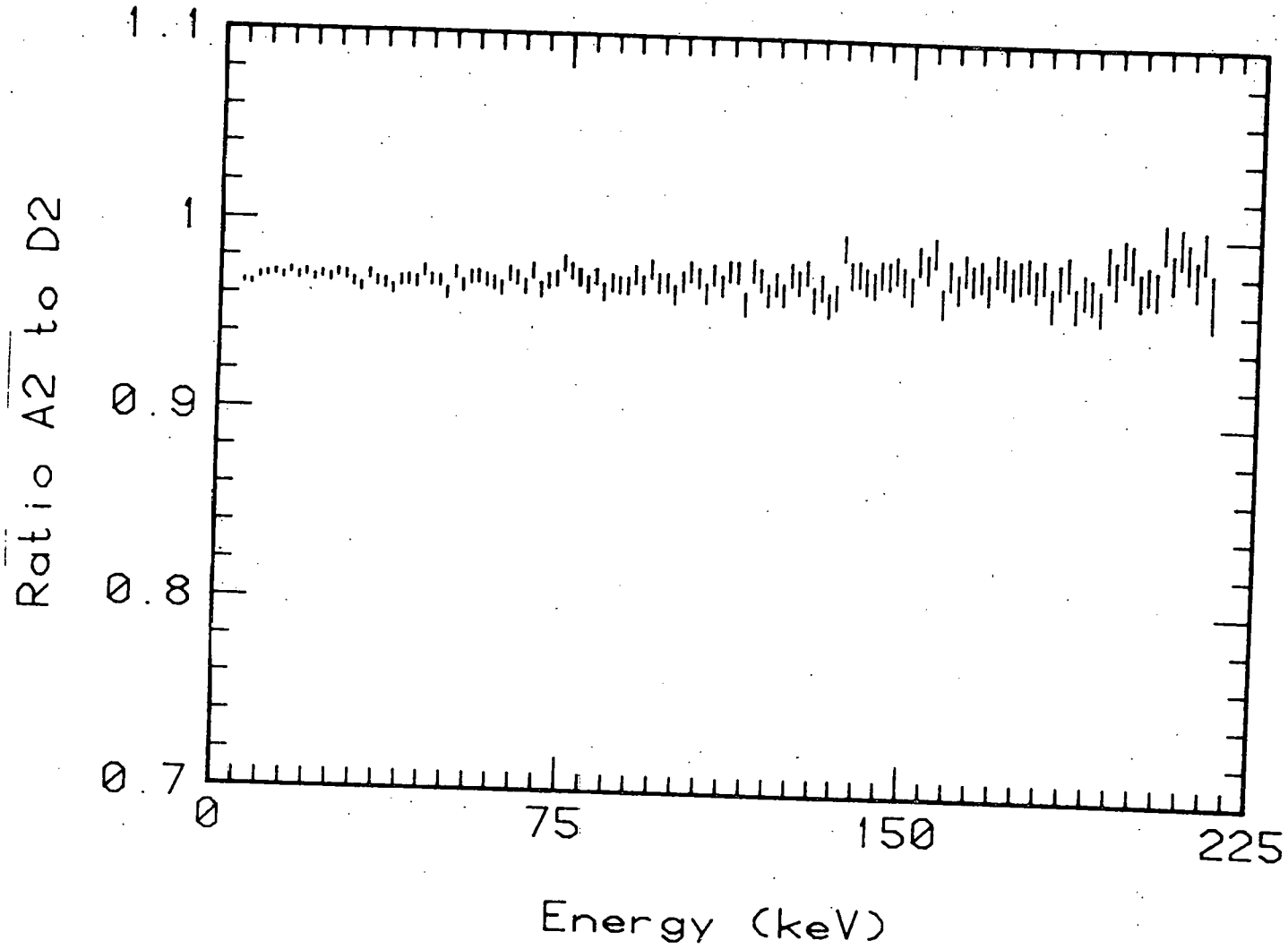

Figure III.1: Ratio of proton recoil distribution in Sector A to that in Sector D from 5 keV to 215 keV at a radius of 26.6 cm.

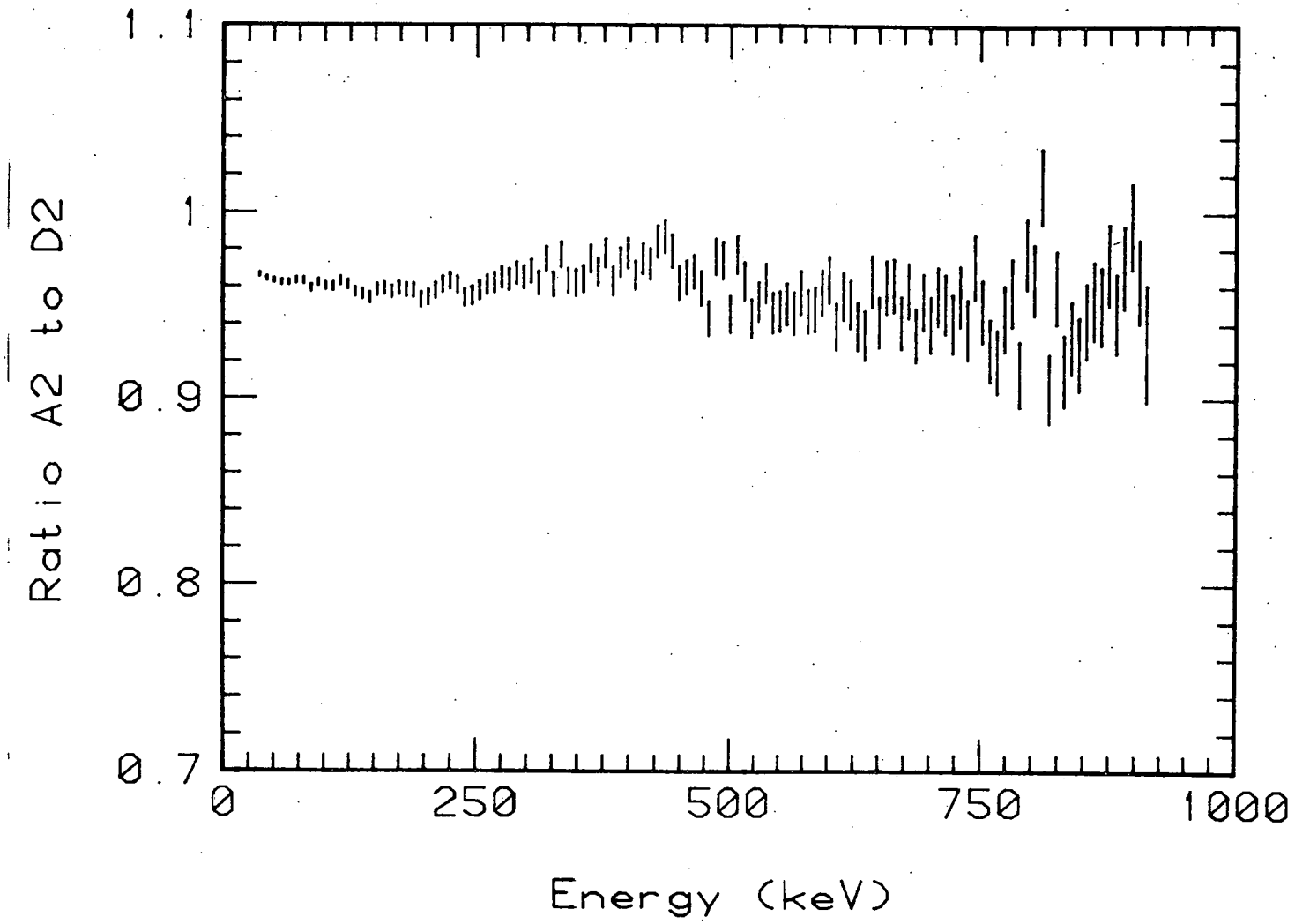

Figure III.2: Ratio of proton recoil distribution in Sector A to that in Sector D from 30 keV to 900 keV at a radius of 26.6 cm.

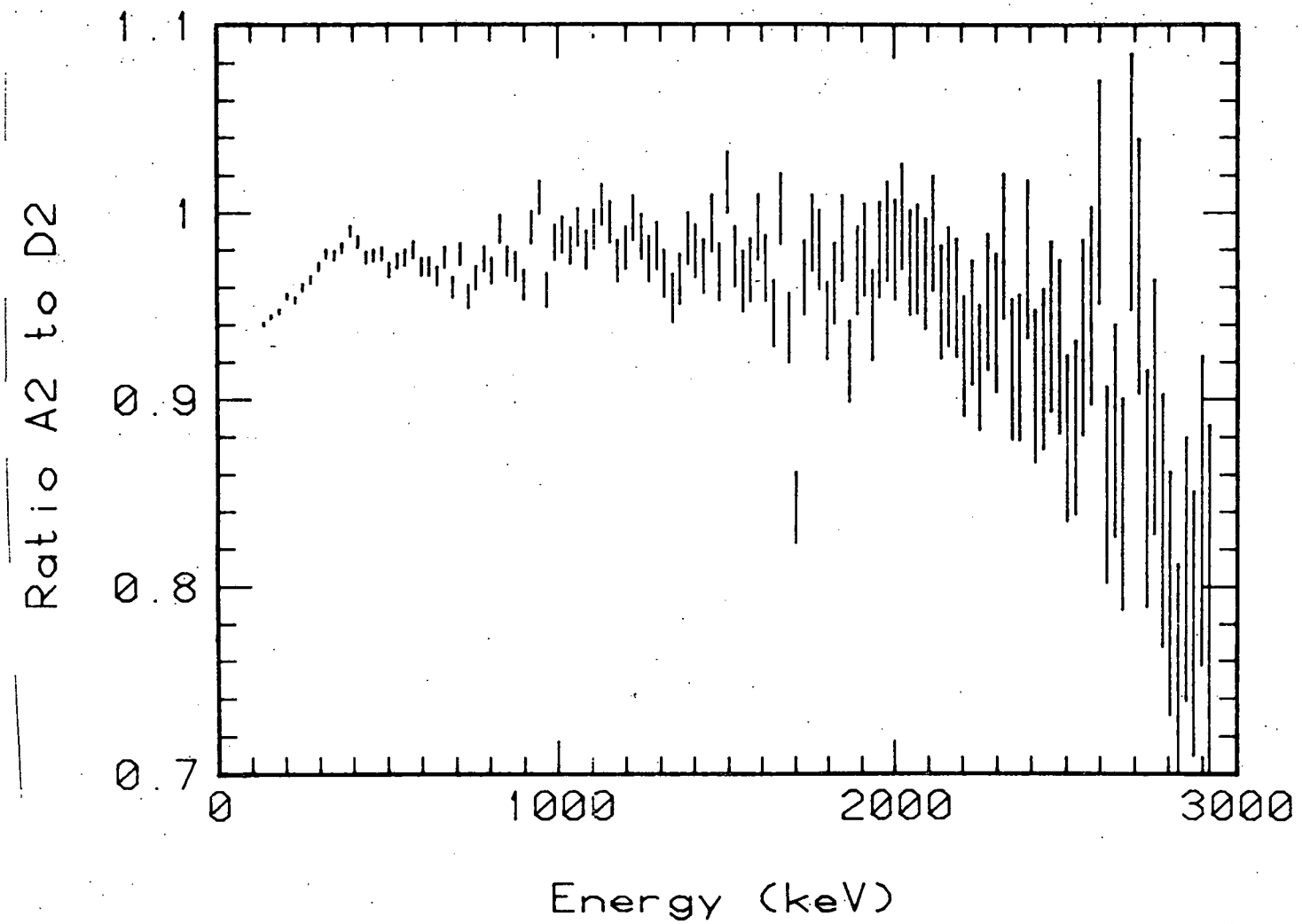

Figure III.3: Ratio of Proton recoil distribution in Sector A to that in Sector D from 100 keV to 3 MeV, at a radius of 26.6 cm.

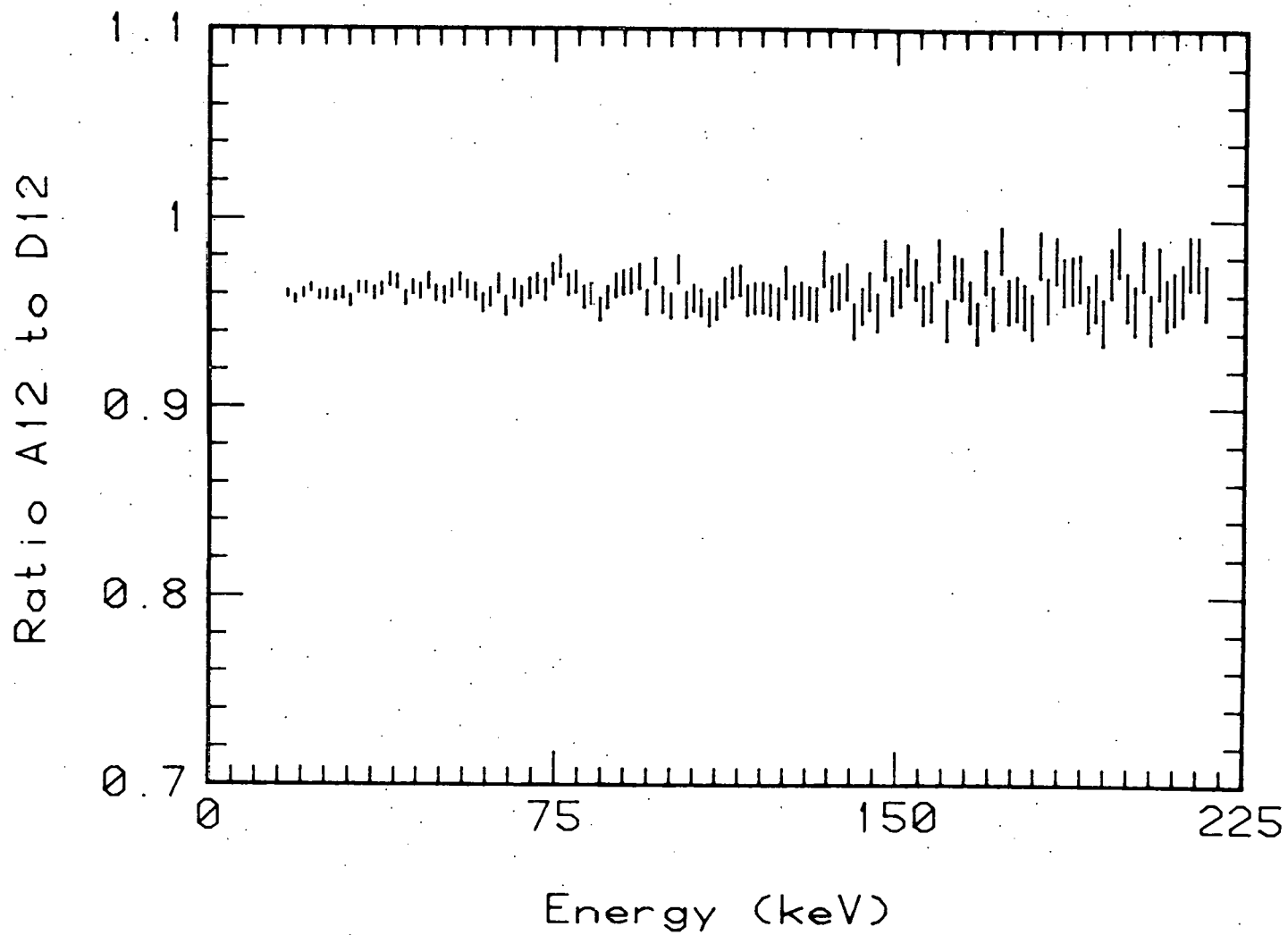

Figure III.4: Ratio of proton recoil distribution in Sector A to that in Sector D from 15 keV to 215 keV, at a radius of 56.3 cm.

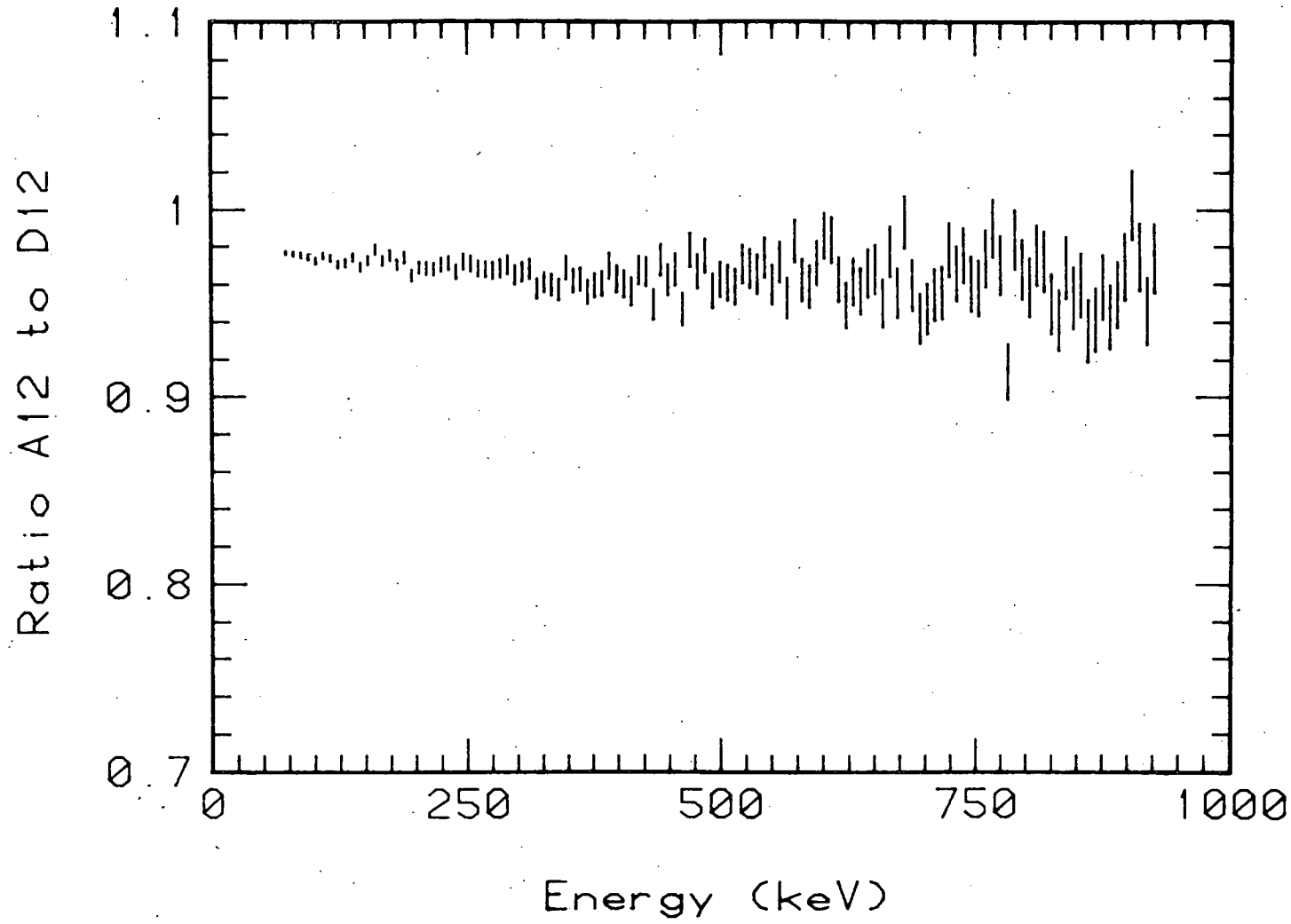

Figure III.5: Ratio of proton recoil distribution in Sector A to that in Sector D from 60 keV to 900 keV, at a radius of 56.3 cm.

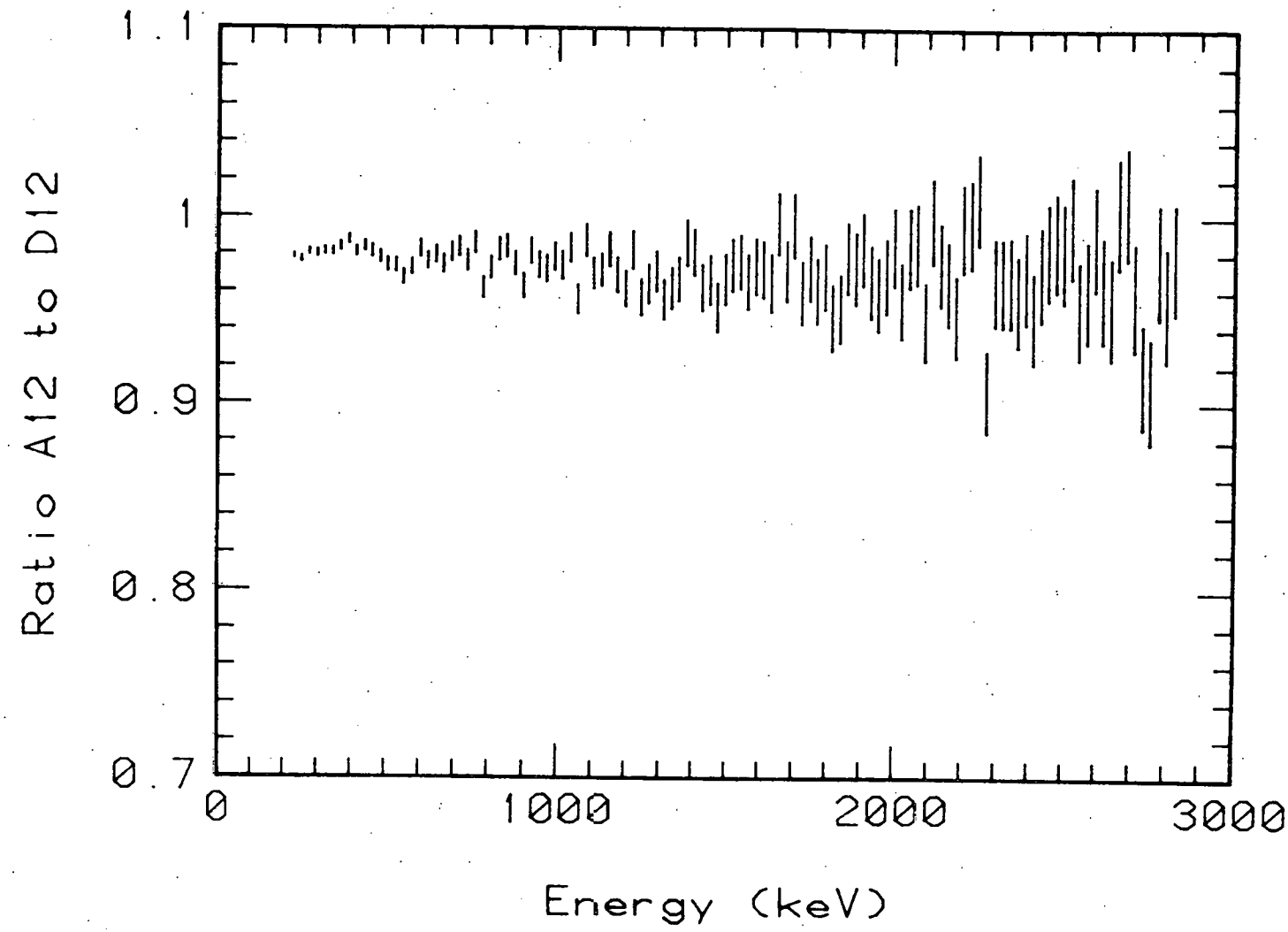

Figure III.6: Ratio of proton recoil distribution in Sector A to that in Sector D from 200 keV to 3 MeV, at a radius of 56.3 cm.

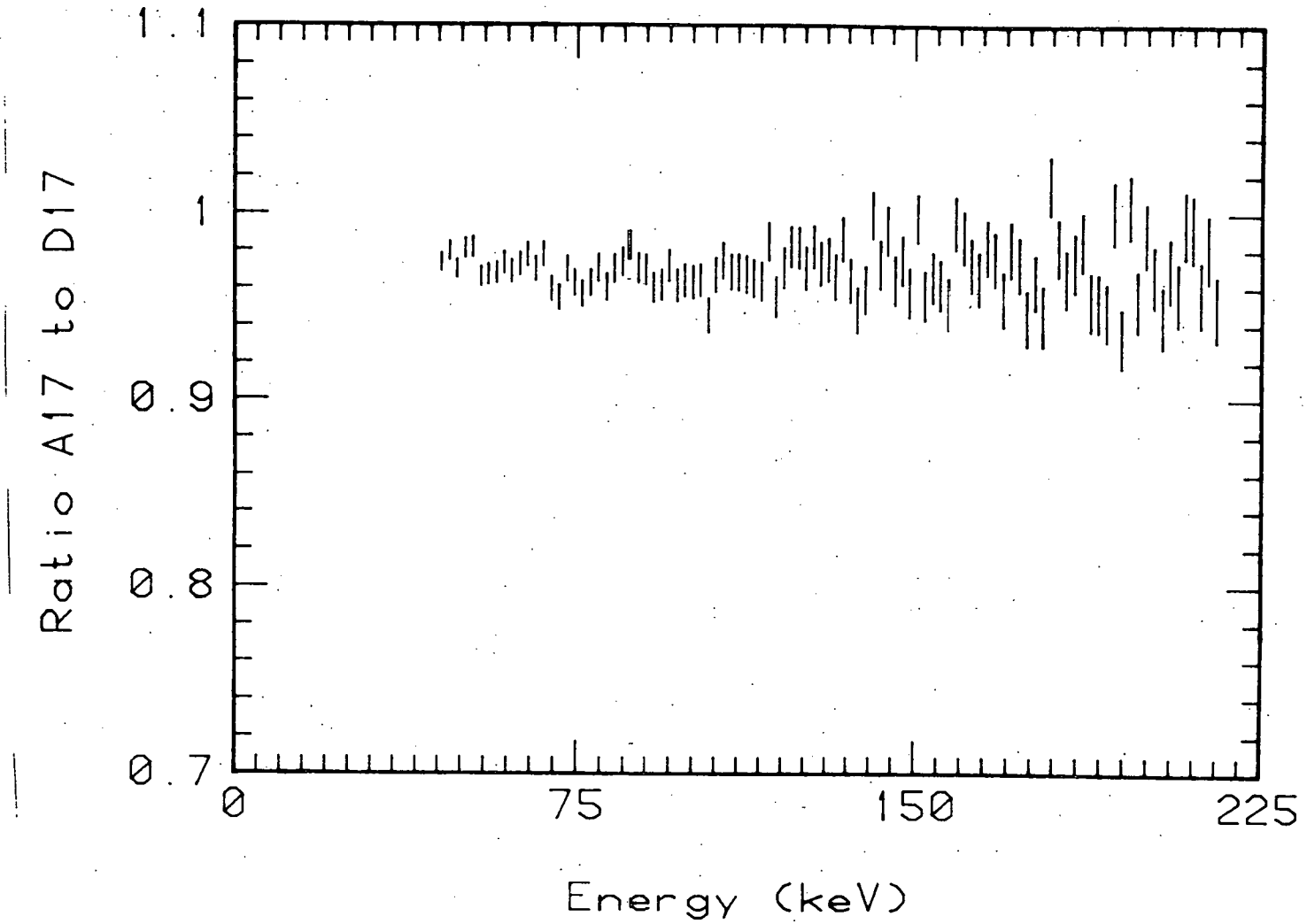

Figure III.7: Ratio of proton recoil distribution in Sector A to that in Sector D from 40 keV to 215 keV, at a radius of 71.1 cm.

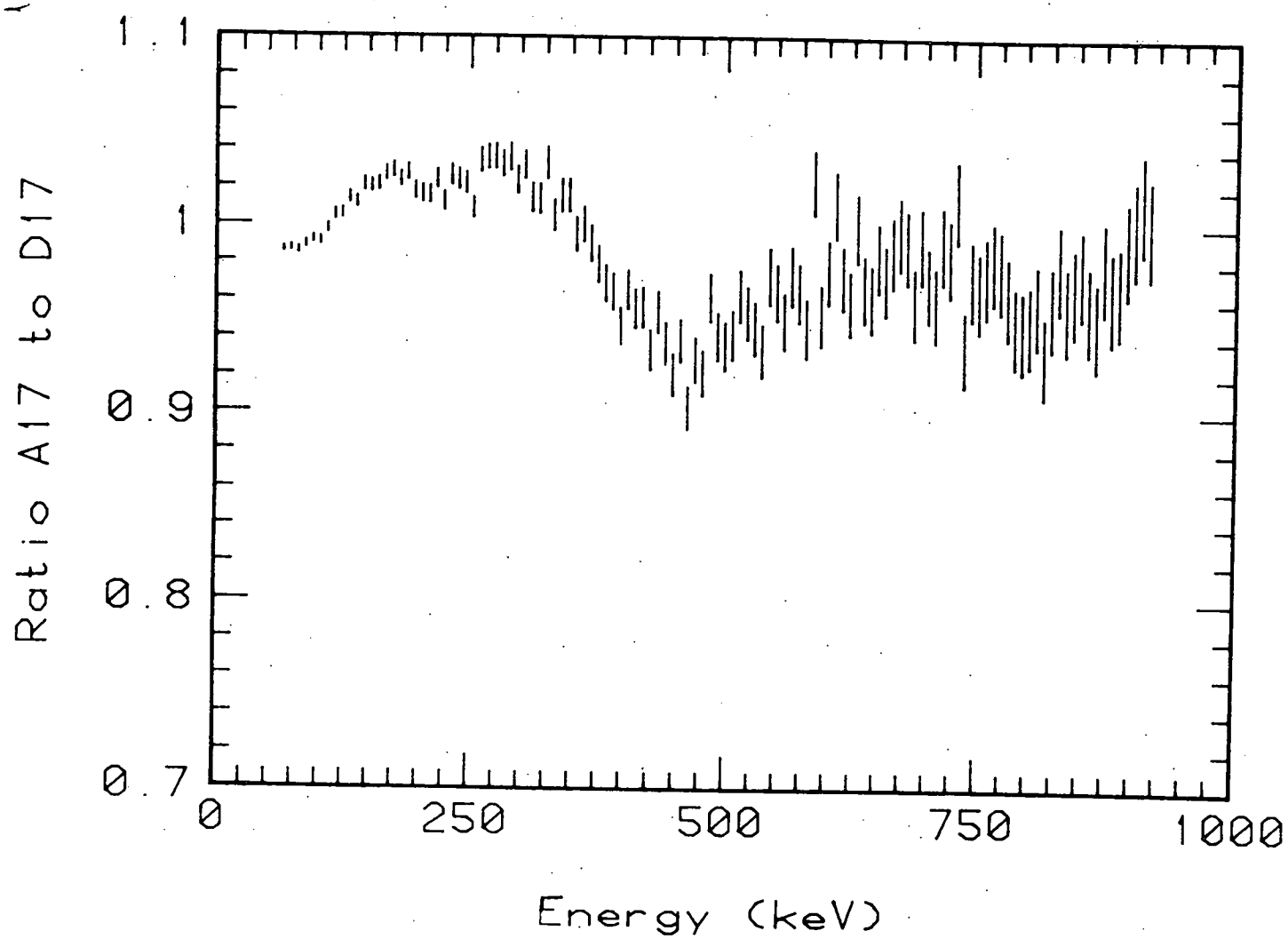

Figure III.8: Ratio of proton recoil distribution in Sector A to that in Sector D from 50 keV to 850 keV, with a radius of 71.1 cm.

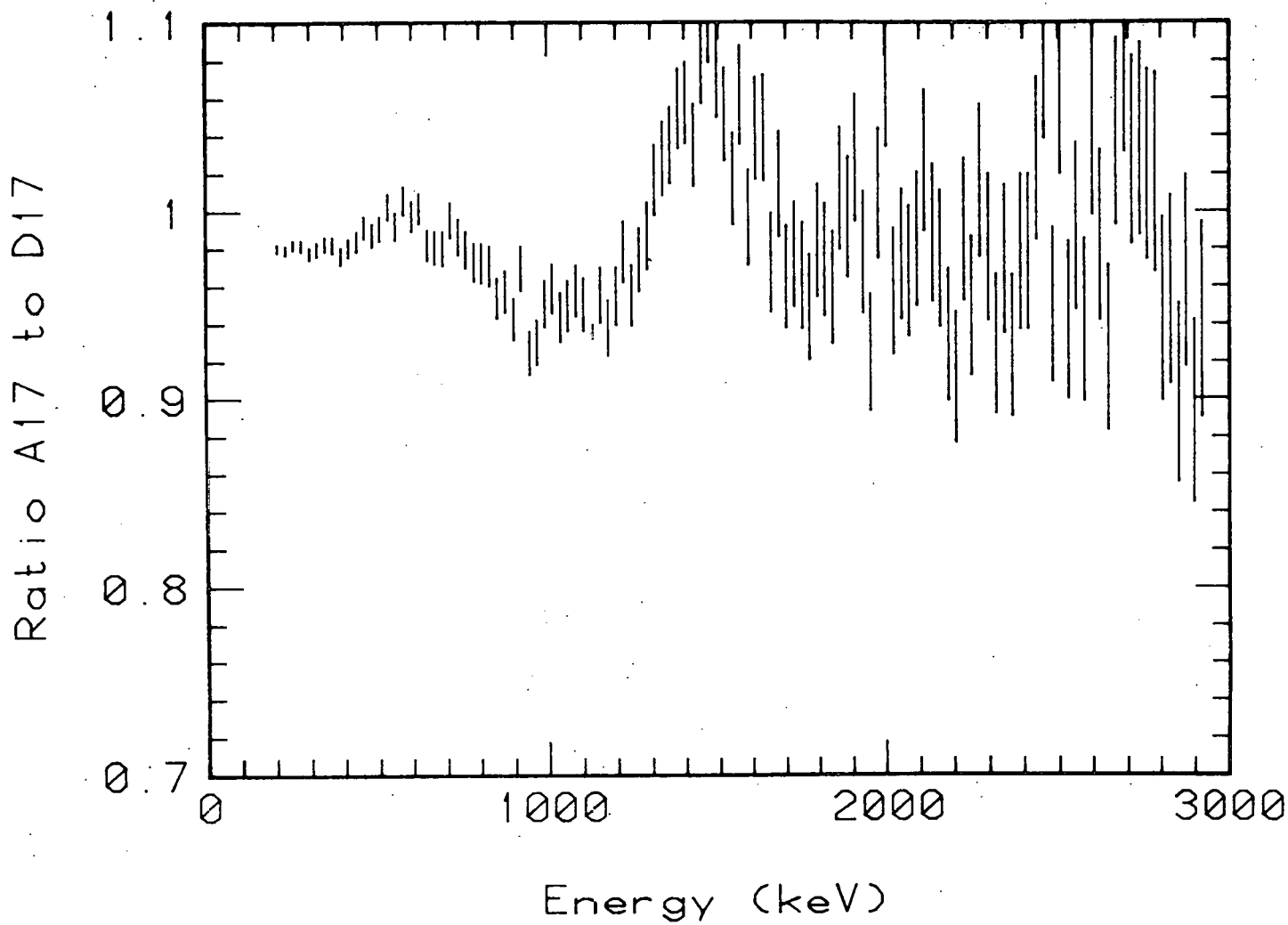

Figure III.9: Ratio of proton recoil distribution in Sector A to that in Sector D from 200 keV to 3 MeV, with a radius of 71.1 cm.

IV. EXPERIMENTAL MEASUREMENTS USING THE FBBF FACILITY

During the progress period the $^{115}In\ (n,\gamma)^{116m}In$ and the $^{115}In(n,n')$ reaction rates were measured in the FBBF facility and the results of these measurements are described in the following section.

A. Preliminary Radial Indium Measurements
(G.A. Harms and F.M. Clikeman)

The activity of indium foils irradiated in the blanket region in the FBBF facility has been measured. The foils were irradiated in sector D and the activities detected from the $^{115}In(n,\gamma)^{116m}In$ and the $^{115}In(n,n')^{115m}In$ reactions. The neutron capture reaction was detectable in all positions while the inelastic scattering reaction was detectable in all positions except D13 and D17. the timing of the experiment was optimized for the neutron capture reation; thus, it is expected that the results of the inelastic scattering reaction can be improved at a later time when the experiment will be repeated using a timing sequence that will optimize the detection of the 4.3 hour halflife of the ^{115m}In isomeric state. Figure IV.1 shows relative ^{116m}In activities as a function of position. Figure IV.2 shows similar results for the inelastic scattering reaction. In both figures the activities are corrected for the cylindrical geometry of the facility by multiplying by 2π times the radius. The one standard deviation error bars based on the counting statistics are shown in both figures. For the neutron capture reaction the error bars correspond to a standard deviation of about 0.7% in the region near the transformer blanket interface and about 1.6% at the blanket reflector interface. For the (n,n') reaction the error bars correspond to about 3.1% standard devia-

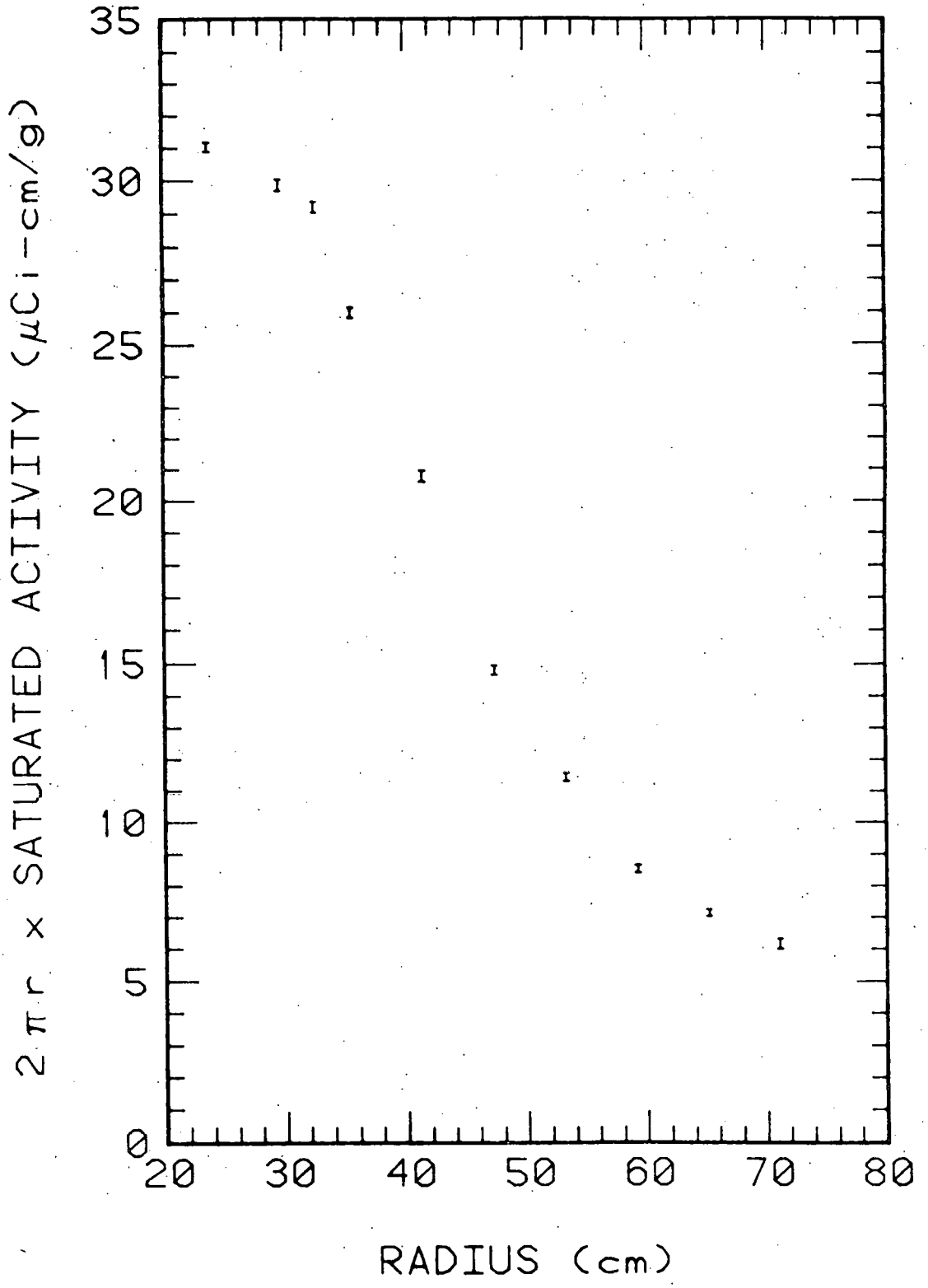

Figure IV.1: Relative ^{116m}In activities in sector D. The errors are shown at one standard deviation and account only for statistical errors in the counting process.

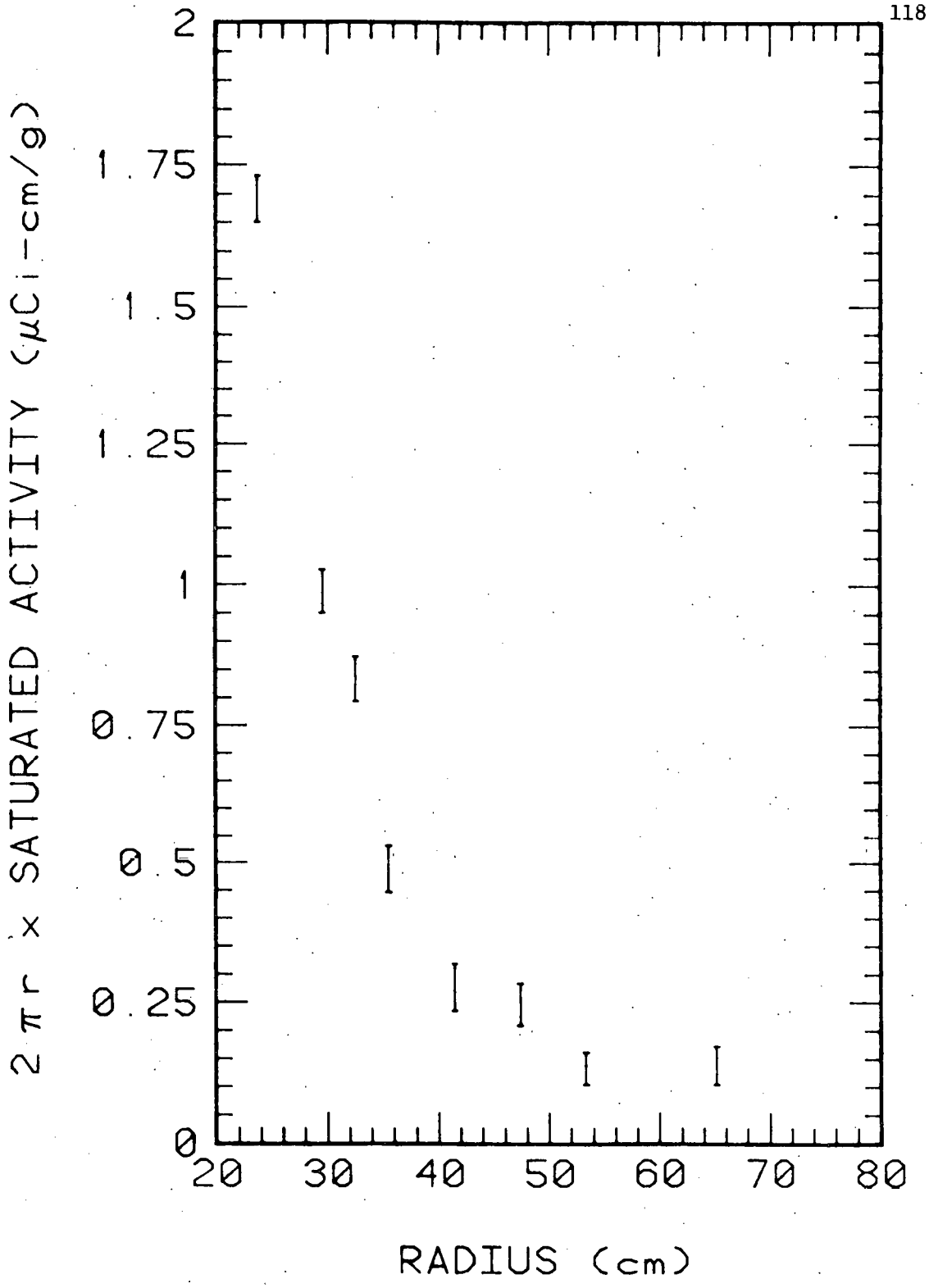

Figure IV.2: Relative ^{115m}In activities in sector D. The errors are shown at one standard deviation and account only for statistical errors in the counting process.

tion near the transformer blanket interface. At the present time the cross section for these reactions are not available, therefore, comparisons with calculated reaction rate as a function of regular position can not be made.

REFERENCES

1. W.W. Little, Jr. and R.W. Hardie, "2DB User's Manual," Pacific Northwest Laboratory, BNWL-831 (July 1968).

2. J.E. Suich and H.C. Honeck, "The HAMMER System, Heterogeneous Analysis by Multigroup Methods of Exponentials and Reactors," Savannah River Laboratory, DP-1064 (January 1967).

3. L.P. Abagyan, N.O. Bazayants, I.I. Bondarenko and M.N. Nikolaev, Group Constants for Nuclear Reactor Calculations, Edited by Professor I.I. Bondarenko, Consultants Bureau, New York, 1964.

4. S. Glasstone and A. Sesonske, Nuclear Reactor Engineering, D. Van Nostrand Company, Inc., Princeton, N.J., 1967.

5. FBBF Quarterly Progress Report for the Period January 1, 1977-March 31, 1977, Purdue University, PNE-77-118, COO-2826-3, (1977).

6. D.J. Malloy, L.B. Luck and G.L. Terpstra, "LAZARUS, A 1-Dimensional Theory Package for Fast Reactor Calculations," Purdue University, PNE-76-112 (1976).

7. FBBF Quarterly Progress Report for the Period January 1, 1976-August 30, 1976, Purdue University, PNE-76-115, COO-2826-1 (1976).

8. FBBF Quarterly Progress Report for the period April 1, 1977-June 30, 1977, Purdue University, PNE-77-119, COO-2826-4 (1977).

9. FBBF Quarterly Progress Report for the period January 1, 1978-March 31, 1978, Purdue University, PNE-78-128, COO-2826-8 (1978).

10. G.G. Simons and L.L. Emmons, "Experimental Evaluation of a Model for Calculating the Gamma-Ray Response of Encapsulated Solid-State Dosimeters," Argonne National Laboratory, ZPR-TM-238 (1976).